BEST AVAILABLE IMAGES

Defective images within this document are accurate representations of the original documents submitted by the applicant.

Defects in the images may include (but are not limited to):

- BLACK BORDERS
- TEXT CUT OFF AT TOP, BOTTOM OR SIDES
- FADED TEXT
- ILLEGIBLE TEXT
- SKEWED/SLANTED IMAGES
- COLORED PHOTOS
- BLACK OR VERY BLACK AND WHITE DARK PHOTOS
- GRAY SCALE DOCUMENTS

IMAGES ARE BEST AVAILABLE COPY.

As rescanning documents *will not* correct images, please do not report the images to the Image Problem Mailbox.

PATENT
Docket No.: **176/60981 (6-11402-1001)**

IN THE UNITED STATES PATENT AND TRADEMARK OFFICE

Applicant	:	Mahin D. Maines	Examiner: Sheridan L. Swope
Serial No.	:	10/045,545	
Cnfrm. No.	:	1814	Art Unit: 1652
Filed	:	January 14, 2002	
For	:	METHODS OF MODIFYING CELL STRUCTURE AND REMODELING TISSUE	

DECLARATION OF MAHIN D. MAINES UNDER 37 C.F.R. § 1.132

I, Mahin D. Maines, pursuant to 37 C.F.R. § 1.132, hereby declare:

1. I am the inventor of the above-identified application.

2. I am currently Professor of Biochemistry and Biophysics at the University of Rochester Medical Center, Rochester, NY.

3. I received a B.A. in Biology from Ball State University in 1964, an M.S. in Chemistry from Ball State University in 1967, and a Ph.D. in Pharmacology from the University of Missouri in 1970. A major focus of my career has been involved with biliverdin reductase, its activities, its properties, and how the protein interacts with other cellular components to regulate cell activities. Since 1981, I have published over twenty-four articles concerning different aspects of biliverdin reductase.

4. I am presenting this declaration to: (i) confirm that the nucleotide sequence of human biliverdin reductase ("BVR") used in the example to the present application was the nucleotide sequence for human BVR that is identified in the application as SEQ ID NO: 2; and (ii) demonstrate that the structure and function of BVR proteins are highly conserved among mammalian BVR and, therefore, results achieved with human and/or rat BVR are predictive of results that can be achieved with other mammalian BVR.

BVR Sequence Used in Examples of Specification

5. The description of the figures that appears in the present application indicates that the BVR expressed in transformed cells is that of human BVR. In performing the experimental work reported in the example, I used the human BVR DNA sequence that is reported in the application as SEQ ID NO: 2. No other human BVR DNA sequence is explicitly recited in the present application.

Conservation of Structure and Function Among Mammalian BVR

6. The present application identifies two human BVR amino acid sequences (SEQ ID NO: 1 and SEQ ID NO: 3) and a single rat BVR amino acid sequence (SEQ ID NO: 4). The two human BVR sequences are 99 percent identical. The human BVR of SEQ ID NO: 1 and the rat BVR of SEQ ID NO: 4 are 82 percent identical.

7. Mammalian BVR proteins are characterized by a number of shared structural features. As identified in the present application, human BVR of SEQ ID NO: 1 is characterized by the following structural features: a basic N-terminal domain characterized by the sequence ERK at residues 6 to 8; a hydrophobic domain characterized by the sequence FGVVVV at residues 9 to 14 (which matches the consensus sequence of SEQ ID NO: 6); a nucleotide binding domain characterized by the sequence GVGRAG at residues 15 to 20 (which matches the consensus sequence of SEQ ID NO: 7); an oxidoreductase domain characterized by the sequence AGKHVLVE at residues 90 to 97 (SEQ ID NO: 8 as corrected); a leucine zipper characterized by the sequence $LX_6LX_6KX_6LX_6L$ at residues 129 to 157 (SEQ ID NO: 9); several kinase motifs characterized by the sequence SRR at residues 44 to 46 (SEQ ID NO: 10), KGS at residues 147 to 149 (SEQ ID NO: 11), and FGF at residues 162 to 164 (which matches the consensus of FGX, SEQ ID NO: 12); a nuclear localization signal characterized by the sequence GLKRNRY at residues 222 to 228 (SEQ ID NO: 13); a myristylation site characterized by the sequence PGLKR at residues 221 to 225 (SEQ ID NO: 14); a zinc finger domain characterized by the sequence $HCX_{10}CC$ at residues 280 to 293 (SEQ ID NO: 15); a protein kinase C ("PKC") enhancing domain characterized by the sequence KKRILHC at residues 275 to 281 (which matches the consensus of SEQ ID NO: 16); and a PKC inhibiting domain characterized by the sequence QKYCCSRK at residues 290 to 296 (which matches the consensus of SEQ ID NO: 17). I have since identified additional kinase motifs within the human BVR sequence, including GRAGSVRM

at residues 17 to 24 which conforms to the XRXXSXRX motif (Kemp et al., "Protein Kinase Recognition Sequence Motifs," *Trends in Biological Sciences* 15(9):342-346 (1990) (copy attached hereto as **Exhibit 1**), and YMKM at residues 198 to 201 which conforms to the YMXM motif (*see* Shoelson et al., "YMXM Motifs of IRS-1 Define Substrate Specificity of the Insulin Receptor Kinase," *Proc. Natl. Acad. Sci. USA* 89:2027-2031 (1992) (copy attached hereto as **Exhibit 2**). The rat BVR sequence of SEQ ID NO: 4 contains an identical hydrophobic domain, an identical nucleotide binding domain, an identical oxidoreductase domain, a conserved leucine zipper domain (i.e., with any residue variations being between L and K residues), identical or conserved kinase motifs, an identical nuclear localization signal, an identical myristylation site, a conserved zinc finger domain, a conserved PKC enhancing domain, and a conserved PKC inhibiting domain. Based on the shared or conserved structural features between the human and rat BVR sequences, one of ordinary skill in the art would expect other mammalian BVR sequences to share these same identical or conserved structural features.

8. The reasonableness of the expectation of shared structural features, based on a comparison of human and rat BVR sequence, is confirmed by the alignment of human and rat BVR sequences with the mouse and pig BVR sequences, which have subsequently been obtained. The mouse BVR sequence, obtained in my laboratory, is reported at Genbank Accession NP_080954, a copy of which is attached hereto as **Exhibit 3**. The pig BVR was also obtained in my laboratory using total RNA isolated from *Sus scrofa* muscle tissue. The RNA was used to make cDNA in a reverse transcription reaction with iScript cDNA synthesis kit (BIO-RAD, #170-8890). 2 μl of the cDNA prep was used to amplify the biliverdin reductase open reading frame with human specific full-length primers under the following conditions: initial denature 94°C, 2 min; 40 cycles: denature temperature 94°C for 30 sec, annealing temperature 65°C for 30 sec, extension temperature 72°C for 1 min; and final extension 72°C, 10 min. The PCR product was purified with QIAquick gel purification kit (Qiagen, #28704) and used for direct sequencing with gene-specific primers giving overlapping fragments with BigDye terminator mix (version 3.1). Independent purification of total RNA from another source of *Sus scrofa* muscle tissue, cDNA synthesis, PCR amplification, and gel purification was done as described above. The PCR product was used to clone into the pETBlue vector plasmid (Novagen, #70599-4). Recombinant DNAs were checked for insert and orientation using PCR analysis with gene specific primers and

restriction endonucleases *Xba*I and *Eco*RI. One of the plasmids pETBlue/SsBVR-3 was used for sequencing analysis. Both independent sets of sequences, from cDNA amplicon and from cloned fragment, were in perfect match with each other. A copy of the pig BVR cDNA and amino acid sequences is attached hereto as **Exhibit 4**. The mouse and pig BVR amino acid sequences were aligned with the human and rat BVR amino acid sequences using the ClustalW alignment program set on its default settings. A copy of the alignment of these four mammalian BVR sequences is attached hereto as **Exhibit 5**.

9. The mouse BVR sequence is about 81 percent identical to the human BVR sequence of SEQ ID NO: 1. Based on the alignment of Exhibit 3, one of ordinary skill in the art would conclude that mouse BVR, when compared to the human BVR of SEQ ID NO: 1, contains an identical hydrophobic domain, an identical nucleotide binding domain, an identical oxidoreductase domain, a conserved leucine zipper domain (i.e., with any residue variations being between L and K residues), identical or conserved kinase motifs, a conserved nuclear localization signal, an identical myristylation site, a conserved zinc finger domain, an identical PKC enhancing domain, and a conserved PKC inhibiting domain. This high structural conservation, particularly within previously identified functional domains of the protein, indicates that the proteins are functionally quite similar.

10. The pig BVR sequence is about 98 percent identical to the human BVR sequence of SEQ ID NO: 1. Based on the alignment of Exhibit 3, one of ordinary skill in the art would conclude that the pig BVR, when compared to the human BVR of SEQ ID NO: 1, contains an identical hydrophobic domain, an identical nucleotide binding domain, an identical oxidoreductase domain, a conserved leucine zipper domain (i.e., with any residue variations being between L and K residues), identical or conserved kinase motifs, an identical nuclear localization signal, an identical myristylation site, a conserved zinc finger domain, an identical PKC enhancing domain, and an identical PKC inhibiting domain. This high structural conservation, particularly within previously identified functional domains of the protein, indicates that the proteins are functionally quite similar.

11. In addition, based on the known biochemical pathways shared by mammalian BVR proteins, one of ordinary skill in the art would have expected the results achieved with one mammalian BVR to be consistent with other mammalian BVR. Prior to my co-pending U.S. Patent Application Serial No. 09/606,129, filed June 28, 2000, it was widely believed that BVR was a general housekeeping enzyme that was conserved among

mammals, catalyzing the NADPH-dependent reduction of biliverdin to produce bilirubin. In particular, Noguchi et al., "Purification and Properties of Biliverdin Reductase from Pig Spleen and Rat Liver," *J. Biochem.* 86(4):833-848 (1979)("Noguchi")(copy attached as **Exhibit 6**) reports that purified pig and rat BVR has both NADH- and NADPH-dependent activities in converting biliverdin to bilirubin, with the NADH-dependent activity being optimal at pH 6.9 and the NADPH-dependent activity being optimal at pH 8.5. Noguchi also indicates that both systems are inhibited by bilirubin, but inhibition of the NADPH-dependent activity was more pronounced. In addition, Noguchi reports that the NADPH-dependent activity for biliverdin had a K_m of 0.3 μM whereas the NADH-dependent activity for biliverdin had a K_m of 1-2 μM. Rigney et al., "The Reaction Mechanism of Bovine Kidney Biliverdin Reductase," *Biochim. Biophys. ACTA* 957:237-242 (1988)(copy attached as **Exhibit 7**) reports that purified bovine BVR has both NADH- and NADPH-dependent activities in converting biliverdin to bilirubin, with the NADH-dependent activity being optimal at pH between 6 and 7 (depending on the buffer system utilized) and the NADPH-dependent activity being optimal at pH 8.5. Rigney et al., "The Kinetics of Ox Kidney Biliverdin Reductase in Pre-steady State: Evidence That the Dissociation of Bilirubin is the Rate-determining Step," *Biochem J.* 259:709-713 (1989)(copy attached as **Exhibit 8**) confirms that the broad features of the reaction mechanism for NADPH- and NADH-dependent activities are the same, with BVR activity exhibiting a pH-dependent burst in the rate of conversion of biliverdin to bilirubin followed by a steady-state rate. As addressed in the present application, at Example 1, human BVR shares the property of dual co-factor activity using NADPH and NADH. In addition to the conserved activity among mammalian BVR, Rigney et al., "Some Physical and Immunological Properties of Ox Kidney Biliverdin Reductase," *Biochem J.* 255:431-435 (1988)("Rigney III")(copy attached as **Exhibit 9**) reports at Table 2 and page 435 (first column) that antibodies raised against ox BVR were able to immunoprecipitate BVR from numerous mammals, including pig, guinea pig, mouse, rat, hamster, fox, wallaby, and human. All of the foregoing confirms that those persons of skill in the art believed BVR to be functionally well-conserved among mammals.

12. Based upon the high degree of structural similarity of the three BVR proteins identified in the present application, addressed in paragraphs 6 and 7 above, as confirmed by their high degree of structural similarity with mouse and pig BVR sequences as addressed in paragraphs 8-10 above, and the functional similarity of many mammalian BVR

proteins as identified in paragraph 11, persons of skill in the art would have expected results achieved with any one mammalian BVR protein to be achievable with other mammalian BVR proteins.

13. I hereby declare that all statements made herein of my own knowledge are true and that all statements made on information and belief are believed to be true; and further that these statements were made with the knowledge that willful false statements and the like so made are punishable by fine or imprisonment, or both, under section 1001 of Title 18 of the United States Code, and that such willful false statements may jeopardize the validity of the application or any patent issuing thereon.

Date: 3/11/04

Mahin D. Maines

Beebe for comments on the manuscript. We acknowledge partial support for studies reviewed here from the US–Spain Joint Committee for Scientific and Technological Cooperation.

References

1 Ham, R. G. and Veomett, M. J. (1980) in *Mechanisms of Development*, p. 429 The C. V. Mosby Company
2 Tata, J. R. (1984) in *Biological Regulation and Development*, Vol. 3B (Goldberger, R. P. and Yamamoto, K. R., eds), p. 13, Plenum Press
3 Gilbert, S. F. (1988) *Developmental Biology*, 2nd Edn, Sinauer
4 Gudernatsch, J. F. (1912) *Wilhelm Roux's Arch. Entwicklungsmech. Org.* 35, 457–483
5 Kopec, S. (1922) *Biol. Bull.* (Woods Hole, MA) 24, 323–342
6 Levi-Montalcini, R. and Angeletti, P. U. (1969) *Physiol Rev.* 48, 534–568
7 Cohen, S. and Savage, C. R., Jr (1974) *Recent Prog. Horm. Res.* 30, 551–574
8 De Pablo, F., Roth, J., Hernandez, E. and Pruss, R. M. (1982) *Endocrinology* 111, 1909–1916
9 Serrano, J., Bevins, C. L., Young, W. S. and De Pablo, F. (1989) *Dev. Biol.* 132, 410–418
10 Girbau M., Bassas, L., Alemany, J. and De Pablo, F. (1989) *Proc. Natl Acad. Sci. USA* 86, 5868–5872
11 De Pablo, F., Girbau, M., Gomez, J. A., Hernandez, E. and Roth, J. (1985) *Diabetes* 34, 1063–1067
12 Girbau, M., Lesniak, M. A., Gomez, J. A. and De Pablo, F. (1988) *Biochem. Biophys. Res. Commun.* 153, 142–148
13 Scavo, L., Alemany, J., Roth, J., and De Pablo, F. (1989) *Biochem. Biophys. Res. Commun.* 162, 1167–1173
14 Beebe, D. C., Silver, M. H., Belcher, K. S., Van Wyk, J. J., Svoboda, M. E. and Zelenka, P. S. (1987) *Proc. Natl Acad. Sci. USA* 84, 2327–2330
15 Alemany, J., Zelenka, P., Serrano J. and De Pablo F. (1989) *J. Biol. Chem.* 264, 17559–17563
16 Spemann H. and Mangold H. (1924) *Wilhelm Roux's Arch. Entwicklungsmech. Org.* 100, 599–638
17 Slack, J. M. W. (1983) in *From Egg to Embryo*, p. 26, Cambridge University Press
18 Nieuwkoop, P. D. (1969) *Wilhelm Roux's Arch. Entwicklungsmech. Org.* 162, 341–373
19 Sargent, T. D., Jamrich, M. and David, I. B. (1986) *Dev. Biol.* 114, 238–246
20 Gurdon, J. B., Brennan, S., Fairman, S. and Mohun, T. J. (1984) *Cell* 38, 691–700
21 Weeks, D. L. and Melton, D. A. (1987) *Cell* 51, 861–867
22 Kimelman, D. and Kirschner, M. (1987) *Cell* 51, 869–877
23 Rosa, F., Roberts, A. B., Danielpour, D., Dart, L. L., Sporn, M. B. and Dawid, I. B. (1988) *Science* 239, 783–785
24 Kimelman, D., Abraham, J. A., Haaparanta, T., Palisi, T. M. and Kirschner, M. W. (1988) *Science* 242, 1053–1056
25 Gillespie, L. L., Paterno, G. D. and Slack, J. M. W. (1989) *Development* 106, 203–208
26 Smith, J. C., Price, B. M. J., Van Nimmen, K. and Huylebroeck, D. (1990) *Nature* 345, 729–731
27 Rosen, O. M. (1987) *Science* 237, 1452–1458
28 Livneh, E., Glazer, L., Segal, D., Schlessinger, J. and Shilo, B-Z. (1985) *Cell* 40, 599–607
29 Mlodzik, M., Hiromi, Y., Weber, U., Goodman, C. S. and Rubin, G. M. (1990) *Cell* 60, 211–224
30 Vassin, H., Bremer, K. A., Knust, E. and Campos-Ortega, J. (1987) *EMBO J.* 6, 3431–3440
31 Greenwald, I. (1985) *Cell* 43, 583–590
32 Yang, Q., Angerer, L. M. and Angerer, R. C. (1989) *Science* 246, 806–808
33 Wright, C. V. E., Cho, K. W. Y., Oliver, G. and De Robertis, E. M. (1989) *Trends Biochem Sci.* 14, 52–56
34 Ruiz I Altaba, A. and Melton, D. A. (1990) *Trends Genet.* 6, 57–64
35 Rappolee, D. A., Brenner, C. A., Schultz, R., Mark, D and Werb, Z. (1988) *Science* 241, 1823–1825
36 Mattson, B. A., Rosenblum, I. Y., Smith, R. M. and Heyner, S. (1988) *Diabetes* 37, 585–589
37 Serrano, J., Shuldiner, A. R., Roberts, C. T., LeRoith, D. and De Pablo, F. *Endocrinology* (in press)
38 Herrmann, B. G., Labeit, S., Poustka, A., King, T. R and Lehrach, H. (1990) *Nature* 343, 617–622
39 Hamburger, V. and Hamilton, H. L. (1951) *J. Morphol.* 88, 49–92

Protein sequence MOTIFS

A REVIEW of protein kinase recognition sequences is both long overdue and premature. It is overdue because many of the approaches and applications of this field are more than a decade old, and it is premature because we do not know the three-dimensional structure of a single protein kinase substrate complex. The study of protein kinases over the last 35 years has resulted in protein phosphorylation being recognized as one of the most important mechanisms of regulating intracellular processes. There are few, if any, physiological processes in eukaryotes that are not dependent on protein phosphorylation. While this brief review is focused on protein kinase recognition motifs, it should be recognized that protein phosphatases, which catalyse the reverse reaction, are equally important players in the overall process of regulation of protein function by phosphorylation. Undoubtedly, their specificity and regulatory properties are no less important.

B. E. Kemp and **R. B. Pearson** are at the St Vincent's Institute of Medical Research, 41 Victoria Parade, Fitzroy, Victoria 3065, Australia.

Protein kinase recognition sequence motifs

Bruce E. Kemp and Richard B. Pearson

Protein kinases play a crucial role in the regulation of many cellular processes. They alter the functions of their target proteins by phosphorylating specific serine, threonine and tyrosine residues. Identification of phosphorylation site sequences and studies with corresponding model peptides have provided clues to how these important enzymes recognize their substrate proteins. This knowledge has made it possible to identify potential sites of phosphorylation in newly sequenced proteins as well as to construct specific model substrates and inhibitors.

All protein kinases contain a common catalytic domain which typically extends over 240 residues[1], including the binding sites for ATP and the protein substrate (Fig. 1). The ATP-binding site is located at the amino terminus of the domain as characterized by the Rossmann motif, GXGXXG, while the centrally located Asp184 is responsible for base catalysed transfer of the phosphate to the protein substrate[2]. The binding site for the protein substrate is not unequivocally established, although some evidence favours the idea that it is located in the carboxy-terminal 60 residues of the catalytic domain[3].

Early studies found that protein kinases phosphorylated their target proteins at discrete sites. These enzymes were shown to prefer certain exogenous substrates (such as casein, phosvitin and histones) and only phosphorylated a limited number of available sites. Indeed, Krebs and Fischer showed that phosphorylase kinase only phosphorylated Ser14 in phosphoryl-

ase which contains 64 Ser and Thr residues. Langan's pioneering work on histone phosphorylation demonstrated that several protein kinases may phosphorylate a common substrate at multiple sites. The importance of substrate specificity was further highlighted by the discovery of the cAMP-dependent protein kinase by Walsh and his colleagues. This enzyme did not phosphorylate phosphorylase but did phosphorylate a wide range of exogenous proteins. The idea that the multiple functions of the second messenger cAMP were all mediated by the cAMP-dependent protein kinase implied the enzyme recognized a panel of protein substrates that were subject to hormonal regulation. This raised the question of how protein kinases recognized specific residues out of the numerous hydroxyl groups in their substrates.

It became evident that the local sequence around the phosphorylation site played a vital role in recognition by the cAMP-dependent protein kinase and that arginine residues were involved. The cAMP-dependent protein kinase phosphorylated β casein B at Ser124 in the sequence TERQSLT (nos 120–126) but not in the more common variant β casein A[2] where Ser replaces Arg at position 122 (Ref. 4). This observation suggested that the cAMP-dependent protein kinase substrate recognition motif may be the RXS* sequence[†]. Studies in several laboratories in the mid-1970s demonstrated that the cAMP-dependent protein kinase readily phosphorylated short synthetic peptides[5] and provided compelling evidence for the role of Arg residues. Significantly, the synthetic peptide modelled on the liver pyruvate kinase phosphorylation site sequence, LRRASLG (Kemptide), was phosphorylated with kinetic constants comparable to native protein substrates. This data suggests that all of the information necessary for recognition by the cAMP-dependent protein kinase could be present in the local phosphorylation site sequence and that RRXS was a preferred motif (reviewed in Ref. 5). While the primary sequence and proximity of Arg residues plays an important role, higher orders of structure can have an overriding influence.

[†]The phosphate acceptor site is indicated S* to distinguish it from serine phosphate (S(P)) which may act as a specificity determinant for some protein kinases. Where the specificity determinants are known, less essential residues are marked X and determinant residues are shown in bold. The complete phosphorylation site sequence is given where the major determinants are not known (see Table I).

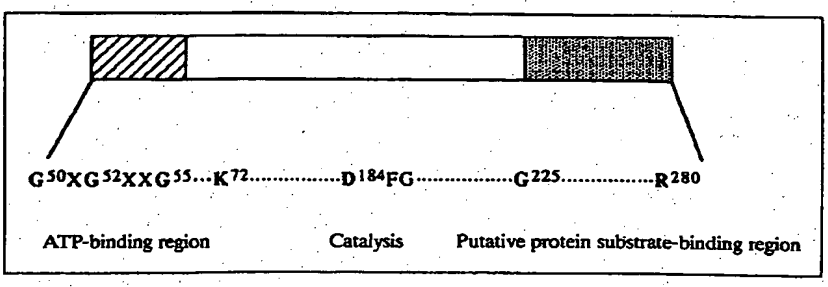

Figure 1
General structure of a protein kinase catalytic domain. Residues conserved in almost all known serine, threonine and tyrosine protein kinases are numbered according to the cAMP-dependent protein kinase catalytic subunit.

For example, lysozyme does not act as a substrate for the cAMP-dependent protein kinase unless it is chemically modified.

Protein kinase specificities

The study of sequences surrounding the local phosphorylation site and the phosphorylation of model peptides has enabled the identification of phosphorylation site motifs for a number of protein kinases (see Table I). Although this is an extensive list, the explosion of protein kinase sequences generated by DNA cloning has outstripped our knowledge of their substrate specificities and identification of natural substrates.

All of the calmodulin-dependent protein kinases studied to date utilize basic residues as specificity determinants. The specificity of phosphorylase kinase was studied in detail by Graves and his colleagues[6]. In the model palindromic peptide LSYRRYSL (nos 1–8), Ser2 is phosphorylated by phosphorylase kinase, whereas the cAMP-dependent protein kinase phosphorylates Ser7 on the carboxyl side of the adjacent arginines[6]. While there is a strong influence of a carboxyl basic residue S*XR in the phosphorylase peptide, this is not an absolute requirement since the enzyme can phosphorylate sites without a basic residue in this position. The non-charged adjacent residues may also influence the phosphorylation of model peptides. The myosin light-chain kinases from both smooth and skeletal muscle also show restricted substrate specificity for myosin light chains. While the skeletal muscle isoenzyme will phosphorylate light chains from skeletal, cardiac and smooth muscle, Stull and his colleagues have shown that the smooth muscle enzyme has a strong preference for light chains from the same muscle. The smooth muscle myosin light-chain kinase requires the sequence KKRXXRXXS*, with the number and spatial arrangement of the basic residues essential for favourable kinetics of phosphorylation and for directing the phosphate to the correct site[7]. In skeletal muscle myosin light chains the local phosphorylation site sequence contains Glu at residue 10 in the sequence PKKAKRRAAEGSS*NVFS (nos 1–17). Synthetic peptide analogs of the native sequence are phosphorylated with low V_{max} values, whereas those containing Arg at position 10, analogous to the smooth muscle light chains, are readily phosphorylated by skeletal muscle enzyme. This is a good example of a negative determinant that is apparent from peptide studies but presumably not accessible in the intact protein. To some extent studying the recognition requirements of protein kinases with highly restricted specificity ranges, such as phosphorylase kinase and the myosin light-chain kinases, is made difficult because of the lack of multiple natural phosphorylation site sequence for comparisons. This is also a problem for the tyrosine kinases. On the other hand, the multifunctional calmodulin-dependent protein kinases have broad specificities and recognize the motif RXXS*X in both proteins and peptide substrates[8]. The specificity requirements of the other members of the calmodulin-dependent protein kinase family are being explored in several laboratories.

Protein kinase C has been the subject of numerous substrate specificity studies. The initial studies were carried out on brain enzyme which consists of multiple isoenzymes. All protein kinase C preparations have a requirement for basic residues but there can be considerable variation in the juxtaposition and choice of Arg over Lys around the

phosphorylation site. Synthetic peptides containing the motif XRXXS*XRX tend to be the best substrates and indeed this arrangement is present in the pseudosubstrate autoregulatory region of the enzyme (see below). With the availability of individual recombinant isoenzymes of protein kinase C, Parker and his colleagues are exploring the basic residue requirements of the individual isoenzymes.

The specificity and recognition sites for the cyclic nucleotide-dependent protein kinases have been extensively studied (reviewed in Ref. 5). For the cAMP-dependent protein kinase, the most typical motif is RRXS*X but RXS*X and KRXXS*X are also encountered. The phosphorylation site sequence RRS* occurs in both cardiac troponin and hormone-sensitive lipase, but limited synthetic peptide studies indicate that the Arg adjacent to the Ser(*) is less important than the second Arg. There is also evidence from synthetic peptide studies that more distal Arg residues on the amino-terminal side may have a positive influence. Indeed the heat-stable inhibitor (Walsh inhibitor) of this enzyme has the pseudosubstrate motif GRTGRRNA*I with Ala occupying the equivalent of the Ser phosphate acceptor site. In scanning sequences for cAMP-dependent protein kinase sites the search pattern is RXS*, then RRXS* or KRXXS*, and not S*XR as the carboxy-terminal basic residue tends to be deleterious. The only known examples of RXS* motifs where X is not Arg are exogenous substrates phosphorylated *in vitro*. The sites phosphorylated *in vivo* by the cAMP-dependent protein kinase all contain multiple adjacent Arg residues in the arrangements RRXS* or RRS*, with two having the latter motif. A hydrophobic residue is often, but not exclusively, found after the Ser. While the yeast cAMP-dependent protein kinase specificity differs in several respects, the fact that it can be complemented by the mammalian enzyme in yeast suggests that the differences do not override the natural function. Recognition site specificity of the cGMP-dependent protein kinase has been studied in detail by Glass and his colleagues[5]. From model peptide studies, there is evidence for a requirement for an Arg located on the carboxy-terminal side of the phosphorylated residue in the sequence S*R or T*R; however this is not an absolute requirement as the enzyme has been shown to phosphorylate sites without this motif. The precise requirements are insufficiently clear to allow cGMP-dependent protein kinase phosphorylation sites to be confidently identified by scanning amino acid sequences alone.

Table I. Protein kinase phosphorylation site motifs

Protein kinase	Recognition motif	Refs
Serine and threonine kinases		
Phosphorylase kinase	KRKQIS*VR	Chan[6]
Myosin light chain kinase (smooth muscle) Myosin light chain kinase (skeletal muscle)	XKKRXXRXXS*X	Kemp[5]
Myosin-I heavy chain kinase	KXXS*X or RXT*X	Brzeska[10]
Calmodulin-dependent protein kinase I	NYLRRLS*DSNF	Czernik[11]
Multifunctional calmodulin-dependent protein kinase II	XRXXS*X	Pearson[8]
Calmodulin-dependent protein kinase III	RAGET*RFT*DT*RK	Nairn[12]
cAMP-dependent protein kinase (mammalian) (yeast)	XRRXS*X XRRXS*X	Zetterqvist[5]
cGMP-dependent protein kinase	XS*RX	Glass[5]
Protein kinase C (α, β, γ)	XRXXS*XRX	Graff[13]
S6 kinase II	XRXXS*X	Erikson[14]
dsRNA-dependent kinase pp68	SELS*RR	Colthurst[15]
dsDNA-dependent kinase	PEET*QT*QDQPMEEEE	Lees-Miller[16]
Protease activated kinase I & II	AKRRRLSS*LRA	Wettenhall[9]
Cell cycle kinase cdc-28, MPF	XKS*PX or XKT*PX	Langan[18]
Proline-dependent protein kinase	XS*PX or XT*PX	Vulliet[19]
Growth factor regulated kinase	PLT*PSGEA	Countaway[20]
Casein kinase I	XS(P)XXS*X or XEXXS*X	Pinna[5]
Casein kinase II	XS*XXEX	Pinna[5]
Mammary gland casein kinase	XS*XEX or XS*XS(P)X	Pinna[5]
Glycogen synthase kinase-3	XS*XXXS(P)X	Fiol[21]
AMP-activated protein kinase (acetyl CoA carboxylase kinase) (HMG-CoA reductase kinase) (hormone sensitive lipase kinase)	MRSSMS*GLHL MIHNRS*KINL MRRSVS*EAAL	Hardie[22]

As early as 1970 Ribadeau-Dumas *et al.*[9] made correct predictions about the specificity requirements of the casein kinase from the mammary gland Golgi apparatus (S*XE or S*XS(P)) based on the sequence of the polyphosphorylated region in casein. Casein kinase II specificity has been studied extensively, in particular in the laboratories of Pinna and Krebs. This enzyme has a very widespread distribution and recognizes the motifs S*XXE and S*XXS(P). Not every site conforming to the motif is phosphorylated, casein kinase II phosphorylates Ser17 and not Ser18 in the peptide from β casein A[2], ESLSSSEE (nos 14–21). On the other hand, the mammary gland enzyme phosphorylates Ser18 and not Ser17 in this sequence. Casein kinase I and II have been shown to participate in hierarchal phosphorylation reactions by several groups. Roach and his colleagues found that prior phosphorylation of glycogen synthase by cAMP-dependent protein kinase at Ser7 caused casein kinase I to phosphorylate Ser10, whereas phosphorylation of glycogen synthase by casein kinase II provides the recognition

Table I. Protein kinase phosphorylation site motifs (continued)

Protein kinase	Recognition motif	Refs
Pyruvate dehydrogenase kinase	S*MSDPGVS*YRYGMGTS*VE	Edelman[23]
Branched chain α-ketoacid dehydrogenase kinase	GHHS*TSDO and SYRS*VDE	Paxton[24]
Heme regulated eIF-2a kinase	LSELS*RR	Kudlicki[25]
Endogenous eIF-4E kinase	KNDKS*KTWQ	Rychlik[26]
Histone H4 kinase I	VKRIS*GLG	Masaracchia[5]
Histone H4 kinase II	AcS*GRGKGG	Masaracchia[5]
Isocitrate dehydrogenase\ kinase (*E. coli*)	GIRS*LNVALR	Thorsness[27]
β-Adrenergic receptor kinase	GYS*S*NGNT*GEQS*G(X)$_{16}$G T*ED(X)$_5$GT*VPS*DNIDS*Q(X)$_3$ S*T*NDS*LL	Hausdorff[28]
Rhodopsin kinase	DEAS*T*T*VKTETS*QVA	Palczewski[29]
Tropomyosin kinase	DNALNDITS*L-COOH	Watson[30]
Tyrosine kinases		
p60$^{v\text{-}src}$	RLIEDNEY*TARQGAK	Geahlen[5]
p56^{lck}	RLIEDNEY*TAREGAK	Geahlen[5]
p40^{thymus}	PEEDGERY*DEDEE	Geahlen[5]
p85$^{gag\text{-}fes}$	REEADGVY*AASGGLR	Geahlen[5]
p90$^{gag\text{-}yes}$	RKIEDNEY*TAREGAK	Geahlen[5]
p120$^{gag\text{-}abl}$	EEKEY*HAE	Geahlen[5]
EGF receptor	TAENAEY*LRVAP	Geahlen[5]
Insulin receptor	TRDIY*ETDY*Y*RK	Geahlen[5]
p75^{liver}	DRVY*VHPF	Geahlen[5]
Spleen tyrosine kinase	EDAEY*AARRRG	Geahlen[5]

[a] R. E. H. Wettenhall and N. Morrice, unpublished.

Ser(P) for glycogen synthase kinase-3. This enzyme recognizes the motif XS*XXXS(P)X. It is of interest that all four of the Ser/Thr kinases studied that utilize Glu or Asp as specificity determinants also recognize Ser(P). There are also examples where phosphorylation at one site by a particular protein kinase can suppress the phosphorylation of a nearby residue by another protein kinase. The nearby phosphorylation sites in the hormone sensitive lipase, MRRSVSEA (nos 560–567) exhibit this behaviour with mutually exclusive phosphorylation[17] by the cAMP-dependent protein kinase (Ser563) and calmodulin-dependent protein kinase II (Ser565). It seems likely that examples of hierarchal phosphorylation will become more frequent as the specificities of additional protein kinase are studied. So far hierarchal phosphorylation has been observed between nearby phosphorylation site sequences, as well as over distances of 25 residues in the case of the regulatory subunit R_{II} phosphorylation by casein kinase II and glycogen synthase kinase-3; it is possible that even more distant interactions involving higher orders of structure may occur.

The recognition sites for a number of tyrosine protein kinases have been examined. Inspection of the known phosphorylation sites indicates that acidic residues are often located near the tyrosine phosphate acceptor site and their importance has been demonstrated with model peptides in several instances. In general, few natural substrates (excluding autophosphorylation) have been reported for tyrosine protein kinases and this has meant that we have not had the benefit of comparisons. In summarizing our knowledge of tyrosine phosphorylation site motifs, Geahlen and Harrison[5] noted: 'Observations drawn from the study of synthetic peptides have frustrated efforts to clearly define primary structural determinants that are involved in the recognition of substrates by tyrosine kinases. It is perhaps some consolation to investigators of tyrosine kinase substrate specificity that not all peptides containing tyrosine residues are substrates'. Clearly some fresh approaches are required.

Phosphorylation site motifs

The progress in recognizing specific phosphorylation site motifs for many protein kinases has led to the expectation of being able to scan protein sequences and identify phosphorylation sites for given protein kinases. However, considerable caution is required as there are too many exceptions at present to accept the phosphorylation site motifs listed in Table I as 'canons' of recognition. We do not know precisely which nominal specificity determinants actually have corresponding residues in protein kinase active sites and which just favour an optimum conformation. Hopefully this dilemma will be short lived with the imminent solution of the X-ray structure of the cAMP-dependent protein kinase complex with substrate and inhibitor peptides. Phosphorylation site sequence studies such as those made by Cohen and his colleagues have been of enormous value in contributing to our knowledge of protein kinase specificity and the development of the concepts of recognition motifs, but their most enduring value is in answering the difficult question of which sites are actually functionally significant *in vivo*. Structures resembling protein kinase phosphorylation site motifs also play an important role in the regulation of protein kinases. These structures, called pseudosubstrate prototopes, are located in the regulatory domains of protein kinases and are responsible for maintaining protein kinases in inactive

forms[3]. The pseudosubstrate sequences typically contain an alanine in place of the serine or threonine found in the phosphorylation site motifs. For protein kinase C, the pseudosubstrate sequence occurs between residues 19 and 31, RFARKGA*LRQKNV, which resembles the substrate motif RXXS*XR (Table I) with Ala25 in place of the phosphate acceptor site. In this case, activation of protein kinase C by binding of diacylglycerol is thought to induce a conformational change that removes the pseudosubstrate structure from the active site allowing access to substrates. One cannot fail to be impressed with the way nature has utilized the same features responsible for substrate recognition to regulate these important enzymes.

References

Because of the limit on the number of references it has not been possible to cite many significant contributions, but these can be traced from those given.

1 Hanks, S. K., Quinn, A. M. and Hunter, T. (1988) *Science* 241, 42–52
2 Taylor, S. S. (1989) *J. Biol. Chem.* 264, 8443–8446
3 House, C., Robinson, P. J. and Kemp, B. E. (1989) *FEBS Lett.* 249, 243–247
4 Kemp, B. E., Bylund, D. B., Huang, T. S. and Krebs, E. G. (1975) *Proc. Natl Acad. Sci. USA* 72, 3448–3452
5 Kemp, B. E. (ed.) (1990) *Peptides and Protein Phosphorylation*, pp. 1–314, Uniscience CRC Press
6 Chan, K. F. J., Hurst, M. O. and Graves, D. J. (1982) *J. Biol. Chem.* 257, 3655–3659
7 Kemp, B. E. and Pearson, R. B. (1985) *J. Biol. Chem.* 260, 3355–3359
8 Pearson, R. B., Woodgett, J. R., Cohen, P. and Kemp, B. E. (1985) *J. Biol. Chem.* 260, 14471–14476
9 Ribadeau-Dumas, B., Grosclaude, F. and Mercier, J. C. (1970) *Eur. J. Biochem.* 14, 451–459
10 Brzeska, H., Lynch, T. J., Martin, B. and Korn, E. D. (1989) *J. Biol. Chem.* 264, 19340–19348
11 Czernik, A. J., Pang, D. T. and Greengard, P. (1987) *Proc. Natl Acad. Sci. USA* 84, 7518–7522
12 Nairn, A. C. and Palfrey, H. C. (1987) *J. Biol. Chem.* 262, 17299–17303
13 Graff, J. M., Stumpo, D. J. and Blackshear, P. J. (1989) *J. Biol. Chem.* 264, 11912–11919
14 Erikson, E. and Maller, J. L. (1988) *Second Messengers and Phosphoproteins* 12, 135–143
15 Colthurst, D. R., Campbell, D. G. and Proud, C. G. (1987) *Eur. J. Biochem.* 166, 357–363
16 Lees-Miller, S. P. and Anderson, C. W. (1989) *J. Biol. Chem.* 264, 17275–17280
17 Yeaman, S. J. (1990) *Biochim. Biophys. Acta* 1052, 128–131
18 Langan, T. A. (1978) *Methods Cell Biol.* 19, 143–152
19 Vulliet, P. R., Hall, F. L., Mitchell, J. P. and Hardie, D. G. (1989) *J. Biol. Chem.* 264, 16292–16298
20 Countaway, J. L., Northwood, I. C. and Davis, R. J. (1989) *J. Biol. Chem.* 264, 10828–10835
21 Fiol, C. J., Mahrenholz, A. M., Wang, Y., Roeske, R. W. and Roach, P. J. (1987) *J. Biol. Chem.* 262, 14042–14048
22 Hardie, D. G., Carling, D. and Sim, A. T. R. (1989) *Trends Biochem. Sci.* 14, 20–23
23 Edelman, A. M., Blumenthal, D. K. and Krebs, E. G. (1987) *Annu. Rev. Biochem.* 56, 567–613
24 Paxton, R., Kuntz, M. and Harris, R. A. (1986) *Arch. Biochem. Biophys.* 244, 187–201
25 Kudlicki, W., Wettenhall, R. E. H., Kemp, B. E., Szyszka, R., Kramer, G. and Hardesty, B. (1987) *FEBS Lett.* 215, 16–20
26 Rychlik, W., Russ, M. A. and Rhoads, R. E. (1987) *J. Biol. Chem.* 262, 10434–10437
27 Thorsness, P. E. and Koshland, D. E. (1987) *J. Biol. Chem.* 262, 10422–10425
28 Hausdorff, W. P., Bouvier, M., O'Dowd, B. F., Irons, G. P., Caron, M. G. and Lefkowitz, R. T. (1989) *J. Biol. Chem.* 264, 12657–12665
29 Palczewski, K., Arendt, A., McDowell, J. H. and Hargrave, P. A. (1989) *Biochemistry* 28, 8764–8770
30 Watson, M. H., Taneja, A. K., Hodges, R. S. and Mak, A. S. (1988) *Biochemistry* 27, 4506–4512

This article is the second in our series on 'conserved protein sequence motifs involved in recognition and targeting'. The series commenced in August 1990.

Proc. Natl. Acad. Sci. USA
Vol. 89, pp. 2027–2031, March 1992
Biochemistry

YMXM motifs of IRS-1 define substrate specificity of the insulin receptor kinase

(signal transduction/phosphatidylinositol 3′-kinase/oncogene/tyrosine kinase/*src* homology domain 2)

STEVEN E. SHOELSON†, SWATI CHATTERJEE, MANAS CHAUDHURI, AND MORRIS F. WHITE

Research Division, Joslin Diabetes Center, Departments of Medicine, Brigham and Women's Hospital and Harvard Medical School, Boston, MA 02215

Communicated by Josef Fried, December 6, 1991

ABSTRACT **Of 34 tyrosine residues in insulin receptor substrate 1 (IRS-1), 14 are adjacent to acidic residues, suggesting that they might be phosphorylation sites. Synthetic peptides corresponding to sequences surrounding these tyrosines were used as substrates of the insulin receptor kinase. Surprisingly six of these, each within YMXM motifs, were phosphorylated with greatest efficiency (K_m, 24–92 μM; k_{cat}/K_m, 0.6–2.1 × 10^4 M^{-1}·sec^{-1}). Substituted YMXM peptides revealed a strong preference of the insulin receptor kinase for methionine at Y + 1 and Y + 3 positions. When phosphorylated, related YMXM sequences are recognition motifs for binding to proteins with *src*-homology (SH2) domains. The combined hydrophobic and flexible nature of methionine side chains adjacent to the targeted tyrosines provides a versatile contact for recognition by diverse proteins involved in signal transduction.**

Insulin binding to the extracellular α subunits of the insulin receptor activates tyrosine kinase activity intrinsic to the intracellular β subunits (1–4). This finding sparked a search for cellular substrates that could link the insulin receptor to postreceptor signaling events. The first identified endogenous substrate of the insulin receptor was pp185, a cytoplasmic phosphoprotein of 165–185 kDa (5). Recently, a cDNA corresponding to a component of the pp185 band was sequenced to provide the deduced primary structure of insulin receptor substrate 1 (IRS-1) (6, 7). As IRS-1 has little extended sequence homology with other known proteins, an intrinsic function for it has not been assigned. IRS-1 is phosphorylated on tyrosine residues after insulin stimulation (7), although the exact sites of phosphorylation have yet to be determined. Of a total of 34 tyrosines, 14 are preceded by acidic amino acids, suggesting that they might be targets of the insulin receptor kinase. Surprisingly, 6 of these are in YMXM motifs and two more are in YXXM motifs.

The platelet-derived growth factor (PDGF) receptor and polyoma virus middle-sized tumor antigen (middle T antigen) contain similar YMXM and homologous YVXM motifs, which are phosphorylated and thought to be essential for binding to phosphatidylinositol 3′-kinase (PI 3-kinase) (8, 9). The 85-kDa regulatory subunit of PI 3-kinase contains two SH2 domains (10, 11), which are thought to mediate its interactions with the PDGF receptor, the $pp60^{c\text{-}src}$/middle T antigen complex, and other proteins involved in cellular signaling (8). In fact, immunoprecipitation studies suggest that PI 3-kinase activity is closely associated with IRS-1 after insulin stimulation of intact cells (7, 12, 13). Thus, phosphorylated IRS-1 might act as a "docking protein" to bind and regulate PI 3-kinase and additional signal-transducing proteins containing SH2 domains as well.

The publication costs of this article were defrayed in part by page charge payment. This article must therefore be hereby marked "*advertisement*" in accordance with 18 U.S.C. §1734 solely to indicate this fact.

In this study, we show that peptides corresponding to IRS-1 YMXM motifs are excellent substrates of the insulin receptor kinase. In fact, within a given sequence the presence of methionine residues at Y + 1 and Y + 3 positions is even more important than acidic residues N-terminal to tyrosine for catalytic efficiency. These findings suggest that in addition to being recognition elements for interactions with SH2 domain-containing proteins, residues within YMXM sequences form a recognition motif for insulin receptor-catalyzed phosphorylation. These studies define structural requisites for efficient phosphorylation of a cellular substrate of the insulin receptor and may extrapolate directly to other members of the family of tyrosine kinases and their interactions with additional elements of signaling cascades.

EXPERIMENTAL PROCEDURES

Peptide Synthesis. Solid-phase syntheses were performed on an Applied Biosystems model 430A synthesizer using standard dicyclohexylcarbodiimide-mediated preformed symmetrical anhydride coupling protocols. Amino acids with standard butoxycarbonyl/benzyl protecting groups were purchased from Applied Biosystems; additional solvents and reagents were the highest purity available. Peptide products were cleaved from the resin, side-chain protecting groups were removed, and methionine sulfoxide was reduced during "low-high" cleavages with trifluoromethanesulfonic acid (14). Peptides were typically quite pure; those having ≤95% purity by analytical reversed-phase HPLC were purified further by preparative HPLC (Waters Prep 4000) on a Dynamax-300A 12-μm C8 column (41.4 × 250 mm) equipped with a matched guard column. Peptides were eluted with a mobile phase composed of acetonitrile in 0.05% aqueous trifluoroacetic acid (80 ml/min). Amino acid analyses of all peptides used for kinetic analyses were as predicted.

Insulin Receptor Preparation. Chinese hamster ovary (CHO) cells, transfected with human insulin receptor constructs and expressing 10^6 receptors per cell (15), were grown in suspension in a 10-liter spinner flask in modified McCoy's 5A medium (GIBCO) containing 0.0345 mg of L-proline per ml and no $CaCl_2$ (16, 17). Cells were solubilized in 1.0% Triton X-100 and receptors were partially purified on wheat germ agglutinin (WGA)/agarose as described (17, 18). WGA-purified protein was stored at −70°C until needed. Identical aliquots of receptor were used for all assays.

Substrate Phosphorylation Experiments. WGA-purified insulin receptor (600 μl; 1.5 pmol) was incubated sequentially with 1 μM insulin (1 h at 4°C) and 50 μM ATP/5 mM $MnCl_2$ (1 h at 22°C) for maximal phosphorylation. The peptides were diluted appropriately in a mixture of 50 μM [γ-^{32}P]ATP/5 mM $MnCl_2$ in 50 mM Hepes containing 0.1% Triton X-100. Substrate phosphorylation reactions were initiated by the

Abbreviations: IRS-1, insulin receptor substrate 1; PDGF, platelet-derived growth factor; middle T antigen, polyoma virus middle-sized tumor antigen; PI 3-kinase, phosphatidylinositol 3′-kinase; SH2 and SH3, *src* homology domains 2 and 3; WGA, wheat germ agglutinin.

†To whom reprint requests should be addressed.

addition of 13 μl (32 fmol) of activated (insulin stimulated and ATP phosphorylated) insulin receptor, allowed to proceed at 22°C for 5 min (final vol, 40 μl), and terminated by addition of 65 μl of 5% trichloroacetic acid. Incorporated phosphate was determined by a modification of the phosphocellulose adsorption method (19). High molecular weight species were removed by precipitation after incubation in the presence of 0.16% bovine serum albumin for 30 min at 4°C. Portions of each supernatant solution containing phosphorylated peptides were spotted onto 2-cm^2 pieces of P81 phosphocellulose paper (Whatman) and washed four times for 30 min each in 1.0 liter of 0.075 M phosphoric acid. The papers were rinsed in acetone and allowed to air dry; incorporated phosphate was determined by Cerenkov counting.

Kinetic Analyses. Values for ^{32}P incorporation into the peptide substrates (cpm) were converted to pmol/min rates (V) to facilitate direct comparisons between peptides; dividing each pmol/min value by 1.3×10^{-5} mg (the amount of WGA-purified protein) converts it to the corresponding pmol per min per mg of protein value. K_m and V_{max} values and the corresponding standard errors were determined with the assistance of the ENZYME program (20), which follows algorithms for appropriate weighting of data described by Cleland (21); each peptide was analyzed in two to five separate experiments (see Table 2). The amount of insulin receptor in the WGA-purified protein isolated from human insulin receptor construct-transfected CHO cells, estimated by [^{125}I]insulin binding and Scatchard analyses using the LIGAND program (22), was 25 nmol/mg (range, 10–40 nmol/mg), which corresponds to 1% of the lectin-bound protein. This value was used to determine turnover rates (k_{cat}) and catalytic efficiency (k_{cat}/K_m).

RESULTS

Peptide Design. Peptides corresponding to sequences of IRS-1 surrounding tyrosine residues were synthesized. All consensus sites for tyrosine phosphorylation within YMXM motifs were prepared, as were additional consensus sequences not found in YMXM motifs (Table 1). Each peptide was designed to include (*i*) the specificity residue Y, (*ii*) acidic residues N-terminal to Y, (*iii*) residues at Y + 1 to Y + 5 positions, including the entire YMXMSP sequence, when appropriate, and (*iv*) as many native basic residues as possible, up to a total of three. If sufficient basic residues were not present within the native sequence, lysine residues were added at the C or N termini to a total of three to guarantee adsorption to the phosphocellulose paper used in the phosphopeptide assay (23). Therefore, peptides varied in length (10–18 residues) and position of the tyrosine residue.

Each peptide contains only one tyrosine with the exception of Y46,‡ which contains two side-by-side tyrosines flanked by glutamic acid residues (Table 1). Peptides Y460 and Y546 contain YXXM motifs in which the Y + 1 position is isoleucine or threonine, respectively, with acidic residues at appropriate positions relative to Y (Table 1). Peptides Y608, Y628, Y658, Y727, Y939, and Y987 each contain complete YMXM motifs with at least one acidic residue N-terminal to Y (Table 1). A final peptide, Y998, contains a single tyrosine residue that is neither in a YMXM motif nor adjacent to an N-terminal acidic residue; like four of the YMXM peptides, however, it does contain a serine and proline at the Y + 4 and Y + 5 positions (Table 1).

‡Peptides are named according to the position of tyrosine in the sequence of IRS-1 (e.g., a peptide corresponding to the sequence surrounding Y^{987} is called Y987); an analogue of Y^{987} in which methionine at the +1 position is mutated to threonine is called Y987(M988T). Peptide sequences are listed in Table 1.

Table 1. Synthetic peptides corresponding to native and modified sequences of IRS-1

Position/name	Sequence
Double tyrosine	
Y46	RLE**YY**ENEKK
YXXM motifs	
Y460	*K*RGEEELSN**YI**C**M**GGK
Y546	*KK*VSIEE**YT**E**M**MPA*K*
YMXM motifs	
Y608	*KK*HTDDG**YM**P**M**SPGVA
Y628	RKGNGDG**YM**P**M**SPKSV
Y658	*KK*RVDPNG**YM**M**M**SPSGS
Y727	*KKK*LPA*T*GD**YM**N**M**SPVGD
Y939	*KK*GSEE**YM**N**M**DLGPGR
Y987	*KK*SRGD**YM**T**M**QIG
Nonspecific sequence	
Y998	*K*PRNS**Y**VDT**SP**VAP*K*
Modified Y987 sequences	
Y987(D986N)	*KK*SRG*N***YM**T**M**QIG
Y987(M988I)	*KK*SRGD**YI**T**M**QIG
Y987(M988T)	*KK*SRGD**YT**T**M**QIG
Y987(M988Nle)	*KK*SRGD**Y***ŧ***T**M**Q**IG
Y987(M990T)	*KK*SRGD**YM**T**T**QIG

Phosphorylated tyrosines are boldface and underlined, as are additional elements of the YMXM specificity motif. Non-native residues are in italics; basic residues were added for assay purposes and there is a cysteine to alanine substitution for peptide Y727. For modified Y987 sequences, substituted positions are italicized.
†Norleucine.

Additional analogues of Y987 (a low K_m substrate with a complete YMXM motif) were prepared to test the functional importance of residues surrounding the targeted tyrosine (Table 1). To determine directly the effect of isoleucine or threonine in place of methionine at the Y + 1 position, as occurs naturally in sequences surrounding Y460 and Y546, these residues were substituted into the sequence of Y987. In addition, norleucine, which is isomorphic with methionine, was substituted at the Y + 1 position to further test requirements for side-chain hydrophobicity and flexibility. The function of methionine at the Y + 3 position of Y987 was also tested by analogous substitution to threonine, and the requirement for an acidic residue (aspartic acid at Y − 1) was tested by a conservative substitution to asparagine.

Peptide Phosphorylations and Kinetic Analyses. All peptides (Table 1) were phosphorylated by the insulin-stimulated and autoactivated receptor kinase in a time- and temperature-dependent fashion and displayed saturable kinetics (Fig. 1 *A* and *C*), which yielded linear Lineweaver–Burk plots (Fig. 1 *B* and *D*). In every case, phosphorylation reactions were linear for at least 5 min (data not shown), validating conditions used for determinations of K_m and V_{max} values (Table 2). Rates of peptide phosphorylation (V_{max}) and peptide concentrations required for half-maximal saturation (K_m) varied dramatically between peptides (Fig. 1). The slopes of double reciprocal plots, which are proportional to K_m/V_{max} (the inverse of catalytic efficiency), clustered into two groups (Fig. 1 *B* and *D*). Notably, native sequences having entire YMXM motifs displayed the smallest slopes (Fig. 1*D*) and were therefore phosphorylated most efficiently. By contrast, YXXM peptides and other sequences not containing complete YMXM motifs all displayed steeper slopes (Fig. 1*B*), demonstrating that they were phosphorylated less efficiently.

Calculation of kinetic constants revealed that K_m values for YMXM peptides ranged from 24 to 92 μM, lower than values previously reported for any peptides used as exogenous substrates of the insulin receptor (Table 2). Values for V_{max}, which range from 0.9 to 1.7 pmol/min (69–131 nmol·min^{-1}·mg^{-1}), are difficult to compare to previous studies as

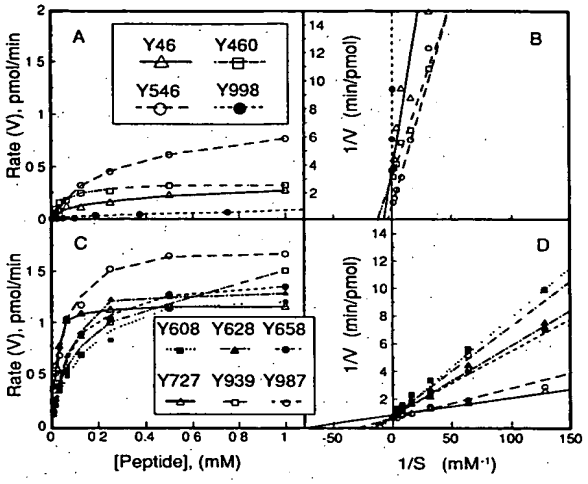

FIG. 1. Phosphorylation of peptides corresponding to native IRS-1 sequences by the insulin receptor kinase. Representative V vs. substrate concentration (A and C) and double reciprocal plots (B and D) are shown for phosphorylation of non-YMXM sequences (A and B) and YMXM sequences (C and D). Peptide sequences are identified in Table 1; methods used for phosphorylation reactions and data handling are described in *Experimental Procedures*.

this number varies with kinase specific activity. Values for k_{cat}/K_m, determined in this study, range from 0.6 to 2.1×10^4 $M^{-1}\cdot s^{-1}$. Therefore, in terms of substrate binding (estimated by K_m), turnover rates (k_{cat}), and overall catalytic efficiency (k_{cat}/K_m), all of the YMXM peptide sequences are excellent substrates of the insulin receptor kinase.

Similar analyses were performed with YXXM motifs (peptides Y460 and Y546; Table 1). Interestingly, K_m for peptide Y460 phosphorylation (isoleucine at the Y + 1 position) was 73 μM, within the range of values for YMXM peptides; this peptide was a less efficient substrate because V_{max} was 0.30 pmol/min, well below the range for YMXM peptides, which suggests that side-chain flexibility in addition to hydrophobicity at the Y + 1 position might be necessary for high turnover and catalytic efficiency. By contrast, the reduced catalytic efficiency of peptide Y546 (threonine at the Y + 1 position) was due to a high K_m for phosphorylation, which at 300 μM was substantially greater than corresponding values for YMXM peptides; in this case V_{max}, at 1.4 pmol/min, was similar to the YMXM peptides. Within a limited context, these results begin to suggest that the unique character of methionine (being flexible and hydrophobic) performs a special function in enhanced catalytic efficiency.

Table 2. Summary of kinetic constants

Peptide	K_m, μM	V_{max}, pmol/min	k_{cat}, s^{-1}	k_{cat}/K_m, $M^{-1}\cdot s^{-1}$
Double tyrosine				
Y46	140 ± 85	0.3 ± 0.06	0.14	1.0×10^3
YXXM motifs				
Y460	73 ± 15	0.3 ± 0.03	0.16	2.1×10^3
Y546	300 ± 30	1.4 ± 0.07	0.73	2.4×10^3
YMXM motifs				
Y608	90 ± 20	1.1 ± 0.09	0.57	6.2×10^3
Y628	60 ± 8	1.2 ± 0.06	0.63	1.0×10^4
Y658	86 ± 16	1.6 ± 0.12	0.83	9.7×10^3
Y727	24 ± 2.9	0.9 ± 0.06	0.47	2.0×10^4
Y939	61 ± 29	1.7 ± 0.3	0.89	1.5×10^4
Y987	34 ± 8.8	1.4 ± 0.11	0.73	2.1×10^4
Nonspecific sequence				
Y998	3200 ± 600	0.4 ± 0.04	0.21	6.5×10
Modified Y987 sequences				
Y987(D986N)	250 ± 69	3.9 ± 0.6	2.0	8.1×10^3
Y987(M988I)	80 ± 15	0.9 ± 0.07	0.47	5.9×10^3
Y987(M988T)	250 ± 80	2.7 ± 0.44	1.4	5.6×10^3
Y987(M988Nle)	24 ± 7.1	1.3 ± 0.12	0.68	2.8×10^4
Y987(M990T)	370 ± 110	1.2 ± 0.13	0.63	1.7×10^3

To test this more directly, the Y + 1 position within YMXM peptide Y987 was substituted with isoleucine, threonine, and norleucine (Table 1). In fact, both M988I and M988T substitutions reduced catalytic efficiency (k_{cat}/K_m) nearly 4-fold (Fig. 2B, compare slopes); the reasons for reduced efficiency were different for the two peptides, however. The M988I substitution increased K_m 2- to 3-fold and reduced V_{max} nearly 2-fold (Table 2). By contrast, the M988T substitution increased both K_m (7- to 8-fold) and V_{max} (2-fold). Thus, in a single, defined YMXM sequence M988I and M988T substitutions have the same general effect as observed for the YXXM peptides (Y460 and Y546). Substitution of methionine with norleucine, whose side chain mimics that of methionine regarding both hydrophobicity and flexibility, had no observable effect on K_m, V_{max}, and k_{cat}/K_m (Fig. 2B; Table 2).

For further comparison, we substituted the Y + 3 methionine of peptide Y987 and the acidic residue N-terminal to tyrosine (Y − 1). Surprisingly, the M991T substitution had an effect even greater than the related Y + 1 substitutions (Fig. 2D), with a 12-fold reduction in catalytic efficiency (k_{cat}/K_m) resulting exclusively from an increase in K_m (Table 2). Therefore, methionine residues at Y + 1 and Y + 3 positions play a very special role in directing efficient catalysis by the insulin receptor kinase. Acidic residues, which exist near autophosphorylated tyrosines in the insulin receptor and other protein tyrosine kinases, are presumed to be important for intermolecular substrate recognition as well (23–27). The only acidic residue in the Y987 sequence was substituted with

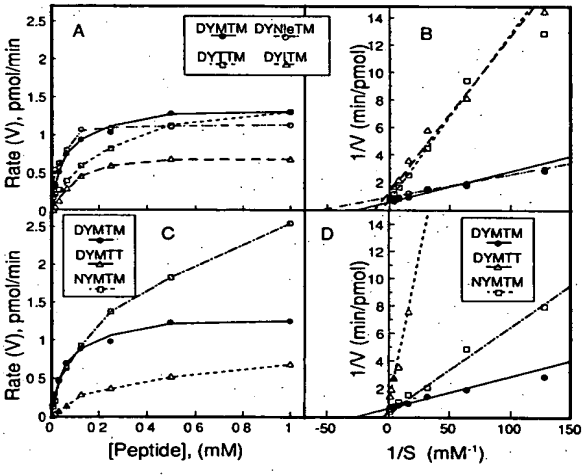

FIG. 2. Insulin receptor-catalyzed phosphorylation of substituted peptides corresponding to the IRS-1 sequence surrounding Y987. Representative V vs. substrate concentration (A and C) and double reciprocal plots (B and D) are shown for phosphorylation of peptides substituted at the Y + 1 position (A and B) or Y − 1 and Y + 3 positions (C and D). Peptide sequences are identified in Table 1; methods used for phosphorylation reactions and data handling are described in *Experimental Procedures*.

asparagine to assess the isolated effect of having no negative charge N-terminal to tyrosine (Fig. 2*D*). K_m was increased 8-fold while V_{max} was increased nearly 3-fold. These changes caused a net 2.5-fold reduction in catalytic efficiency (k_{cat}/K_m). Surprisingly, this is less deleterious than the corresponding effects observed for substituting methionine residues at either Y + 1 or Y + 3 positions (Table 2).

Two additional peptides corresponding to IRS-1 sequences not associated with YXXM or YMXM motifs were studied for comparison. Y46 contains a paired YY sequence flanked by acidic residues (EYYENE), resembling to a degree the major phosphorylation site of the insulin receptor itself (DIYETDYY) (28–30). The K_m for peptide Y46 phosphorylation was 134 μM, higher than that observed for YMXM peptides (Table 2), and V_{max} was 3- to 4-fold lower. Therefore, although Y46 can be considered to be a good substrate of the insulin receptor, it was phosphorylated with lower efficiency (6- to 36-fold) than YMXM peptides. Peptide Y998, which contains serine and proline at the Y + 4 and Y + 5 positions but lacks an acidic residue and methionine altogether, has a K_m for phosphorylation that is markedly elevated (3.2 mM). In addition, V_{max} is reduced (0.4 pmol/min) so k_{cat}/K_m is dramatically reduced (65 $M^{-1}\cdot s^{-1}$), which demonstrates the importance of primary sequence in directing insulin receptor kinase action and suggests that the effects of acidic residues N-terminal to tyrosine and methionine residues at Y + 1 and Y + 3 positions are cumulative.

DISCUSSION

Unlike serine/threonine-protein kinases, whose substrate recognition sequences are well defined by basic residues neighboring the phosphate acceptor (31–33), recognition sequences for substrates of protein tyrosine kinases are not well characterized. Autophosphorylated tyrosines within protein tyrosine kinase sequences are frequently located near acidic residues, which has led most investigators to focus on these positions as consensus sequences for tyrosine phosphorylation (23–27, 34–37). Synthetic peptides corresponding to autophosphorylation sites are phosphorylated by tyrosine kinases with K_m values typically in the millimolar range, which is considerably higher than values obtained for peptide substrates of serine/threonine kinases (23–27, 31–37). Unrelated peptides such as angiotensin and gastrin analogues are also phosphorylated by protein tyrosine kinases. Angiotensins I and II (both containing the DRVY*IHPF sequence) are phosphorylated with K_m values in the 1–4 mM range (26, 34), while gastrin analogues having five sequential glutamates N-terminal to tyrosine are phosphorylated with K_m values in the 50–200 μM range (35, 36). In fact, of all synthetic peptides studied previously as tyrosine kinase substrates, gastrin had the lowest K_m, a fact supporting the notion that acidic residues are important for tyrosine phosphorylation. However, systematic studies to define substrate specificity showed that when acidic residues of various peptides were replaced by uncharged amino acids, effects on V_{max}/K_m were often relatively small (2- to 4-fold) (23–27, 34–37).

The insulin receptor has tyrosine kinase activity similar to that of the viral transforming proteins, their cellular counterparts, and growth factor receptors. The insulin receptor phosphorylates the src peptide and angiotensin with K_m values in the millimolar range (26) and, in addition, phosphorylates a peptide corresponding to its own major autophosphorylation site (residues 1154–1164) (28–30) with a K_m value of 0.2–0.3 mM (18, 23, 30, 37). While the sequence at residues 1154–1164 might be a preferred substrate sequence, it was the recent identification of an endogenous substrate that allowed us to test sequences that might direct intermolecular substrate recognition. Finding biologically important sites of substrate phosphorylation will facilitate testing the importance of elements of secondary or tertiary structure in addition to that of primary sequence. For the insulin receptor, IRS-1 may be such a substrate. IRS-1 is a component of pp185 that is immunoprecipitated from insulin-stimulated cells by anti-phosphotyrosine antibodies. IRS-1 is phosphorylated on tyrosine residues in response to insulin (5–7) and appears to link the receptor to other components of the intracellular signaling cascade (e.g., PI 3-kinase; ref. 7).

As yet, we do not know which of the 34 tyrosine residues in IRS-1 are actually phosphorylated, although 14 have acidic residues N-terminal to the tyrosine position, which would categorize them as conventional consensus sequences for tyrosine kinase recognition. Surprisingly, 6 of these are within YMXM motifs and 2 more are in YXXM sequences, which previous studies (8–10, 38) suggest are important for interactions with PI 3-kinase and other proteins having SH2 domains. In this report, we show that synthetic peptides corresponding to IRS-1 YMXM sequences are excellent substrates for the insulin receptor kinase. In fact, calculated values of K_m are lower than has been reported previously for peptides phosphorylated by any tyrosine kinase, with the exception of epidermal growth factor receptor-catalyzed phosphorylation of gastrin (which contains the homologous EEEEEAYGWM sequence; refs. 35 and 36).

Amino acid substitution studies show that different positions within the YMXM motif effect catalytic efficiency. Substitutions of methionine at Y + 1 decrease catalytic efficiency for tyrosine phosphorylation ≈4-fold, estimated by (*i*) comparisons of k_{cat}/K_m for peptides Y460 and Y546 (YXXM motifs) and the six YMXM peptides, and (*ii*) direct comparisons between k_{cat}/K_m for the wild-type Y987 sequence and substituted peptides Y987(M988I) and Y987(M988T). Notably, norleucine and methionine at the Y + 1 position are functionally indistinguishable. Substitution of methionine at Y + 3 with threonine has an even greater effect on peptide Y987 phosphorylation, in this case reducing k_{cat}/K_m ≈12-fold due to an effect on K_m. Both of these effects are greater than that produced by substituting aspartic acid with asparagine at Y − 1 of peptide Y987 (≈2.5-fold reduction in k_{cat}/K_m). Sequences having neither N-terminal acidic residues nor methionine at Y + 1 and Y + 3 positions are phosphorylated much less efficiently. We do not know the significance of residues at the Y + 2 position (proline, methionine, asparagine, or threonine in the YMXM sequences studied here). Four of the six YMXM sequences of IRS-1 also have serine and proline at the Y + 4 and Y + 5 positions, although peptides with or without the YMXMSP residues are phosphorylated with equal efficiency. Furthermore, the Y998 sequence contains serine and proline at the Y + 4 and Y + 5 positions but without an acidic residue or methionine phosphorylation was inefficient. The function (if any) served by these residues appears not to be related to phosphorylation.

What, if anything, is special about Y + 1 and Y + 3 positions, and why does methionine at these positions enhance kinetic efficiency? Sequences directly contiguous to and including YMXM are predicted by the Chou–Fasman algorithm (41) to be unstructured, although β-turns are predicted to flank each of the YMXM motifs of IRS-1 (data not shown). Alternatively, it has been proposed that substrates might adopt amphiphilic helical structures at the kinase catalytic surface (42); if so, methionine residues at Y + 1 and Y + 3 positions might be positioned appropriately for direct participation in binding. While we have not yet been able to analyze structure, the unique character of methionine may play a special role here. Isoleucine, leucine, and valine, while also highly hydrophobic, have branched and thus relatively rigid side chains. By contrast, the side chain of methionine is unbranched, providing considerable structural flexibility. In support of this, norleucine, which is equally flexible and hydrophobic compared to methionine, has an identical capacity to direct insulin receptor kinase action. This feature of methionine has recently

been proposed to provide a malleable nonpolar surface for signal peptide recognition (43) and plasticity in protein interactions with calmodulin (39), which would allow structurally diverse nonpolar surfaces to conform to the respective recognition surfaces of the proteins to which they bind (40). Such a malleable, nonpolar surface might provide a mechanism to explain how the same IRS-1 YMXM motifs interact with the insulin receptor kinase and PI 3-kinase and, potentially, other tyrosine kinases and proteins with SH2 domains as well. The side chains of residues in the YMXM domain might be sufficiently flexible to provide a nonpolar surface that accommodates itself equally to the surfaces of kinase active sites and SH2 protein binding pockets.

Relationships between IRS-1 and other signal transduction proteins may be quite complex, as IRS-1 contains multiple copies of the YMXM motif that could interact selectively with different tyrosine kinases as well as distinct effector molecules containing various isoforms of the SH2/SH3 domain. Furthermore, other proteins involved in signal transduction contain related sequences. The PDGF receptor phosphorylates itself within YMXM or YVXM motifs (44), the src-associated middle T antigen contains a phosphorylated EEEEEEYMPM sequence (8, 45), and similar sequences within the colony-stimulating factor 1 receptor (DTYVEM) and *kit* oncogene (DSTNEYMDM) may be phosphorylated, as well (8). Whether YMXM motifs define a recognition sequence for efficient tyrosine phosphorylation by these and other protein tyrosine kinases remains to be tested. For the src-associated middle T antigen and the PDGF receptor, these sequences are thought to be involved in recognition by PI 3-kinase through interaction with one or the other of its SH2 domains (8, 9, 38, 44). Similarly, studies to block interactions between IRS-1 and PI 3-kinase with synthetic phosphopeptides corresponding to IRS-1 YMXM sequences suggest that these interactions involve SH2 domains as well (unpublished data).

In conclusion, YMXM, a redundant sequence motif identified in IRS-1, is shown to define substrate specificity of the insulin receptor kinase. Methionine residues at the Y + 1 and Y + 3 positions are particularly important for efficient kinase recognition, in addition to acidic residues N-terminal to tyrosine. Knowing a target motif for the action of the insulin receptor kinases, and possibly other tyrosine kinases as well, may enhance our understanding of tyrosine kinase signaling pathways. Furthermore, a tyrosine kinase target motif may facilitate identification of additional known or newly identified proteins that might be involved in related signaling pathways. Certainly, as genomic sequencing efforts progress, it will be increasingly useful to have identified short peptide motifs to help decipher which of these DNA sequences encodes proteins acting as potential targets of tyrosine kinase action.

This work was supported in part by the National Science Foundation (S.E.S.), National Institutes of Health (M.F.W.), and Diabetes and Endocrinology Research Center Grant DK08366. S.C. is supported by a Fellowship from the Juvenile Diabetes Foundation; S.E.S. is a Capps' Scholar in Diabetes at Harvard Medical School and the recipient of a Career Development Award from the Juvenile Diabetes Foundation.

1. Kasuga, M., Zick, Y., Blithe, D. L., Crettaz, M. & Kahn, C. R. (1982) *Nature (London)* **298**, 667–669.
2. Kasuga, M., Karlsson, F. A. & Kahn, C. R. (1982) *Science* **215**, 185–187.
3. Rosen, O. M., Herrera, R., Olowe, Y., Petruzzelli, L. M. & Cobb, M. H. (1983) *Proc. Natl. Acad. Sci. USA* **80**, 3237–3240.
4. Yu, K. & Czech, M. P. (1984) *J. Biol. Chem.* **259**, 5277–5286.
5. White, M. F., Maron, R. & Kahn, C. R. (1985) *Nature (London)* **318**, 183–186.
6. Rothenberg, P. L., Lane, W. S., Karasik, A., Backer, J. M., White, M. F. & Kahn, C. R. (1991) *J. Biol. Chem.* **266**, 8302–8311.
7. Sun, X. J., Rothenberg, P., Kahn, C. R., Backer, J. M., Araki, E., Wilden, P. A., Cahill, D. A., Goldstein, B. J. & White, M. F. (1991) *Nature (London)* **352**, 73–77.
8. Cantley, L. C., Auger, K. R., Carpenter, C., Duckworth, B., Graziani, A., Kapeller, R. & Soltoff, S. (1991) *Cell* **64**, 281–302.
9. Escobedo, J. A., Kaplan, D. R., Kavanaugh, W. M., Turck, C. W. & Williams, L. T. (1991) *Mol. Cell. Biol.* **11**, 1125–1132.
10. Koch, C. A., Anderson, D., Moran, M. F., Ellis, C. & Pawson, T. (1991) *Science* **252**, 668–674.
11. Moran, M. F., Koch, C. A., Anderson, D., Ellis, C., England, L., Martin, G. S. & Pawson, T. (1990) *Proc. Natl. Acad. Sci. USA* **87**, 8622–8626.
12. Ruderman, N. B., Kapeller, R., White, M. F. & Cantley, L. C. (1990) *Proc. Natl. Acad. Sci. USA* **87**, 1411–1415.
13. Edemann, G., Yohezawa, K. & Roth, R. A. (1990) *J. Biol. Chem.* **265**, 396–400.
14. Tam, J. P. & Merrifield, R. B. (1987) in *The Peptides: Analysis, Synthesis, Biology*, eds. Udenfriend, S. & Meienhofer, J. (Academic, New York), pp. 185–248.
15. Ebina, Y., Edery, M., Ellis, L., Beaudoin, J., Roth, R. A. & Rutter, W. J. (1985) *Proc. Natl. Acad. Sci. USA* **82**, 8014–8018.
16. Shymko, R. M., Gonzales, N. S., Backer, J. M., White, M. F. & De Meyts, P. (1989) *Biochem. Biophys. Res. Commun.* **164**, 191–198.
17. Shoelson, S. E., Lu, Z., Parlautan, L., Lynch, C. S. & Weiss, M. A. (1992) *Biochemistry*, in press.
18. Shoelson, S. E., White, M. F. & Kahn, C. R. (1988) *J. Biol. Chem.* **263**, 4852–4860.
19. Glass, D. B., Masaracchia, R. A., Feramisco, J. R. & Kemp, B. E. (1978) *Biochem. J.* **87**, 566–575.
20. Lutz, R. A., Bull, C. & Rodbard, D. (1986) *Enzyme* **36**, 197–206.
21. Cleland, W. W. (1979) *Methods Enzymol.* **63**, 103–138.
22. Munson, P. J. & Rodbard, D. (1980) *Anal. Biochem.* **107**, 220–239.
23. Stadtmauer, L. A. & Rosen, O. M. (1986) *J. Biol. Chem.* **261**, 10000–10005.
24. Hunter, T. (1982) *J. Biol. Chem.* **257**, 4843–4848.
25. Patschinsky, T., Hunter, T., Esch, F. S., Cooper, J. A. & Sefton, B. M. (1982) *Proc. Natl. Acad. Sci. USA* **79**, 973–977.
26. Stadtmauer, L. A. & Rosen, O. M. (1983) *J. Biol. Chem.* **258**, 6682–6685.
27. Geahlen, R. L. & Harrison, M. L. (1989) in *Peptides and Protein Phosphorylation*, ed. Kemp, B. E. (CRC, Boca Raton, FL), pp. 239–250.
28. Ebina, Y., Ellis, L., Jarnagin, K., Edery, M., Graf, L., Clauser, E., Ou, J.-H., Masiarz, F., Kan, Y. W., Goldfine, I. D., Roth, R. A., & Rutter, W. J. (1985) *Cell* **40**, 747–758.
29. Ullrich, A., Bell, J. R., Chen, E. Y., Herrera, R., Petruzzelli, L. M., Dull, T. J., Gray, A., Coussens, L., Liao, Y.-C., Tsubokawa, M., Mason, A., Seeburg, P. H., Grunfeld, C., Rosen, O. M. & Ramachandran, J. (1985) *Nature (London)* **313**, 756–761.
30. White, M. F., Shoelson, S. E., Keutmann, H. & Kahn, C. R. (1988) *J. Biol. Chem.* **263**, 2969–2980.
31. Kemp, B. E. & Pearson, R. B. (1990) *Trends Biochem. Sci.* **15**, 342–346.
32. Kemp, B. E., ed. (1990) *Peptides and Protein Phosphorylation* (CRC, Boca Raton, FL).
33. Kennely, P. J. & Krebs, E. G. (1991) *J. Biol. Chem.* **266**, 15555–15558.
34. Wong, T. W. & Goldberg, A. R. (1983) *J. Biol. Chem.* **258**, 1022–1025.
35. Baldwin, G. S., Burgess, A. W. & Kemp, B. E. (1982) *Biochem. Biophys. Res. Commun.* **109**, 656–662.
36. Baldwin, G. S., Knesel, J. & Monckton, J. M. (1983) *Nature (London)* **301**, 435–438.
37. Shoelson, S. E., White, M. F. & Kahn, C. R. (1989) *J. Biol. Chem.* **264**, 7831–7836.
38. Auger, K. R., Carpenter, C. L., Shoelson, S. E., Piwnica-Worms, H. & Cantley, L. C. (1992) *J. Biol. Chem.*, in press.
39. O'Neil, K. T. & DeGrado, W. F. (1990) *Trends Biochem. Sci.* **15**, 59–64.
40. Gellman, S. H. (1991) *Biochemistry* **30**, 6633–6636.
41. Fasman, G., ed. (1989) *Prediction of Protein Structure and the Principles of Protein Conformation* (Plenum, New York).
42. Radziejewski, C., Miller, W. T., Mobashery, S., Goldberg, A. R. & Kaiser, E. T. (1989) *Biochemistry* **28**, 9047–9052.
43. Bernstein, H. D., Poritz, M. A., Strub, K., Hoben, P. J., Brenner, S. & Walter, P. (1989) *Nature (London)* **340**, 482–486.
44. Escobedo, J. A., Navankasattusas, S., Kavanaugh, W. M., Milfay, D., Fried, V. A. & Williams, L. T. (1991) *Cell* **65**, 75–82.
45. Hunter, T., Hutchinson, M. A. & Eckhart, W. (1984) *EMBO J.* **3**, 73–79.

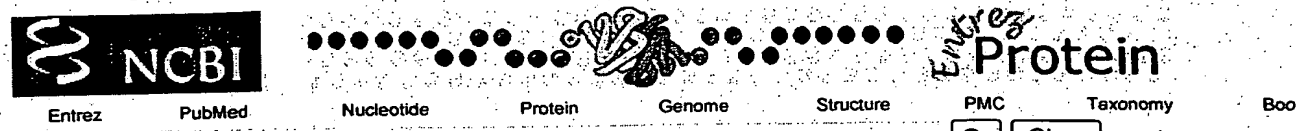


```
LOCUS       NP_080954                 295 aa            linear   ROD 22-DEC-2003
DEFINITION  biliverdin reductase A [Mus musculus].
ACCESSION   NP_080954
VERSION     NP_080954.3  GI:31982541
DBSOURCE    REFSEQ: accession NM_026678.3
KEYWORDS    .
SOURCE      Mus musculus (house mouse)
  ORGANISM  Mus musculus
            Eukaryota; Metazoa; Chordata; Craniata; Vertebrata; Euteleostomi;
            Mammalia; Eutheria; Rodentia; Sciurognathi; Muridae; Murinae; Mus.
REFERENCE   1  (residues 1 to 295)
  AUTHORS   Whitby,F.G., Phillips,J.D., Hill,C.P., McCoubrey,W. and Maines,M.D.
  TITLE     Crystal structure of a biliverdin IXalpha reductase enzyme-cofactor
            complex
  JOURNAL   J. Mol. Biol. 319 (5), 1199-1210 (2002)
   PUBMED   12079357
COMMENT     PROVISIONAL REFSEQ: This record has not yet been subject to final
            NCBI review. The reference sequence was derived from BC052146.1.
            On Jun 19, 2003 this sequence version replaced gi:27764877.
FEATURES             Location/Qualifiers
     source          1..295
                     /organism="Mus musculus"
                     /db_xref="taxon:10090"
                     /chromosome="2"
                     /map="2 62.0 cM"
     Protein         1..295
                     /product="biliverdin reductase A"
     Region          <55..119
                     /region_name="Oxidoreductase family, NAD-binding Rossmann
                     fold"
                     /note="GFO_IDH_MocA"
                     /db_xref="CDD:6445"
     CDS             1..295
                     /gene="Blvra"
                     /coded_by="NM_026678.3:182..1069"
                     /note="go_component: soluble fraction [goid 0005625]
                     [evidence ISS] [pmid 12079357];
                     go_function: nucleotide binding [goid 0000166] [evidence
                     ISS] [pmid 12079357];
                     go_function: biliverdin reductase activity [goid 0004074]
                     [evidence ISS] [pmid 12466851];
                     go_process: heme catabolism [goid 0042167] [evidence ISS]
                     [pmid 12079357]"
                     /db_xref="GeneID:109778"
                     /db_xref="LocusID:109778"
                     /db_xref="MGI:88170"
ORIGIN
        1 mstepkrkfg vvvvgvgrag svrirdskdp hssaflnlig yvsrrelgsl dnvrqisled
       61 alrsqevdva yictessshe dyirqflqag khvlveypma lsfaaaqelw elaaqkgrvl
      121 heehiellme efeflkreva gkellkgslr ftaspleeek fgfpafsgis rltwlvslfg
      181 elslisatme nrkedqymkm tvqletqnks plswieekgp glkrnrhisi hfksgsleev
      241 pnvgvnknif lkdqdifiqk llgqvsaedl aaekkrilhc lelasdiqrl chrkq
```

Jan 29 2004 15:38:25

Pig Biliverdin Reductase Sequence Cloned By Maines Lab

```
ATG AAT GCA GAG CCC GAG AGG AAG TTT GGC GTG GTG GTG GTT GGT GTT GGC CGA GCC GGC TCC
  M   N   A   E   P   E   R   K   F   G   V   V   V   V   G   V   G   R   A   G   S
GTG CGG ATG AGG GAC TTG CGG AAT CCA CAC CCT TCC TCA GCG TTC CTG AAC CTG ATT GGC TTC
  V   R   M   R   D   L   R   N   P   H   P   S   S   A   F   L   N   L   I   G   F
GTG TCG AGA AGG GAG CTC GGG AGC ATT GAT GGA GTC CAG CAG ATT TCT TTG GAG GAT GCT CTT
  V   S   R   R   E   L   G   S   I   D   G   V   Q   Q   I   S   L   E   D   A   L
TCC AGC CAA GAG GTG GAG GTC GCC TAT ATC TGC AGT GAG AGC TCC AGC CAT GAG GAC TAC ATC
  S   S   Q   E   V   E   V   A   Y   I   C   S   E   S   S   S   H   E   D   Y   I
AGG CAG TTC CTT AAT GCT GGC AAG CAC GTC CTT GTG GAA TAC CCC ATG ACA CTG TCA TTG GCG
  R   Q   F   L   N   A   G   K   H   V   L   V   E   Y   P   M   T   L   S   L   A
GCC GCT CAG GAA CTG TGG GAG CTG GCT GAG CAG AAA GGA AAA GTC TTG CAC GAG GAG CAT GTT
  A   A   Q   E   L   W   E   L   A   E   Q   K   G   K   V   L   H   E   E   H   V
GAA CTC TTG ATG GAG GAA TTC GCT TTC CTG AAA AAA GAA GTG GTG GGG AAA GAC CTG CTG AAA
  E   L   L   M   E   E   F   A   F   L   K   K   E   V   V   G   K   D   L   L   K
GGG TCG CTC CTC TTC ACA GCT GGC CCG TTG GAA GAA GAG CGG TTT GGC TCC CCT GCA TTC AGC
  G   S   L   L   F   T   A   G   P   L   E   E   E   R   F   G   S   P   A   F   S
GGC ATC TCT CGC CTG ACC TGG CTG GTC TCC CTC TTT GGG GAG CTT TCT CTT GTG TCT GCC ACT
  G   I   S   R   L   T   W   L   V   S   L   F   G   E   L   S   L   V   S   A   T
TTG GAA GAG CGA AAG GAA GAT CAG TAT ATG AAA ATG ACA GTG TGT CTG GAG ACA GAG AAG AAA
  L   E   E   R   K   E   D   Q   Y   M   K   M   T   V   C   L   E   T   E   K   K
AGT CCA CTG TCA TGG ATT GAA GAA AAA GGA CCT GGT CTA AAA CGA AAC AGA TAT TTA AGC TTC
  S   P   L   S   W   I   E   E   K   G   P   G   L   K   R   N   R   Y   L   S   F
CAT TTC AAG TCT GGG TCC TTG GAG AAT GTG CCA AAC GTA GGA GTG AAT AAG AAC ATA TTT CTG
  H   F   K   S   G   S   L   E   N   V   P   N   V   G   V   N   K   N   I   F   L
AAA GAT CAA AAT ATA TTT GTC CAG AAA CTC TTG GGC CAG TTC TCT GAG AAG GAA CTG GCT GCT
  K   D   Q   N   I   F   V   Q   K   L   L   G   Q   F   S   E   K   E   L   A   A
GAA AAG AAA CGC ATC CTG CAC TGC CTG GGG CTT GCA GAA GAA ATC CAG AAA TAT TGC TGT TCA
  E   K   K   R   I   L   H   C   L   G   L   A   E   E   I   Q   K   Y   C   C   S
AGG AAG TAA
  R   K   .
```

```
CLUSTAL W (1.82) Multiple Sequence Alignments

Sequence format is Pearson
Sequence 1: Human_BVR       296 aa
Sequence 2: Rat_BVR         295 aa
Sequence 3: Mouse_BVR       295 aa
Sequence 4: Pig_BVR         296 aa
Start of Pairwise alignments Aligning...
Sequences (1:2) Aligned. Score:  82
Sequences (1:3) Aligned. Score:  81
Sequences (1:4) Aligned. Score:  98
Sequences (2:3) Aligned. Score:  88
Sequences (2:4) Aligned. Score:  83
Sequences (3:4) Aligned. Score:  82
Start of Multiple Alignment
There are 3 groups Aligning...
Group 1: Sequences:   2      Score:6353
Group 2: Sequences:   2      Score:6075
Group 3: Sequences:   4      Score:5825
Alignment Score 9407

CLUSTAL W (1.82) multiple sequence alignment


Human_BVR       MNAEPERKFGVVVVGVGRAGSVRMRDLRNPHPSSAFLNLIGFVSRRELGSIDGVQQISLE 60
Pig_BVR         MNAEPERKFGVVVVGVGRAGSVRMRDLRNPHPSSAFLNLIGFVSRRELGSIDGVQQISLE 60
Rat_BVR         MDAEPKRKFGVVVVGVGRAGSVRLRDLKDPR-SAAFLNLIGFVSRRELGSLDEVRQISLE 59
Mouse_BVR       MSTEPKRKFGVVVVGVGRAGSVRIRDSKDPH-SSAFLNLIGYVSRRELGSLDNVRQISLE 59
                *.:**:******************:** ::*: *:*******:********:* *:*****

Human_BVR       DALSSQEVEVAYICSESSSHEDYIRQFLNAGKHVLVEYPMTLSLAAAQELWELAEQKGKV 120
Pig_BVR         DALSSQEVEVAYICSESSSHEDYIRQFLNAGKHVLVEYPMTLSLAAAQELWELAEQKGKV 120
Rat_BVR         DALRSQEIDVAYICSESSSHEDYIRQFLQAGKHVLVEYPMTLSFAAAQELWELAAQKGRV 119
Mouse_BVR       DALRSQEVDVAYICTESSSHEDYIRQFLQAGKHVLVEYPMALSFAAAQELWELAAQKGRV 119
                *** ***::*****:*************:***********:**:********** ***:*

Human_BVR       LHEEHVELLMEEFAFLKKEVVGKDLLKGSLLFTSDPLEEDRFGFPAFSGISRLTWLVSLF 180
Pig_BVR         LHEEHVELLMEEFAFLKKEVVGKDLLKGSLLFTAGPLEEERFGSPAFSGISRLTWLVSLF 180
Rat_BVR         LHEEHVELLMEEFEFLRREVLGKELLKGSLRFTASPLEEERFGFPAFSGISRLTWLVSLF 179
Mouse_BVR       LHEEHIELLMEEFEFLKREVAGKELLKGSLRFTASPLEEEKFGFPAFSGISRLTWLVSLF 179
                *****:******* **::** **:****** **:.****::** ****************

Human_BVR       GELSLVSATLEERKEDQYMKMTVCLETEKKSPLSWIEEKGPGLKRNRYLSFHFKSGSLEN 240
Pig_BVR         GELSLVSATLEERKEDQYMKMTVCLETEKKSPLSWIEEKGPGLKRNRYLSFHFKSGSLEN 240
Rat_BVR         GELSLISATLEERKEDQYMKMTVQLETQNKGLLSWIEEKGPGLKRNRYVNFQFTSGSLEE 239
Mouse_BVR       GELSLISATMENRKEDQYMKMTVQLETQNKSPLSWIEEKGPGLKRNRHISIHFKSGSLEE 239
                *****:***:*:*********** ***::*. ***************::.::*.*****:

Human_BVR       VPNVGVNKNIFLKDQNIFVQKLLGQFSEKELAAEKKRILHCLGLAEEIQKYCCSRK 296
Pig_BVR         VPNVGVNKNIFLKDQNIFVQKLLGQFSEKELAAEKKRILHCLGLAEEIQKYCCSRK 296
Rat_BVR         VPSVGVNKNIFLKDQDIFVQKLLDQVSAEDLAAEKKRIMHCLGLASDIQKLCHQKK 295
Mouse_BVR       VPNVGVNKNIFLKDQDIFIQKLLGQVSAEDLAAEKKRILHCLELASDIQRLCHRKQ 295
                **.************:**:****.*.* ::********:*** **.:**: *  ::
```

J. Biochem. 86, 833–848 (1979)

Purification and Properties of Biliverdin Reductases from Pig Spleen and Rat Liver[1]

Masato NOGUCHI, Tadashi YOSHIDA, and Goro KIKUCHI

Department of Biochemistry, Tohoku University School of Medicine, Sendai, Miyagi 980

Received for publication, March 14, 1979

Biliverdin reductase was purified from pig spleen soluble fraction to a purity of more than 90% as judged by sodium dodecyl sulfate-polyacrylamide gel electrophoresis. The enzyme was a monomer protein with a molecular weight of about 34,000. Its isoelectric point was at 6.1–6.2. The enzyme was strictly specific to biliverdin and no other oxidoreductase activities could be detected in the purified enzyme preparation. The purified enzyme could utilize both NADPH and NADH as electron donors for the reduction of biliverdin. However, there were considerable differences in the kinetic properties of the NADPH-dependent and the NADH-dependent biliverdin reductase activities: K_m for NADPH was below 5 μM while that for NADH was 1.5–2 mM; the pH optimum of the reaction with NADPH was 8.5 whereas that of the reaction with NADH was 6.9; K_m for biliverdin in the NADPH system was 0.3 μM whereas that in the NADH system was 1–2 μM. In addition, both the NADPH-dependent and NADH-dependent activities were inhibited by excess biliverdin, but this inhibition was far more pronounced in the NADPH system than in the NADH system. IXα-biliverdin was the most effective substrate among the four biliverdin isomers, and the dimethylester of IXα-biliverdin could not serve as a substrate. Biliverdin reductase was also purified about 300-fold from rat liver soluble fraction. The hepatic enzyme was also a monomer protein with a molecular weight of 34,000 and showed properties quite similar to those of the splenic enzyme as regards the biliverdin reductase reaction. The isoelectric point of the hepatic enzyme, however, was about 5.4. It was assumed that NADPH rather than NADH is the physiological electron donor in the intracellular reduction of IXα-biliverdin. The stimulatory effects of bovine and human serum albumins on the biliverdin reductase reactions were also examined.

Biliverdin is the final product of physiological heme degradation in mammalian tissues; this process is thought to be catalyzed by the microsomal heme oxygenase (*1–6*), and biliverdin is then reduced to bilirubin by biliverdin reductase [EC 1.3.1.24], consuming reduced pyridine nucleotides (*7*). Despite the importance of biliverdin reductase in linear tetrapyrrole metabolism, the molecular

[1] This work was supported in part by research grants from the Scientific Research Fund (Nos. 348177 and 238012) of the Ministry of Education, Science and Culture of Japan, and a grant from the Foundation for the Promotion of Research on Medicinal Resources, Japan.

and catalytic properties of this enzyme have not been well elucidated. In 1965 Singleton and Laster (*8*) obtained a 15-fold purified preparation of biliverdin reductase from guinea pig liver soluble fraction and reported that the enzyme was more active with NADH than NADPH. However, Tenhunen *et al.* (*9*) reported in 1970 that biliverdin reductase partially purified (52-fold) from rat liver soluble fraction had an absolute and stoichiometric requirement for NADPH. Subsequently Colleran and O'Carra (*10*, *11*) indicated that guinea pig liver extracts contained both NADH-dependent and NADPH-dependent activities and that these activities were due to a single enzyme system capable of utilizing both NADH and NADPH. They also found that biliverdin reductase was essentially specific to IXα-biliverdin; the IXβ- and IXδ-isomers were very poor substrates and the IXγ-isomer did not serve as a substrate. IXα-biliverdin reduction was markedly inhibited by excess biliverdin. These studies by Colleran and O'Carra provided information on the general features of the biliverdin reductase reaction. However, to clarify further the nature of biliverdin reductase as well as the properties of the reaction catalyzed by this enzyme, it is essential to have a highly purified preparation of this enzyme. Previous efforts to purify this enzyme have not been wholly successful.

In the present report, we describe the purification of biliverdin reductase, as well as the properties of the biliverdin reductase reaction catalyzed by the purified enzyme preparation.

MATERIALS AND METHODS

Materials—Fresh pig spleens used as a source of splenic biliverdin reductase were obtained at a local slaughterhouse. The hepatic biliverdin reductase was prepared from the livers of Wistar rats, 120–150 g body weight.

Reagents and biochemicals were obtained from the following sources: Sephadex G-100, Sephadex G-200, and QAE-Sephadex, from Pharmacia Fine Chemicals, Uppsala; CM-cellulose (CM-23) and DEAE-cellulose (DE-32), from Whatman Biochemicals, Maidstone; Wakogel B-10, Wakogel C-200, human serum albumin, from Wako Pure Chemical Industries, Osaka; crystalline bilirubin, chlorohemin, bovine serum albumin, FMN, yeast alcohol dehydrogenase, ovalbumin, and horse heart myoglobin, from Sigma Chemical Company, St. Louis; pig heart malate dehydrogenase, chymotrypsinogen A, ox liver catalase, and rabbit muscle lactate dehydrogenase, from Boehringer Mannheim-Yamanouchi, Tokyo; pyridine nucleotides, from Oriental Yeast Company, Tokyo; FAD, from Wakamoto Pharmaceutical Company, Tokyo; Ampholine, from LKB Produkter, Bromma. Other reagents were also obtained commercially. Hydroxyapatite was prepared according to the method described by Bernardi (*12*).

IXα-biliverdin was prepared by the oxidation of crystalline bilirubin with ferric chloride in boiling glacial acetic acid essentially according to the method described by Lemberg (*13*), and pure biliverdin-IXα was isolated from the mixture of oxidation products of bilirubin by silica gel column chromatography, instead of by crystallization. Namely, the amorphous powder of crude biliverdin obtained from 0.5 g of crystalline IXα-bilirubin by the procedures described by Lemberg was divided into two equal portions. Each portion was suspended in a small volume of pyridine (about 10 ml) and applied to a silica gel column (3.6×27 cm) (Wakogel C-200) in chloroform–acetic acid (97 : 3). On elution with the same solution, a small amount of bilirubin that remained unoxidized was eluted first, then unidentified brown and reddish purple pigments were eluted successively. When these pigments were completely eluted from the column, IXα-biliverdin (clear dark green color) was eluted with a slightly more polar eluant (chloroform–methanol–acetic acid, 92 : 5 : 3). Further elution with more polar eluants (chloroform–methanol–acetic acid, 77 : 20 : 3 and methanol–acetic acid, 97 : 3) yielded other unidentified greenish-brown and brown pigments. Of the fractions eluted with the second eluant, those which gave only one spot on analytical thin layer chromatography were collected. The analytical thin layer chromatography was carried out on 20×5 cm plates precoated with 0.25 mm layers of Wakogel B-10 activated at 150°C for 3 h. The pure biliverdin obtained above gave a single spot with an R_f value of 0.25–0.27 when developed with chloroform–methyl alcohol–acetic acid (94 : 5 : 1).

The biliverdin preparations obtained from the two silica gel columns were combined and the

solvent was evaporated off under reduced pressure at 30–40°C. The pigment was redissolved in 1% NaOH and precipitated by adding 1% acetic acid. The precipitate was collected by centrifugation, washed several times with distilled water to remove salts, then freeze-dried. The biliverdin powder obtained was stored at 4°C in the dark. From 0.5 g of crystalline bilirubin, 30–50 mg of pure IXα-biliverdin was usually obtained.

The purity of biliverdin prepared by this method was confirmed in various systems of analytical thin layer chromatography (*14–16*) and from the absorption spectrum, using crystalline IXα-biliverdin (kindly provided by Dr. McDonagh) and its dimethyl ester as standards. The pure biliverdin preparation showed two absorption maxima at 384 nm and 670 nm with millimolar extinction coefficients of 49.0 and 15.0, respectively, in potassium phosphate buffer (pH 7.4) (*cf.* Fig. 7).

For daily use, 2–3 mg of the purified biliverdin was dissolved in about 0.3 ml of 0.1 N KOH and diluted with 0.1 M potassium phosphate buffer (pH 7.4) to approximately 0.2 mM. The precise concentration of biliverdin in the solution was estimated on the basis of the absorbance at 670 nm.

Four biliverdin isomers were prepared from the products (verdohemochrome) of the coupled oxidation of pyridine hemin with ascorbic acid as the dimethyl esters, according to the procedure of Bonnet and McDonagh (*14*). Each isomer was further purified by thin layer chromatography according to the methods of O'Carra and Colleran (*15*). The dimethyl ester of each isomer was converted to the free acid by incubation with 1% KOH at 37°C for 2 h in the dark. The mixture was then neutralized with acetic acid and the acid form of biliverdin was extracted with chloroform. Chloroform was evaporated off and the pigment was dissolved in 0.1 N KOH, then diluted with 0.1 M potassium phosphate buffer (pH 7.4) as described above.

Estimation of Molecular Weight by Gel Filtration and by Sodium Dodecyl Sulfate (SDS)-Polyacrylamide Gel Electrophoresis—Estimation of the molecular weight of biliverdin reductase by gel filtration was performed according to the method of Andrews (*17*) with a column (2.5 × 100 cm) of Sephadex G-200 previously equilibrated with 50 mM potassium phosphate buffer (pH 7.4) and calibrated with the following proteins (molecular weights in parentheses): yeast alcohol dehydrogenase (150,000), pig heart malate dehydrogenase (67,000), ovalbumin (45,000), and chymotrypsinogen A (25,000). Electrophoresis on SDS-polyacrylamide gel was performed as described by Weber and Osborn (*18*). Calibration proteins and their molecular weights were: catalase (58,000), ovalbumin (45,000), lactate dehydrogenase (36,000), chymotrypsinogen A (25,000), and horse heart myoglobin (17,200). To assess the purity of the biliverdin reductase preparation, the gel was stained with Coomassie blue and the relative optical densities of the protein bands on the gel were measured with a Hitachi gel scanner, recording the difference in absorbances at 550 nm and 400 nm.

Determination of Protein—Protein was determined by the method of Lowry *et al.* (*19*), using bovine serum albumin as a standard.

Assay of Biliverdin Reductase Activity—The reaction was conducted in a cuvette placed in a constant temperature chamber at 37°C attached to a Hitachi 200-20 double-beam spectrophotometer, and the enzymic conversion of biliverdin to bilirubin was monitored in terms of the increase in absorbance at 468 nm. The standard assay mixture contained, in a final volume of 2 ml, 0.1 M potassium phosphate buffer (pH 7.4), 10 μM IXα-biliverdin, 1 mg/ml bovine serum albumin, 100 μM NADPH (or 2 mM NADH), and an appropriate amount of the enzyme preparation. The concentration of NADH used in the standard assay system was lower than the saturating concentration (K_m for NADH was 1.5–2.0 mM, as described later), but the NADH-dependent biliverdin reductase activity could be adequately detected at this NADH concentration. Reduced pyridine nucleotide was omitted in the reference cuvette. The reaction was started by the addition of reduced pyridine nucleotide, after preincubation for 5 min at 37°C. Formation of bilirubin was calculated by assuming that the difference in the millimolar extinction coefficients of bilirubin and biliverdin at 468 nm is 46.0: the millimolar extinction coefficients of bilirubin and biliverdin at 468 nm were 52.0 and 6.0, respectively, under the experimental conditions employed.

As shown in Fig. 1, however, the time course of the NADPH-dependent reaction displayed a sigmoidal curve, whereas the reaction with NADH did not. This was true for the reactions with

either the pig spleen enzyme or the rat liver enzyme. Therefore, to express the enzyme activity, we defined one unit of biliverdin reductase as the amount of the enzyme which catalyzed the reduction of half of 20 nmol of biliverdin in one min under the standard assay conditions; since the concentration of biliverdin in the standard reaction mixture was 10 μM, the enzyme units correspond to the reciprocals of the time in minutes required to obtain an increase of absorbance of 0.23 at 468 nm, as indicated by the dashed lines in Fig. 1. The enzyme units thus defined were linearly proportional to the amounts of enzyme protein used in both the NADPH-dependent and NADH-dependent reactions, as shown in the inset in Fig. 1. Therefore, this measure was employed in most of the experiments in the present study, although other measures were also employed in some experiments for convenience, as indicated in the appropriate tables and figures.

A Hitachi 323 recording spectrophotometer was used in some experiments.

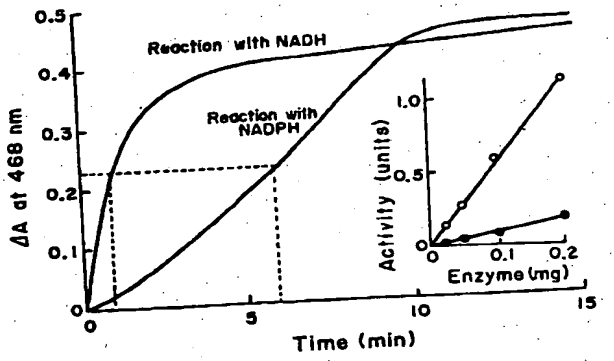

Fig. 1. Time courses of the NADPH-dependent and NADH-dependent biliverdin reductase reactions under the standard assay conditions. The reaction mixture, containing 1.06 mg protein of the CM-cellulose fraction of splenic biliverdin reductase, was preincubated for 5 min at 37°C and the reaction was started by adding NADPH (final 100 μM) or NADH (final 2 mM). The increase of absorbance at 468 nm was recorded. *Inset:* The relationship between the activity units and the amount of enzyme. ●, NADPH-dependent reaction; ○, NADH-dependent reaction.

RESULTS

Purification of Biliverdin Reductase from Pig Spleen—Fresh pig spleens (1.2 kg) were homogenized in 0.02 M potassium phosphate buffer (pH 7.4) containing 0.134 M KCl with a Waring blender to give a 20% homogenate. The homogenate was centrifuged succesively at 8,000 × *g* for 15 min and at 56,000 × *g* for 2 h, and the supernatant obtained was used as the starting extract. The results of a typical purification experiment are shown in Table I.

TABLE I. Summary of the purification of biliverdin reductase from pig spleen. The procedures are described in detail in the text.

Fraction	Total protein (mg)	Biliverdin reductase activity				Ratio of activities measured with NADH and with NADPH
		With NADPH (100 μM)		With NADH (2 mM)		
		Specific activity (unit/mg)	Total activity (unit)	Specific activity (unit/mg)	Total activity (unit)	
56,000 × *g* supernatant	66,300	0.0349	2,310	0.298	19,700	8.5
Solid ammonium sulfate (35–70%)	27,600	0.107	2,950	0.646	17,800	6.0
CM-cellulose	20,700	0.104	2,150	0.606	12,500	5.8
1st Hydroxyapatite	8,770	0.240	2,100	1.46	12,800	6.1
1st Sephadex G-100	876	1.06	929	7.19	6,300	6.8
DEAE-cellulose	76.6	8.86	679	61.6	4,720	7.0
2nd Hydroxyapatite	41.0	12.4	508	86.1	3,530	7.0
Electrofocusing	—	—	150	—	1,050	7.0
2nd Sephadex G-100	2.54	23.0	58.4	161	409	7.0
3rd Sephadex G-100	0.900	24.0	21.6	160	144	6.7

Ammonium sulfate fractionation: The 56,000 × *g* supernatant was fractionated with solid ammonium sulfate between 0.35 and 0.7 saturations and the precipitate obtained was suspended in 1 mM potassium phosphate buffer (pH 6.5) then dialyzed against 100 volumes of the same buffer for 6 h (solid ammonium sulfate fraction).

CM-cellulose column chromatography: The solid ammonium sulfate fraction (about 500 ml) was passed through a column of CM-cellulose (5 × 30 cm) previously equilibrated with 1 mM potassium phosphate buffer (pH 6.5). In this procedure almost all of the hemoglobin was retained on the column, whereas biliverdin reductase was not adsorbed. The column was washed with the same buffer until no further biliverdin reductase activity emerged, and the washings were combined with the flow-through (CM-cellulose fraction).

1st hydroxyapatite column chromatography: The CM-cellulose fraction was diluted with potassium phosphate buffer (pH 7.4) to reduce the protein concentration to about 5 mg/ml, then the solution was divided into five equal portions and applied separately to five hydroxyapatite columns (5 × 10 cm) equilibrated with 10 mM potassium phosphate buffer (pH 7.4). Each column was washed with 100 ml of the same buffer, and biliverdin reductase was eluted with 70 mM potassium phosphate buffer (pH 7.4). The five eluates were combined (1st hydroxyapatite fraction, about 800 ml).

1st Sephadex G-100 gel filtration: Proteins in the 1st hydroxyapatite fraction were precipitated by the addition of solid ammonium sulfate (0.8 saturation), then taken up in a small volume of 20 mM potassium phosphate buffer (pH 7.4) and dialyzed against 100 volumes of the same buffer for 6 h. The dialyzed solution (about 120 ml) was divided into four equal portions and each portion was applied separately to a Sephadex G-100 column (5 × 100 cm) equilibrated with 20 mM potassium phosphate buffer (pH 7.4). Elution was performed with the same buffer and the active fractions from the four columns were pooled (1st Sephadex G-100 fraction).

DEAE-cellulose column chromatography: The 1st Sephadex G-100 fraction was applied to a column of DEAE-cellulose (2.5 × 45 cm) equilibrated with 20 mM potassium phosphate buffer (pH 7.4). Elution was performed with 200 ml of the same buffer, followed by a linear gradient formed from 500 ml of the starting buffer and 500 ml of 250 mM potassium phosphate buffer (pH 7.4). The enzyme activity emerged in the early portion of the gradient and the active fractions were combined (DEAE-cellulose fraction).

2nd hydroxyapatite column chromatography: The DEAE-cellulose fraction was diluted with distilled water to reduce the buffer concentration to 10 mM, then applied to a column of hydroxyapatite (2.5 × 10 cm) previously equilibrated with 10 mM potassium phosphate buffer (pH 7.4). Proteins were eluted from the column first with 100 ml of the same buffer, then with a linear gradient formed from 200 ml of the starting buffer and 200 ml of 150 mM potassium phosphate buffer (pH 7.4). The enzyme-active fractions were combined (2nd hydroxyapatite fraction).

Preparative electrofocusing: The 2nd hydroxyapatite fraction was concentrated to about 15 ml by ultrafiltration and subjected to preparative electrofocusing in the pH range of 5 to 7, using an LKB electrofocusing column of 110 ml capacity operated according to the manufacture's instructions. After running at 600 volts for 45 h, the content of the column was pumped out at a rate of 2 ml per min and fractions of 2.3 ml were collected. The fractions between pH 5.9 and 6.5 were combined (electrofocusing fraction). The isoelectric point of biliverdin reductase from pig spleen was estimated to be 6.1–6.2.

2nd Sephadex G-100 gel filtration: The electrofocusing fraction was applied to a column of Sephadex G-100 (5 × 100 cm) equilibrated with 20 mM potassium phosphate buffer (pH 7.4) and proteins were eluted with the same buffer. The active fractions were combined (2nd Sephadex G-100 fraction).

3rd Sephadex G-100 fraction: The 2nd Sephadex G-100 fraction was concentrated to about 5 ml by ultrafiltration and was further fractionated on a column of Sephadex G-100 (2.5 × 100 cm), using 50 mM potassium phosphate buffer (pH 7.4). The active fractions were pooled (3rd Sephadex G-100 fraction).

The purified enzyme preparation in 50 mM potassium phosphate buffer (pH 7.4) could be stored at −20°C for several months without loss of activity.

It should be noted (Table I) that biliverdin

reductase was active with both NADH and NADPH, and the ratio of the activities with NADH and NADPH remained nearly constant throughout the purification procedure; in all instances the activities obtained with NADH were about 7 times higher than those obtained with NADPH under the assay conditions employed.

Molecular Properties of the Splenic Biliverdin Reductase—The purified biliverdin reductase preparation finally obtained gave a distinct major protein band when subjected to SDS-polyacrylamide gel electrophoresis (Fig. 2), and its molecular weight was estimated to be about 34,000. In addition to the major band, one or two faint bands were occasionally seen on the gel: the apparent molecular weights of these additional proteins were in the range of 50,000 to 70,000 and their relative densities varied from preparation to preparation. The major protein detected on the SDS-polyacrylamide gel usually constituted 90% or more of the total protein loaded as determined with a gel scanner. The purified biliverdin reductase preparation also gave a molecular weight of 34,000 as estimated by gel filtration on a Sephadex G-200 column (data not shown). Therefore, we conclude that biliverdin reductase from pig spleen is a monomer protein with an apparent molecular weight of 34,000.

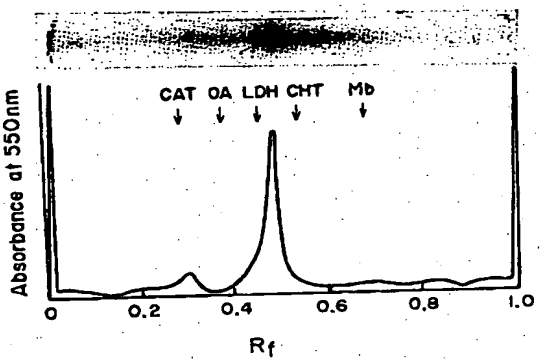

Fig. 2. Estimation of the molecular weight of the purified splenic biliverdin reductase by SDS-polyacrylamide gel electrophoresis. The purified biliverdin reductase preparation (about 6 μg protein) was loaded onto a 7.5% polyacrylamide gel (0.6×7 cm) containing 0.1% SDS. Coomassie blue was employed as the tracking dye. The marker proteins (indicated by arrows in the figure) were, from left to right: catalase (CAT); ovalbumin (OA); lactate dehydrogenase (LDH); chymotrypsinogen A (CHT); myoglobin (Mb).

The purified biliverdin reductase from pig spleen did not appear to contain any cofactor as judged from the absorption spectrum in the visible region, although this conclusion is not definitive, since the enzyme solutions available for spectrophotometric study were of relatively low concentration (about 50 μg/ml). The addition of FAD or FMN was rather inhibitory to the biliverdin reductase reaction.

Specificity of Splenic Biliverdin Reductase and Effects of Various Compounds on the Enzyme Activity—The purified splenic biliverdin reductase preparation did not exhibit any other pyridine nucleotide-dependent activity such as glucose dehydrogenase, alcohol dehydrogenase, aldehyde dehydrogenase, glutathione reductase or DT-diaphorase, when tested under appropriate assay conditions (data not shown). The biliverdin reductase activity was susceptible to thiol reagents; in these experiments, reaction mixtures containing 6 μg protein of the purified enzyme were treated with various thiol reagents and preincubated for 5 min at 37°C, then the reactions were started by the addition of NADPH. The activity was completely inhibited by 25 μM *p*-chloromercuribenzoate, whereas the inhibition by this reagent at 1 μM was only 15%. The activity was also inhibited by about 30% by 0.5 mM or 1.0 mM *N*-ethylmaleimide. The inhibition by 1 mM iodoacetamide or 1 mM arsenobenzoate, however, was less than 10%. The reaction was not affected by EDTA or other chelating agents.

Kinetic Properties of the Splenic Biliverdin Reductase Reaction—Although the purified biliverdin reductase was active with both NADH and NADPH, there were considerable differences between the kinetic properties of the reactions with NADH and NADPH.

pH optimum: The pH optimum of the reaction with NADH was 6.9, whereas that with NADPH was 8.5 (Fig. 3). In the following experiments, however, reactions were carried out at pH 7.4 unless otherwise stated.

Inhibition by excess biliverdin: The reactions with NADH and NADPH were inhibited by excess biliverdin and, as shown in Fig. 4, the inhibition was apparently independent of the concentration of NADPH or NADH. However, the reaction with NADPH was far more susceptible to excess biliverdin than the reaction with NADH; for

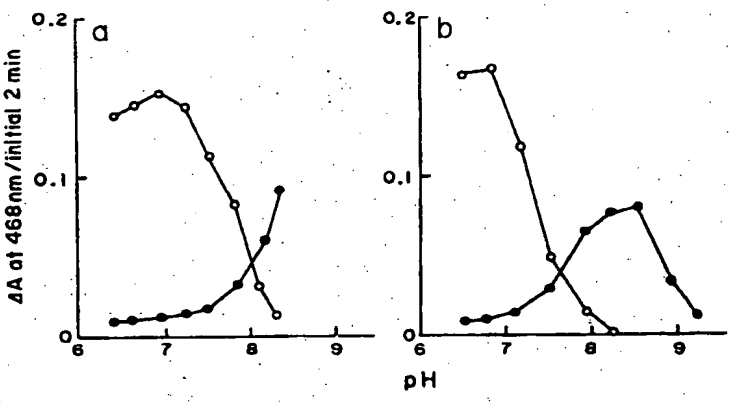

Fig. 3. The pH-activity relationships of the biliverdin reductase reactions. The reaction mixtures contained, in a final volume of 2 ml, 1.8 μg protein of purified splenic biliverdin reductase, 10 μM biliverdin, 1 mg/ml bovine serum albumin, 0.1 mM NADPH (or 2 mM NADH), and 100 mM potassium phosphate buffer in *a* or 100 mM Tris-HCl buffer in *b*. The actual pH of each assay mixture was determined at 37°C after the reaction. Other conditions were the same as the standard assay conditions. ●, NADPH-dependent reaction; ○, NADH-dependent reaction.

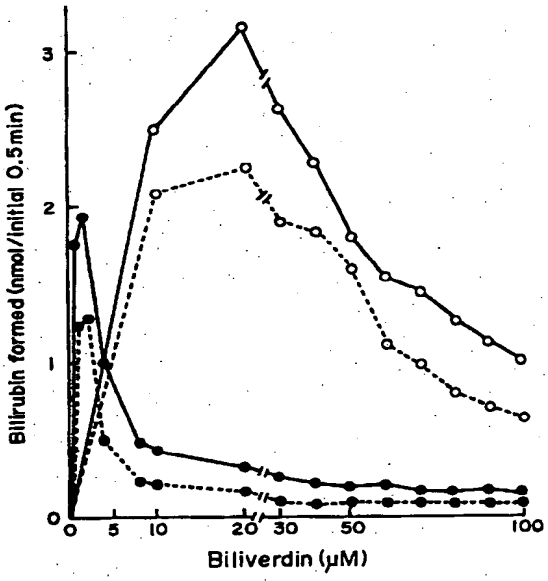

Fig. 4. Inhibition of biliverdin reductase by excess biliverdin. Each reaction mixture contained, in a final volume of 2 ml, 100 mM potassium phosphate buffer (pH 7.4), 1 mg/ml bovine serum albumin, and 3.7 μg protein of purified splenic biliverdin reductase. —●—, With 100 μM NADPH; --●--, with 10 μM NADPH; —○—, with 5 mM NADH; --○--, with 2 mM NADH. Other conditions were as described in "MATERIALS AND METHODS."

instance, the reaction with NADPH was markedly inhibited when the reaction was carried out with 10 μM biliverdin, while 10 μM biliverdin did not appear to inhibit the reaction with NADH appreciably. The data in Fig. 4 could well account for the observation (Fig. 1) that the time course of the reaction with NADPH was sigmoidal, whereas the reaction with NADH was not under the standard assay conditions with 10 μM biliverdin as a substrate.

K_m values for reduced pyridine nucleotides and biliverdin: The K_m values were determined at lower biliverdin concentrations to avoid possible substrate inhibition, and using relatively small amounts of the enzyme to ensure that the reaction was linear at least for the initial 0.5 to 1 min. Figure 5 shows double-reciprocal plots of the concentration of reduced pyridine nucleotides against the initial velocities. The plots obtained in the NADH system or the NADPH system at fixed concentrations of biliverdin as indicated in the figure crossed the axis to the left of the ordinate. This indicates that the biliverdin reductase reaction occurs by a sequential mechanism (*20*). From the data in Fig. 5, the K_m values were calculated according to Cleland (*20*); in the reaction with NADPH, K_m for biliverdin was 0.3–0.5 μM and

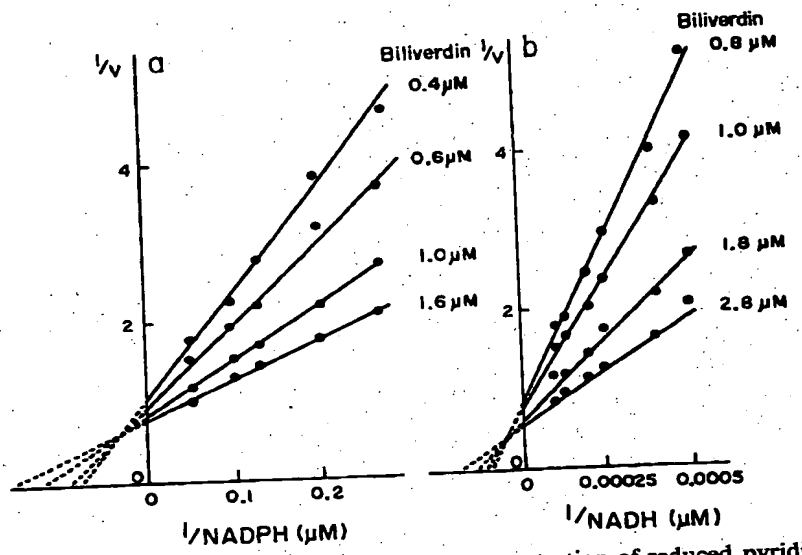

Fig. 5. The reaction rate as a function of the concentration of reduced pyridine nucleotide. The assay mixtures contained, in a final volume of 2 ml, 100 mM potassium phosphate buffer (pH 7.4), 1 mg/ml bovine serum albumin, 1.2 μg protein of purified splenic biliverdin reductase, and the indicated concentrations of biliverdin and NADPH or NADH. The initial velocities were adopted for comparison of the reaction rates. *a*, With NADPH varied; *b*, with NADH varied.

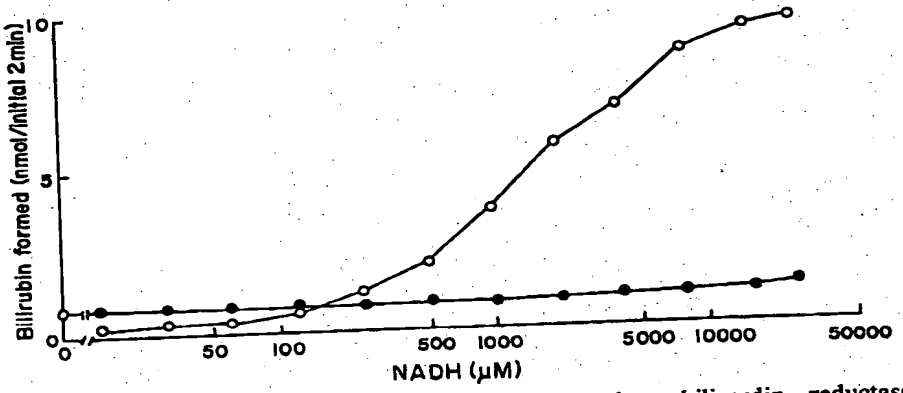

Fig. 6. Competitive inhibition of NADH-dependent biliverdin reductase reaction by NADPH. The assay mixtures contained, in a final volume of 2 ml, 100 mM potassium phosphate buffer (pH 7.4), 10 μM biliverdin, 1 mg/ml bovine serum albumin, 2 μg protein of purified splenic biliverdin reductase, and the indicated concentrations of NADH or both NADH and NADPH. ○, With NADH alone; ●, with the indicated concentrations of NADH plus 100 μM NADPH.

that for NADPH was about 3 μM, while in the reaction with NADH, K_m for biliverdin was 1–2 μM and that for NADH was 1.5–2 mM. It was found that the maximum velocity of the reaction with NADH was about twice that of the reaction with NADPH at pH 7.4.

It should be noted that the K_m value for NADPH is far smaller than that for NADH. Preference for NADPH in the biliverdin reductase reaction was confirmed by the experiments shown in Fig. 6. When NADH alone was employed as a reductant, the rate of reduction of biliverdin

increased with further addition of NADH, but when the reaction mixtures were supplemented with 100 μM NADPH, which appeared to be sufficient to give maximum activity in the NADPH-dependent reaction, the rates in the reaction systems containing both NADH and NADPH did not increase beyond the level which could be reached by employing NADPH alone; in other words, the observed increase in the rate of the reaction with NADH alone was suppressed almost completely by 100 μM NADPH, indicating that NADPH was preferentially utilized for the reduction of biliverdin under these reaction conditions. These data are consistent with the view that NADPH and NADH compete for the same binding site of a single enzyme protein. We have also observed in an independent experiment that reduction of biliverdin in the reaction system with 2 mM NADH was inhibited almost completely by the addition of as little as 5–20 μM $NADP^+$, whereas the extent of the inhibition by 2 mM NAD^+ was about 65%. On the other hand, the reduction of biliverdin in the reaction system with 100 μM NADPH was hardly affected by 2 mM NAD^+, while the reduction was inhibited by about 85% by the addition of 1 mM $NADP^+$. These observations also indicate that biliverdin reductase utilizes NADP-type pyridine nucleotides in preference to NAD-type pyridine nucleotides.

Stoichiometry of Biliverdin Reduction—In biliverdin reduction catalyzed by biliverdin reductase, 1 mol of reduced pyridine nucleotide was apparently consumed per mol of biliverdin reduced or per mol of bilirubin formed in both the NADPH and NADH systems, as shown in Table II.

Comparison of the Effectiveness of Four Biliverdin Isomers as Substrates—Four biliverdin isomers, *i.e.*, the IXα-, IXβ-, IXγ-, and IXδ-isomers, prepared according to Bonnet and McDonagh (*14*), were subjected to enzymic reduction with highly purified splenic biliverdin reductase. Since there is no reliable means to determine accurately the concentrations of the isomers other than IXα-biliverdin, the concentrations of the other isomers were estimated from the absorption at 650–670 nm, assuming that the three isomers have the same millimolar extinction coefficients at 650–670 nm as IXα-biliverdin at 670 nm, namely 15.0. Figure 7 shows the absorption spectra of the four biliverdin isomers used as substrates. The spectra of

TABLE II. Stoichiometry in the biliverdin reductase reaction. The assay mixture (final, 2 ml) contained 0.1 M potassium phosphate buffer (pH 7.4), 13 μM biliverdin, 1 mg/ml bovine serum albumin, 100 μM NAD(P)H, and 1.5 μg protein of purified splenic biliverdin reductase. Biliverdin was omitted in the control. The reaction was started by adding biliverdin after preincubation for 5 min at 37°C. At the indicated times, the difference spectra in the whole range of 340–700 nm were recorded. The amounts of bilirubin formed were determined as described in the text. The amounts of biliverdin lost were calculated from the decrease in absorbance at 670 nm, assuming the millimolar extinction coefficient for the decrement at 670 nm to be 13.0, since bilirubin also absorbed at 670 nm, giving a millimolar extinction coefficient of 2.0. The amounts of NAD(P)H consumed were calculated from the decrease in the absorbance at 340 nm, employing a millimolar extinction coefficient of 23.2 instead of 6.2 for the decrement at 340 nm, since the millimolar extinction coefficients of biliverdin and bilirubin at 340 nm were 25.0 and 8.0, respectively.

Reaction time (min)	Bilirubin formed (nmol)	Biliverdin lost (nmol)	NAD(P)H consumed (nmol)
Reaction with NADPH			
20	6.74	6.54	6.21
40	14.00	13.15	13.53
60	23.04	20.24	22.16
Reaction with NADH			
20	2.22	2.88	2.47
40	5.30	5.65	5.06
60	8.00	8.11	8.53

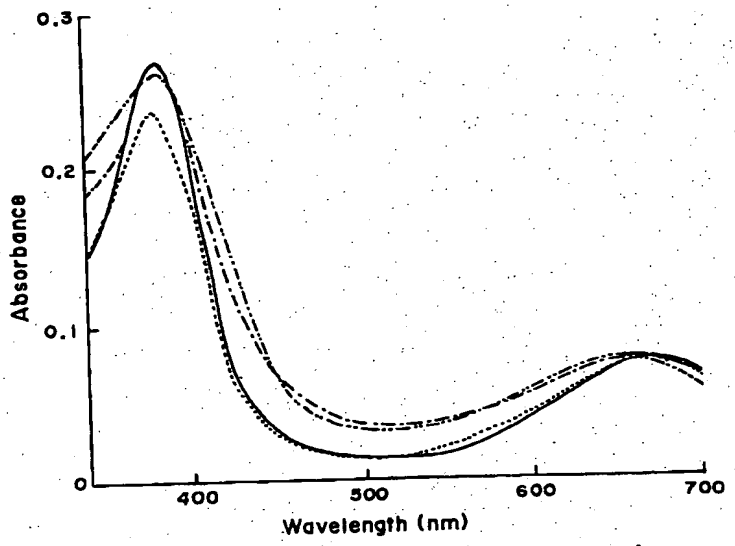

Fig. 7. The absorption spectra of the four biliverdin isomers in assay mixtures for the biliverdin reduction but without pyridine nucleotides. The mixtures contained, in 1.9 ml, 200 μmol of potassium phosphate buffer (pH 7.4), 2 mg of bovine serum albumin, 14 μg of purified splenic biliverdin reductase, and approximately 10 nmol of IXα (——), IXβ (—·—), IXγ (—··—), or IXδ-biliverdin (·····).

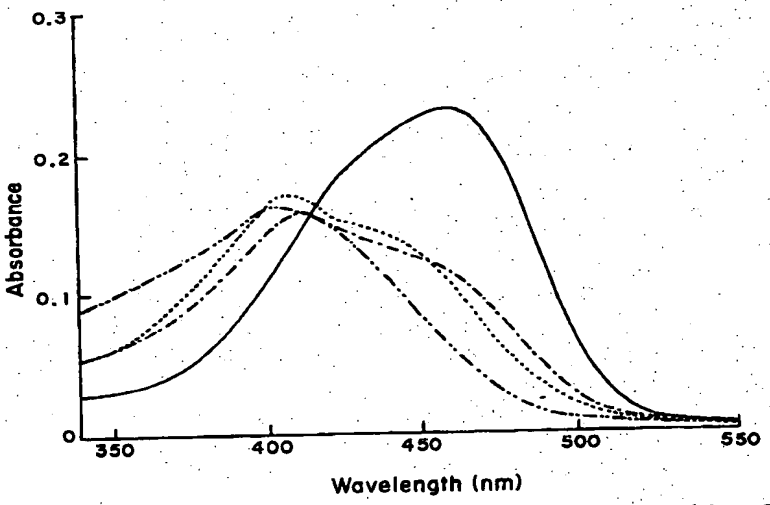

Fig. 8. The absorption spectra of the reaction products extracted into 3 ml of butanol from the reaction mixtures after completion of the reaction. The compositions of the reaction mixtures are given in the legend to Fig. 9. The reactions were started by the addition of 0.1 ml of NADPH (final, 100 μM). ——, IXα-isomer; —·—, IXβ-isomer; —··—, IXγ-isomer; ·····, IXδ-isomer.

the products of the reactions with the four isomers, which were extracted in butanol after completion of the reactions, are compared in Fig. 8. The spectral properties of the isomers shown in Figs. 7 and 8 are quite similar to those described by Blanckeart *et al.* (*16*). In the reaction with the α-isomer of biliverdin, two clear isosbestic points were observed at 408 nm and 525 nm; with the

β-isomer, they were at 398 nm and 518 nm; with the γ-isomer, they were at 388 nm and 492 nm; and with the δ-isomer, they were at 395 nm and 512 nm. Figure 9 shows the rates of reduction

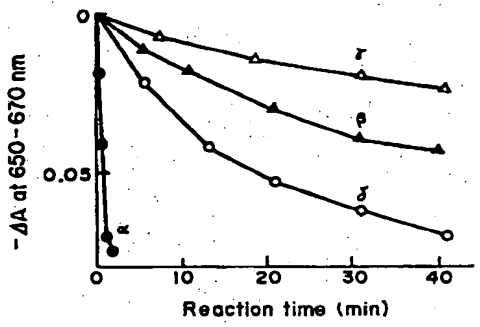

Fig. 9. Comparison of the reduction rates of the four biliverdin isomers. The assay mixture contained, in a final volume of 2 ml, 100 mM potassium phosphate buffer (pH 7.4), 1 mg/ml bovine serum albumin, 14 μg protein of purified splenic biliverdin reductase, and one of the four biliverdin isomers (indicated by α, β, γ, and δ in the figure). The final concentration of each biliverdin isomer was 5 μM.

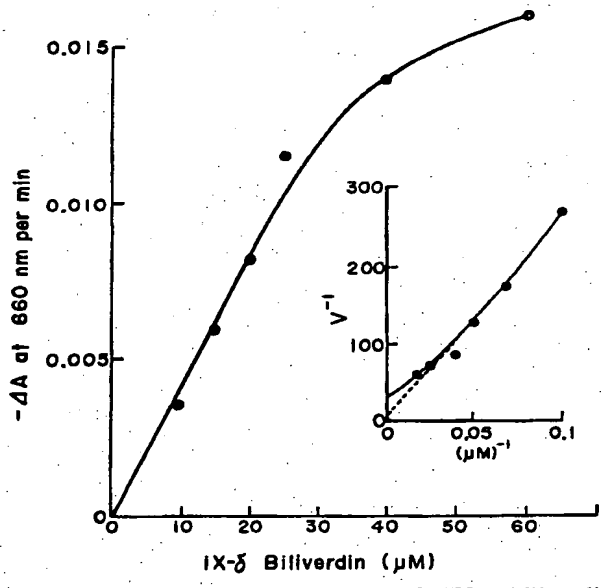

Fig. 10. Kinetics of reduction of IXδ biliverdin. Reaction mixtures contained, in a final volume of 2 ml, 100 mM potassium phosphate buffer (pH 7.4), 1 mg/ml bovine serum albumin, 14 μg of purified splenic biliverdin reductase, and the indicated concentrations of IXδ biliverdin. The reaction was started by the addition of NADPH (final 100 μM). *Inset*: double-reciprocal plot.

of the four biliverdin isomers in the NADPH-dependent reactions. Although the rates of reduction of the β-, γ-, and δ-isomers were extremely low as compared with that of the α-isomer, the initial rates were exactly proportional to the enzyme amounts used (data not shown). Taking the initial rate of reduction of the α-isomer as 100%, the relative initial rates of reduction of the β-, γ-, and δ-isomers were 4%, 2%, and 7%, respectively. The observed low rates of reduction of the unphysiological isomers are probably due to low affinities of these isomers for biliverdin reductase. In fact, as shown in Fig. 10, the half-saturation concentration of IXδ-biliverdin (apparent K_m value) were about 30 μM, which is more than 60 times that for IXα-biliverdin (0.3–0.5 μM) in the NADPH-dependent reaction. The double reciprocal plot of the data, however, was not linear, but was convex downwards, suggesting the occurrence of mild substrate inhibition for the reaction with the δ-isomer of biliverdin. It should also be noted that the maximum velocity of reduction of the δ-isomer, as estimated by extrapolation of the linear part of the double reciprocal plot, was apparently the same as the maximum velocity of reduction of the α-isomer under comparable experimental conditions, except for the biliverdin concentration.

Effects of Bovine and Human Serum Albumins—Previous investigators (*8*, *9*) had noticed that bovine serum albumin and human serum albumin enhanced the biliverdin reductase reaction. However, the relationships between albumin concentration and the extent of the stimulation reported for bovine serum albumin (*8*) and human serum albumin (*9*) were considerably different, so the ways in which these albumins exert their stimulative effects appear to be different. We therefore examined the effects of human serum albumin and bovine serum albumin on the reaction, employing the purified biliverdin reductase. Figure 11 shows the effects of increasing concentrations of albumins on the rate of reduction of biliverdin. In these experiments 10 μM biliverdin was used, as usual. Bovine serum albumin stimulated the reactions with both NADPH and NADH, although the degree of stimulation was considerably greater in the reaction with NADH. Human serum albumin also stimulated both reactions, but excess human serum albumin was rather inhibitory to both

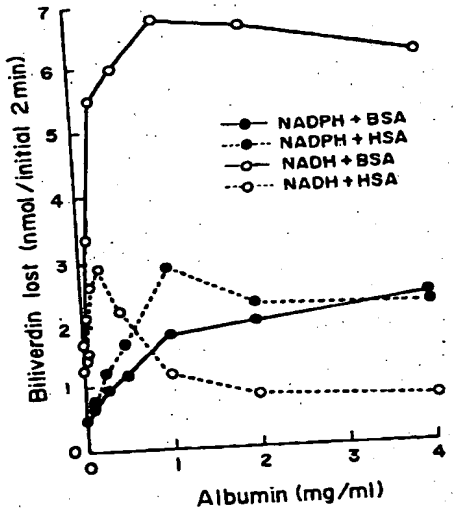

Fig. 11. Effects of bovine serum albumin (BSA) and human serum albumin (HSA) on the biliverdin reductase reaction. In this series of experiments, the reaction rate was measured in terms of the disappearance of biliverdin instead of bilirubin formation, since the spectrum of bilirubin is considerably different according to whether it is bound with albumin or not. The amount of biliverdin lost was calculated from the decrease in absorbance at 670 nm, assuming the millimolar extinction coefficient at 670 nm to be 13.0 for the decrement of biliverdin, as discussed in the text. In the experiments with human serum albumin, however, a slight correction to the millimolar extinction coefficient was made since human serum albumin had a slight metachromagic effect on biliverdin, as mentioned in the text. The reaction mixtures contained, in a final volume of 2 ml, 100 mM potassium phosphate buffer (pH 7.4), 10 μM biliverdin, 100 μM NADPH (or 2 mM NADH), 4 μg protein of purified splenic biliverdin reductase, and the indicated amounts of bovine or human serum albumin.

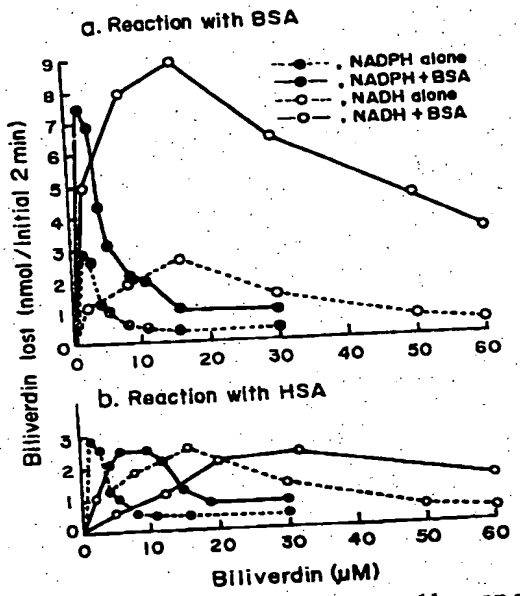

Fig. 12. Effects of addition of bovine and human serum albumins on the biliverdin reductase reaction at various biliverdin concentrations. The amounts of biliverdin reduced were calculated in the same way as in Fig. 11. *a*, The reaction mixture contained, in a final volume of 2 ml, 100 mM potassium phosphate buffer (pH 7.4), 100 μM NADPH (or 2 mM NADH), 4 μg protein of purified splenic biliverdin reductase, the indicated concentrations of biliverdin, and 2 mg of bovine serum albumin (BSA), when added. *b*, The compositions of the reaction mixtures as well as the meaning of the symbols were the same as in *a*, except that 2 mg of human serum albumin (HSA) was employed in place of BSA.

reactions. These results are similar to those reported by previous investigators (*8*, *9*).

Since the biliverdin concentration used in the above experiments was 10 μM, which was quite inhibitory to the reaction with NADPH (*cf.* Fig. 4), it is possible that albumin might have acted to reduce the inhibitory action of excess biliverdin. Therefore the effects of albumins at different concentrations of biliverdin were examined. As shown in Fig. 12, *a*, bovine serum albumin (1 mg/ml) enhanced the reaction to approximately the same degree at any biliverdin concentration tested in the NADPH system or the NADH system. In contrast, as shown in Fig. 12, *b*, human serum albumin (1 mg/ml) reduced the rate of the reaction at relatively low concentrations of biliverdin in the NADH or NADPH system, while at relatively higher concentrations of biliverdin, it apparently reduced the extent of the inhibition by excess biliverdin. However, with both NADPH and NADH, the maximum activities obtained in the presence of human serum albumin were similar to those observed without addition of albumin, indicating that the stimulatory effect of human serum albumin is far smaller than that of bovine serum albumin.

The observed stimulatory effect of human serum albumin could be accounted for by assuming that it binds biliverdin fairly tightly, reducing the effective concentration of biliverdin in the

reaction mixture. In accord with this view, we have observed that the addition of human serum albumin to biliverdin solution gave rise to a slight metachromagy of biliverdin (batho- and hyperchromic shift of the absorption maximum in the ultraviolet region and hyperchromic shift of the absorption maximum in the visible region). On the other hand, such metachromagy of biliverdin was not observable in the presence of bovine serum albumin, and this is in accord with the observation that bovine serum albumin did not significantly alter the pattern of inhibition by excess biliverdin. The possibility that bovine serum albumin might have stimulated the reaction by enhancing the removal of bilirubin as the product from the enzyme surface is also unlikely, since we observed in an independent experiment that the relative ratios of inhibition of the biliverdin reductase reaction by exogeneously added bilirubin were not substantially different whether the reaction mixtures contained bovine serum albumin or not (data not shown). Bovine serum albumin appears to stimulate the activity of biliverdin reductase in a rather direct manner through an as yet unknown mechanism.

Purification and Molecular Properties of Hepatic Biliverdin Reductase—Rat liver biliverdin reductase was purified by a modification of the procedures used for the purification of the enzyme from pig spleen. The results of a typical experiment are shown in Table III. Pooled rat livers (950 g) were homogenized with 4 volumes of 0.02 M potassium phosphate buffer (pH 7.4) containing 0.134 M KCl. The homogenate was successively centrifuged at 8,000 × *g* for 15 min and at 77,000 × *g* for 90 min, and the supernatant obtained was fractionated with solid ammonium sulfate between 0.35–0.7 saturations. The fractionated proteins were subjected successively to chromatographies on a CM-cellulose column (CM 32, 5 × 30 cm) and three separate hydroxyapatite columns (5 × 10 cm) as described for the purification of the splenic enzyme. Hepatic biliverdin reductase, however, was not adsorbed on hydroxyapatite columns which had been equilibrated with 10 mM potassium phosphate buffer, and therefore the flow-through fractions and washings were combined (hydroxyapatite fraction, 1,250 ml). The first Sephadex G-100 fraction was obtained as described in the previous section, and this fraction was loaded onto a DEAE-cellulose column (DE-32, 2.5 × 45 cm) equilibrated with 10 mM potassium phosphate buffer (pH 7.4) containing 30 mM KCl. After washing the column with 200 ml of the same buffer,

TABLE III. Summary of the purification of biliverdin reductase from rat liver. The procedures are described in detail in the text. About 1 mg of protein was used for the assay of biliverdin reductase activity in the fractions from the 77,000 × *g* supernatant to the hydroxyapatite fraction.

Fraction	Total protein (mg)	Biliverdin reductase activity				Ratio of activities measured with NADH and with NADPH
		With NADPH (100 μM)		With NADH (2 mM)		
		Specific activity (unit/mg)	Total activity (unit)	Specific activity (unit/mg)	Total activity (unit)	
77,000 × *g* supernatant	79,800	0.042	3,350	0.183	14,600	4.3
Ammonium sulfate (35–70%)	68,600	0.048	3,290	0.250	17,200	5.2
CM-cellulose	55,700	0.060	3,340	0.302	16,800	5.0
Hydroxyapatite	34,000	0.076	2,580	0.412	14,000	5.4
1st Sephadex G-100	4,470	0.391	1,750	2.12	9,470	5.4
1st DEAE-cellulose	242	2.48	600	15.5	3,750	6.2
2nd DEAE-cellulose	143	3.28	468	19.6	2,800	6.0
QAE-Sephadex	34	7.12	244	51.2	1,760	7.2
Electrofocusing	—	—	81	—	560	6.9
2nd Sephadex G-100	4.2	8.39	35	60.4	254	7.2

biliverdin reductase was eluted with a linear gradient formed from 600 ml of the same buffer and 600 ml of 10 mM potassium phosphate buffer (pH 7.4) containing 90 mM KCl. The most active fractions, which were eluted at about 35–40 mM KCl, were combined (1st DEAE-cellulose fraction, 370 ml) and diluted 3-fold with distilled water. The diluted solution was again charged onto a DEAE-cellulose column (DE-32, 2.5×23 cm) equilibrated with 10 mM potassium phosphate buffer (pH 7.4) containing 30 mM KCl, and the enzyme was eluted in the same manner as in the first DEAE-cellulose column chromatography, except that a 500 ml linear gradient was employed instead of 1,200 ml. The biliverdin reductase activity was again eluted at 35–40 mM KCl. The second DEAE-cellulose fraction (140 ml) was dialyzed against 10 mM potassium phosphate buffer (pH 7.4) containing 60 mM KCl and the dialyzed solution was adsorbed on a QAE-Sephadex column (1.5×30 cm) equilibrated with the same buffer. After rinsing, protein was eluted with a linear gradient formed from 150 ml of the rinsing buffer and 150 ml of 10 mM potassium phosphate buffer (pH 7.4) containing 250 mM KCl. The active fraction (QAE-Sephadex fraction, 110 ml) was concentrated by membrane filtration to about 15 ml and subjected to preparative electrofocusing (110 ml capacity, LKB) in the pH range of 4 to 6. The isoelectric point of the hepatic biliverdin reductase appeared to be 5.4. The electrofocusing fraction (15 ml) was further fractionated on a column of Sephadex G-100 (2.5×100 cm), using 50 mM potassium phosphate buffer (pH 7.4) as an eluant.

In the experiment shown in Table III, the purification was about 300-fold with an activity recovery of about 1.5%. The enzyme preparation finally obtained showed a distinct protein band with a molecular weight of 34,000 on SDS-gel electrophoresis, but there were also several minor protein bands on the gel. Further purification was unsuccessful due to instability of the enzyme. The purified enzyme preparation had a molecular weight of 34,000 as estimated by gel filtration on a Sephadex G-200 column (2.5×100 cm) (data not shown). The hepatic biliverdin reductase also appears to be a monomer protein with a molecular weight of 34,000. The purified hepatic enzyme could be stored at −20°C for several months without appreciable loss of activity.

It should be noted in Table III that, although the NADPH- and NADH-dependent biliverdin reductase activities were both purified concomitantly throughout the overall purification procedure, the extents of purification of the activities at individual steps were not always the same. Also, the ratio of the NADH-dependent and NADPH-dependent activities gradually changed from 4.3 to about 7 as the purification proceeded. The activity ratio of 7 is the same as that observed for the purified or the crude splenic enzyme. To investigate the possibility that the rat liver extract, but not the pig spleen extract, may contain some proteins which readily bind biliverdin, we added IXα-biliverdin to a 77,000×g supernatant of the liver homogenate and fractionated it directly on a Sephadex G-100 column. It was found that most of the pigment added was eluted at the void volume, while small portions were also eluted over all the fractions up to the bed volume. We took the void volume fraction from another 77,000×g supernatant to which biliverdin had not been added, and examined the effect of addition of this fraction on the NADH-dependent and NADPH-dependent activities of the purified biliverdin reductase. As shown in Fig. 13, the NADH-dependent activity decreased progressively with addition of the void volume fraction, whereas this fraction did not affect the NADPH-dependent activity under the

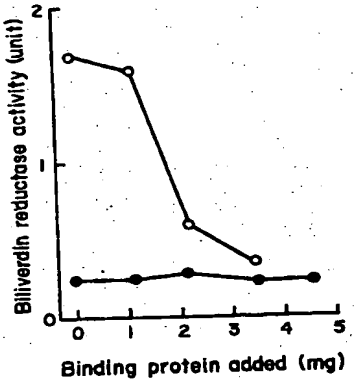

Fig. 13. Effect of biliverdin-binding protein(s) on the biliverdin reductase activity. Reaction mixtures contained, in a final volume of 2 ml, 100 mM potassium phosphate buffer (pH 7.4), 10 μM IXα-biliverdin, 1 mg/ml bovine serum albumin, the indicated amounts of biliverdin binding protein (the void volume fraction described in the text), and 100 μM NADPH (●) or 2 mM NADH (○).

experimental conditions employed. Apparently the enzyme preparations at earlier steps of the purification contained a biliverdin-adsorbing protein(s) and this acted to decrease the concentration of biliverdin available for the reaction. It is conceivable that only the NADH-dependent activity was affected by such a protein(s) since the NADH-dependent activity requires higher concentrations of biliverdin than the NADPH-dependent activity.

Catalytic Properties of the Hepatic Biliverdin Reductase—The purified hepatic biliverdin reductase was found to have catalytic properties very similar to those of the splenic enzyme. The hepatic biliverdin reductase purified from rat liver was active with both NADPH and NADH. K_m for NADPH was 3 μM and that for NADH was 1.5–2.0 mM. Essentially the same relation as depicted in Fig. 5 was also observed with the purified hepatic biliverdin reductase. K_m for IXα-biliverdin was 0.3 μM in the NADPH system and that in the NADH system was about 3 μM. These values are quite similar to those obtained for the reactions with splenic biliverdin reductase. Inhibition by excess biliverdin was also observable, and this inhibition was far more prominent in the reaction with NADPH than in that with NADH. The hepatic enzyme showed a very high activity with IXα-biliverdin as compared with the other isomers, like the splenic enzyme. All those observations indicate that the hepatic and splenic enzymes have essentially similar molecular and catalytic properties.

DISCUSSION

The present study with purified enzyme preparations from pig spleen and rat liver has shown that biliverdin reductase is a monomer protein with an apparent molecular weight of 34,000 and that a single enzyme is responsible for both the NADPH-dependent and NADH-dependent reactions, resolving the previous controversy (*8*, *9*) with respect to the hydrogen donor in the enzyme-catalyzed reduction of biliverdin.

The soluble fraction of rat liver contained a protein(s) which readily binds IXα-biliverdin. It is well known that the soluble liver fraction contains organic anion binding proteins such as ligandin (*21*, *22*) and Z protein (*22*, *23*), which preferentially bind bilirubin, bromsulfophthalein, indocyanine green, fatty acids, and others. The biliverdin binding protein(s) found in the present study may have a larger molecular weight than ligandin (M.W. 44,000 (*24*) or Z-protein (M.W. 12,000 (*23*, *25*)) since the biliverdin-binding protein was eluted at the void volume of a column of Sephadex G-100. No attempt was made to further characterize this protein.

It is worth noting that although biliverdin reductase was active with both NADH and NADPH, there were considerable differences in kinetic properties between the reactions with NADH and NADPH. Particularly significant is the observation that the inhibition by excess biliverdin was far more marked in the reaction with NADPH than with NADH. O'Carra and Colleran (*11*) also observed similar substrate inhibition and interpreted this as being similar to the type of abortive complex mechanism known to be responsible for substrate inhibition in some other pyridine nucleotide-linked dehydrogenase — notably lactate dehydrogenase (*26*). Namely, in the biliverdin reductase reaction, an inactive ternary complex consisting of enzyme, biliverdin and oxidized pyridine nucleotide may be readily formed, especially in the reaction with NADPH (*11*), because NADP-type pyridine nucleotides have higher affinity for biliverdin reductase compared with the NAD-type ones.

We confirmed, using the highly purified enzymes from pig spleen and rat liver, that biliverdin reductase has a much higher affinity for the α-isomer of biliverdin than for the other three types of isomers, and that the enzyme could reduce the α-isomer much faster than the other unphysiological isomers. This is important in relation to the physiological role of biliverdin reductase, since the microsomal heme oxygenase has been shown to yield almost exclusively IXα-biliverdin (*2*). Colleran and O'Carra (*10*, *11*) reported that the γ-isomer of biliverdin could not serve as a substrate when tested with the crude extract of guinea pig liver. With the purified pig spleen enzyme, however, we found that the γ-isomer could be reduced by the biliverdin reductase system, although the rate of reduction was extremely low, as shown in Fig. 9. On the other hand, the dimethylester of IXα-biliverdin was not a substrate of the purified biliverdin reductase

preparations (data not shown), in agreement with the observation of Colleran and O'Carra with the crude enzyme preparation (*10*, *11*). Free propionate side chain may be an essential requirement for biliverdin as a substrate, and the factor determining the reactivity of the individual biliverdin isomers may be the position of the propionate side chains on the tetrapyrroles, as suggested originally by O'Carra and Colleran (*11*).

It is well documented that NADP is predominantly in the reduced form in the cytoplasm, whereas NAD is predominantly in the oxidized form (*27*). The approximate concentrations of pyridine nucleotides in the liver cytosol fraction have been reported to be as follows: 0.12 mM for NADPH, 0.035 mM for $NADP^+$, 0.07 mM for NADH, and 0.5 mM for NAD^+ (*28*). Taking into account these values as well as the K_m values for NADH and NADPH in the biliverdin reductase reaction, it appears that the enzyme-catalyzed conversion of biliverdin to bilirubin in animal tissues under physiological conditions may depend almost entirely on NADPH.

We thank Dr. A.F. McDonagh, Department of Medicine, University of California School of Medicine, San Francisco, for providing crystalline IXα-biliverdin.

REFERENCES

1. Tenhunen, R., Marver, H.S., & Schmid, R. (1968) *Proc. Natl. Acad. Sci. U.S.* **61**, 748–755
2. Tenhunen, R., Marver, H.S., & Schmid, R. (1969) *J. Biol. Chem.* **244**, 6388–6394
3. Schmid, R. & McDonagh, A.F. (1975) *Ann. N.Y. Acad. Sci.* **244**, 533–552
4. Yoshida, T., Takahashi, S., & Kikuchi, G. (1974) *J. Biochem.* **75**, 1187–1191
5. Yoshida, T. & Kikuchi, G. (1978) *J. Biol. Chem.* **253**, 4224–4229
6. Yoshida, T. & Kikuchi, G. (1978) *J. Biol. Chem.* **253**, 4230–4236
7. O'Carra, P. (1975) in *Porphyrins and Metalloporphyrins* (Smith, K.M., ed.) pp. 123–153, Elsevier Scientific Publishing Co., Amsterdam
8. Singleton, J.W. & Laster, L. (1965) *J. Biol. Chem.* **240**, 4780–4789
9. Tenhunen, R., Ross, M.E., Marver, H.S., & Schmid, R. (1970) *Biochemistry* **9**, 298–303
10. Colleran, E. & O'Carra, P. (1970) *Biochem. J.* **119**, 16P–17P
11. O'Carra, P. & Colleran, E. (1977) in *Chemistry and Physiology of Bile Pigments* (Berk, P.D. & Berlin, N.I., eds.) pp. 69–80, National Institute of Health, Bethesda, Maryland
12. Bernardi, G. (1971) in *Methods in Enzymology* (Jakoby, W.B., ed.) Vol. 22, pp. 325–339, Academic Press, New York
13. Lemberg, R. (1932) *Liebigs Ann.* **499**, 25–40
14. Bonnet, R. & McDonagh, A.F. (1973) *J.C.S. Perkin* I, 881–888
15. O'Carra, P. & Colleran, E. (1970) *J. Chromatogr.* **50**, 458–468
16. Blanckeart, N., Heirwegh, K.P.M., & Compernolle, F. (1976) *Biochem. J.* **155**, 405–417
17. Andrews, P. (1964) *Biochem. J.* **91**, 222–233
18. Weber, K. & Osborn, M. (1969) *J. Biol. Chem.* **244**, 4406–4412
19. Lowry, O.H., Rosebrough, N.J., Farr, A.L., & Randall, R.J. (1951) *J. Biol. Chem.* **193**, 265–275
20. Cleland, W.W. (1963) *Biochim. Biophys. Acta* **67**, 104–137
21. Reyes, H., Levi, A.J., Gatmaitan, Z., & Arias, I.M. (1969) *Proc. Natl. Acad. Sci. U.S.* **64**, 168–170
22. Levi, A.J., Gatmaitan, Z., & Arias, I.M. (1969) *J. Clin. Invest.* **48**, 2156–2167
23. Ockner, R.K. & Manning, J.A. (1974) *J. Clin. Invest.* **54**, 326–338
24. Kirsch, R., Fleischner, G., Kamisaka, K., & Arias, I.M. (1975) *J. Clin. Invest.* **55**, 1009–1019
25. Mishkin, S., Stein, L., Fleischner, G., Gatmaitan, Z., & Arias, I.M. (1975) *Amer. J. Physiol.* **228**, 1634–1640
26. Fromm, H.J. (1961) *Biochim. Biophys. Acta* **52**, 199–200
27. Siess, E.A., Brocks, D.G., Lattke, H.K., & Wieland, O.H. (1977) *Biochem. J.* **166**, 225–235
28. Sols, A. & Marco, R. (1970) *Curr. Top. Cell. Regul.* **2**, 227–273

Biochimica et Biophysica Acta, 957 (1988) 237–242
Elsevier

BBA 33253

The reaction mechanism of bovine kidney biliverdin reductase

Elizabeth Rigney and Timothy J. Mantle

Department of Biochemistry, Trinity College, Dublin (Ireland)

(Received 27 May 1988)

Key words: Biliverdin reductase; Reaction mechanism; (Bovine kidney)

The steady-state kinetics of biliverdin reductase can be studied in detail at pH 9 as under these conditions the K_m for biliverdin is high enough to obtain reliable measurements of the initial rate in the absence of any biliverdin binding proteins. The initial rate kinetics and the product-inhibition studies are consistent with an ordered sequential mechanism provided the biliverdin concentration was below 20 μM. Above this concentration significant flux occurs through a substrate inhibition pathway involving an enzyme-NAD(P)-biliverdin complex. Chloride is shown to cause a significant activation of the enzyme under certain conditions and this is shown to result from an inability of biliverdin to bind to an enzyme-NAD-chloride complex.

Introduction

Biliverdin reductase is an NAD(P)-linked monomeric oxidoreductase which catalyses the reduction of biliverdin to produce the bile pigment, bilirubin. The enzyme is believed to have a function clearing biliverdin from the foetus [1] and recently the product bilirubin has been suggested to play a role as an antioxidant [2,3]. In most species the enzyme exists as a monomer of M_r 34000 [4–6]; however, the guinea pig and hamster enzymes have M_r values that are approximately twice this value [7,8]. Biliverdin reductase is subject to potent substrate inhibition by biliverdin [9,6] although this effect is probably modulated in vivo by intracellular binding proteins [10]. There has been no detailed study of the reaction mechanism of biliverdin reductase, although it has been suggested that the enzyme obeys an ordered mechanism [7,6]. These studies were conducted in the presence of serum albumin which complicates the analysis by binding the substrate biliverdin [6] and also appears to have direct effects on the enzyme activity [11]. While it is highly desirable to analyse the reaction mechanism for biliverdin reductase in the absence of serum albumin this is not possible at a physiological pH, due to the insolubility of the product bilirubin and the low K_m for biliverdin. This last aspect is exacerbated using NADPH as the cofactor [7,11]. We have recently shown that biliverdin binding, both productively and non-productively, is less tight at alkaline pH values (Rigney and Mantle, unpublished data) and have utilised this observation to study the steady-state mechanism at pH 9. Details of this work are presented in the present report.

Materials and Methods

Materials

Biliverdin was synthesised by the method of McDonagh [12]. Biliverdin reductase was purified as described previously [8].

Methods

Enzyme assays. Biliverdin reductase activity was measured by following the production of bilirubin spectrophotometrically by monitoring the increase

Correspondence: T.J. Mantle, Department of Biochemistry, Trinity College, Dublin 2, Ireland.

in absorbance at 460 nm. The buffers used were: 0.1 M Tris-HCl/0.1 M sodium phosphate, and 0.02 M sodium pyrophosphate/0.2 M sodium phosphate at the pH values indicated. In the steady-state study the buffer used was 0.02 M sodium pyrphosphate/0.2 M sodium phosphate (pH 9). The absorption coefficient for bilirubin in this buffer at 460 nm is 54.7 $nM^{-1} \cdot cm^{-1}$ and for biliverdin the value is 4.08 $mM^{-1} \cdot cm^{-1}$ (Rigney, unpublished data). All assays were conducted in triplicate at 30 °C.

Treatment of data. All initial rate data were fitted to a rectangular hyperbola by the method of Wilkinson [13]. Slope and intercept replots were fitted by linear regression.

Results

Effect of pH

Biliverdin reductase was stable for at least 25 min in all of the buffer systems described in this work. The effect of pH on the NADPH- and NADH-dependent activities of biliverdin reductase are shown in Fig. 1. A pH optimum of 8.5 was found with NADPH when all three buffer systems described in the legend to Fig. 1 were used. The optimum pH observed when NADH was the cofactor was found to depend on the buffer system used. In sodium phosphate buffer the pH optimum is at 7 whereas in Tris-HCl the optimum shifts to a lower value. A similar phenomenon was observed with sodium pyrophosphate/sodium phosphate buffer in which case the pH optimum was 6. The effect of pH on the initial-rate kinetics with biliverdin as the variable substrate is shown in Fig. 2. This shows that the substrate inhibition is far more potent at acid and neutral pH values than at alkaline pH values. In addition the apparent K_m values for biliverdin are considerably higher at alkaline values than at acid or neutral values. At pH 9 it is therefore feasible to examine the steady-state kinetics of biliverdin reductase in the absence of serum albumin.

The initial rate kinetics of biliverdin reductase

A linear relationship was demonstrated between enzyme concentration and initial rate over the range 0.3–3.9 μg per assay. All kinetic experiments were conducted within this range. Initial rate measurements when the biliverdin concentration was held constant and the NADPH concentration varied (5–150 μM) yielded linear double-reciprocal plots (Fig. 3). When biliverdin was the variable substrate (0.5–10 μM) at fixed levels of NADPH, linear double-reciprocal plots were obtained (Fig. 3). The slopes and intercepts from each plot were replotted against the reciprocal of the fixed substrate concentration and the kinetic constants calculated by the method of Florini and Vestling [14]. These are shown in Table I for the cases when the data set were analysed with biliverdin as the variable substrate and NADPH was held constant at various fixed levels, and when NADPH was varied and the concentration of biliverdin was held constant at different fixed levels.

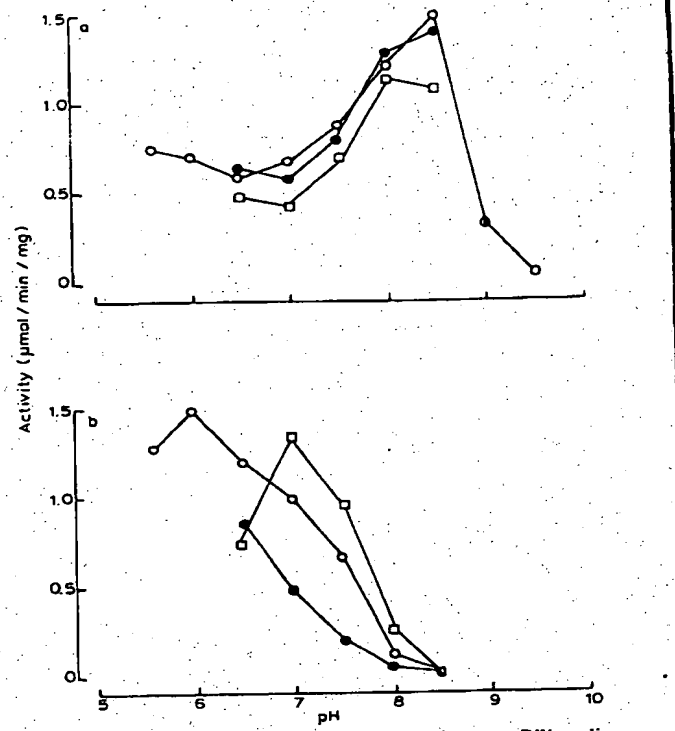

Fig. 1. The pH dependence of biliverdin reductase. Biliverdin reductase (1.95 μg) was assayed at 30 °C in 0.1 M Tris-HCl (●); 0.1 M sodium phosphate (□) and 0.02 M sodium pyrophosphate/0.2 M sodium phosphate (○) containing: (a) Biliverdin (2.5 μM) and NADPH (100 μM). (b) Biliverdin (2.5 μM) and NADH (700 μM).

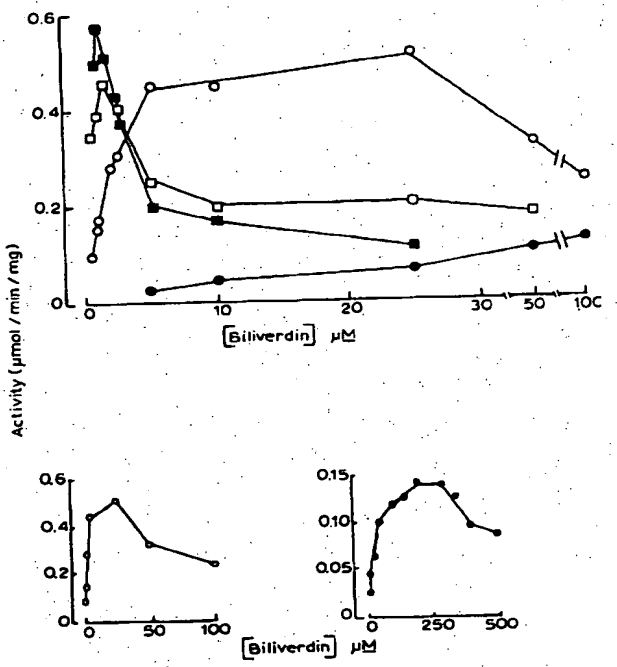

Fig. 2. The effect of pH on biliverdin reductase kinetics. Biliverdin reductase (1 μg) was assayed at 30 °C in a mixture containing NADPH (100 μM) and biliverdin at the concentrations indicated with 0.02 sodium pyrophosphate/0.2 M sodium phosphate: □, pH 5.6, ■, pH 7.5; ○, pH 9; and ●, pH 9.5.

Product inhibition studies

The primary data for all of these experiments are not shown; however, all the inhibition constants can be found in Table II. When inhibition by bilirubin was investigated with biliverdin as the variable substrate at nonsaturating (10 μM) and saturating (100 μM) concentrations of NADPH, mixed inhibition was observed. When the slope and intercept values of the double-reciprocal plots were replotted against the concentration of bilirubin, a linear relationship was obtained and the resultant inhibitor constants K_{ii} (from the intercept replot) and K_{is} (from the slope replot) are shown in Table II. Bilirubin also exhibited mixed inhibition when the variable substrate was NADPH and the bilirubin concentration was held constant at a nonsaturating level (1 μM) or at 10 μM. Unfortunately, it was not possible to saturate the enzyme with biliverdin, as the mechanism becomes complicated by flux through an EBQ complex where B and Q denote biliverdin and NADP, respectively (see below). The 'saturating' concentration of biliverdin (10 μM) was as close to saturation as possible without demonstrating substrate inhibition. When the slope and intercept values were replotted against bilirubin concentra-

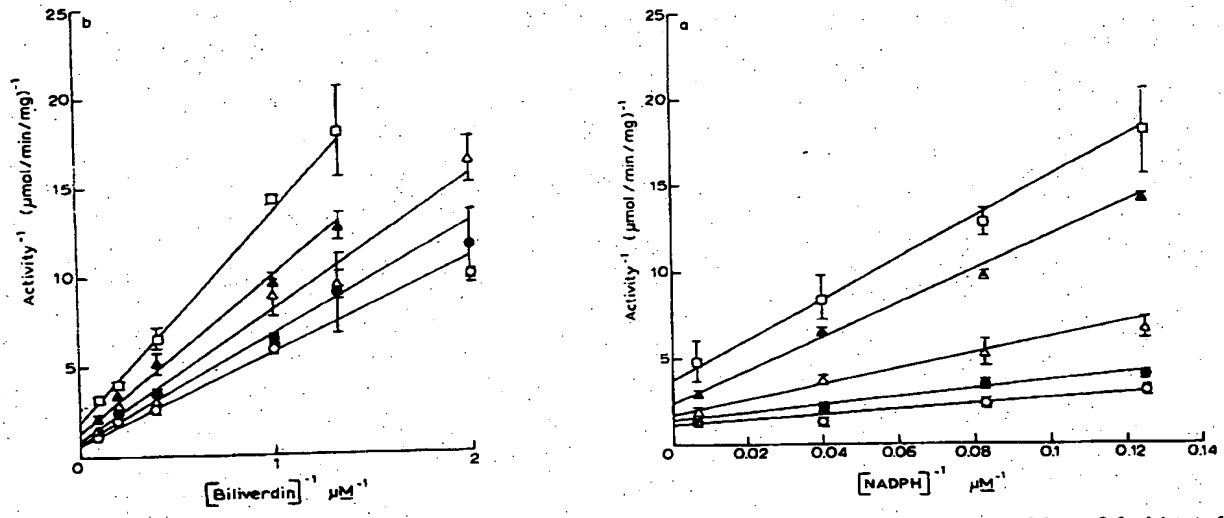

Fig. 3. The initial rate kinetics of biliverdin reductase. (a) The concentrations of biliverdin were 0.75 μM (□), 1 μM (▲), 2.5 μM (△), 5 μM (●) and 10 μM (○). (b) The concentrations of NADPH were 8 μM (□), 12 μM (▲), 25 μM (△), 50 μM (●) and 100 μM (○). All assays were performed in 0.02 M sodium pyrophosphate/0.2 M sodium phosphate (pH 9) with 0.65 μg of biliverdin reductase at 30 °C.

TABLE I

KINETIC CONSTANTS FOR BILIVERDIN REDUCTASE AT pH9

	[NADPH] constant	[Biliverdin] constant
K_a (μM)	12.23 ± 3.93	11.49 ± 5.55
K_b (μM)	6.91 ± 1.53	5.27 ± 1.72
K_{ia} (μM)	9.47 ± 2.12	26.43 ± 12.12
V (μmol/min per mg)	1.31 ± 0.27	1.49 ± 0.47

tion, a linear relationship was obtained and the resultant K_{ii} and K_{is} values are shown in Table II.

NADP showed competitive kinetics with NADPH as the variable substrate at nonsaturating (1 μM) and 'saturating' (10 μM) concentrations of biliverdin (the K_{is} values are shown in Table II). With biliverdin as the variable substrate, NADP showed mixed inhibition at nonsaturating concentrations of NADPH (10 μM), and when the experiment was repeated using saturating concentrations of NADPH (100 μM) the inhibition became uncompetitive. The values for the inhibition constants K_{ii} and K_{is} for both NADP and bilirubin at subsaturating and 'saturating' concentrations of the fixed substrate were calculated from replots of slopes and intercepts against the concentration of the inhibitory product and are listed in Table II.

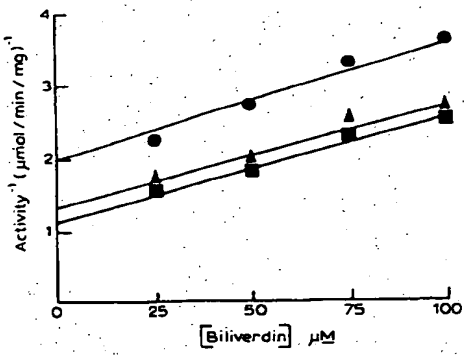

Fig. 4. Substrate inhibition by biliverdin. Dixon plot with NADPH concentrations of 10 μM (●), 25 μM (▲) and 50 μM (■).

Substrate inhibition by biliverdin

The substrate inhibition by biliverdin at pH 9 was further investigated by varying the concentration of NADPH (10–50 μM) and biliverdin (25–75 μM). A Dixon plot of the reciprocal velocity against biliverdin concentration was linear (Fig. 4). The lines at the various concentrations of NADPH were parallel, demonstrating that the substrate inhibition was uncompetitive. The inhibition constant for biliverdin is 48 μM.

Effect of chloride on initial rates

Chloride has a pronounced 'activating' effect on biliverdin reductase activity when NADH is the cofactor; however, no such effect was observed with NADPH at pH 7.2 in the presence of

TABLE II

INHIBITION CONSTANTS FOR BILIVERDIN REDUCTASE

Inhibitor	Variable Substrate	Fixed Substrate Conc. (μM)	K_{is} (μM)	K_{ii} (μM)
Bilirubin	NADPH	1	6.83 ± 2.7	4.93 ± 2.63
		10	5.2 ± 1.35	2.6 ± 0.36
Bilirubin	biliverdin	10	3.91 ± 0.84	6.24 ± 1.69
		100	1.63 ± 0.85	11.17 ± 2.78
$NADP^+$	NADPH	1	84.7 ± 10.74	–
		10	24.3 ± 0.70	–
$NADP^+$	biliverdin	10	690.0 ± 630.0	11.96 ± 5.53
		100	–	90.0 ± 8.8

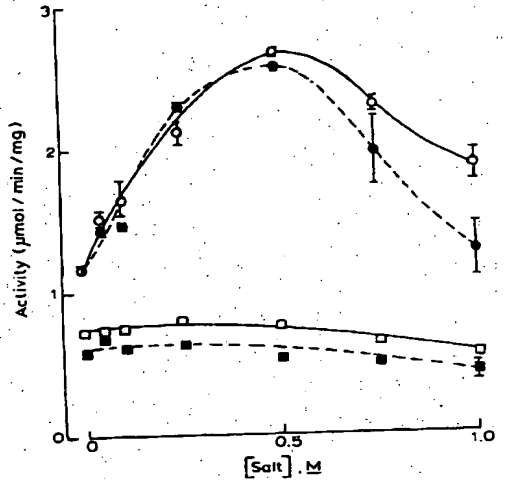

Fig. 5. Effect of chloride on initial rates. Biliverdin reductase (0.35 μg) was assayed in a reaction mixture (2 ml) containing 20 μM biliverdin, 700 μM NADH, 30 μM bovine serum albumin in 0.1 M sodium phosphate (pH 7.2) in the presence of the indicated concentrations of NaCl (●) and KCl (○). The enzyme was also assayed in a mixture containing 2.5 μM biliverdin, 100 μM NADPH in 0.1 M sodium phosphate (pH 8.5) in the presence of the indicated concentrations of NaCl (■) and KCl (□).

bovine serum albumin (Fig. 5). The activation was further investigated by examining the effect of 0.5 M KCl on the initial rate kinetics with biliverdin or NADH as the variable substrate. It can be seen (Fig. 6) that the primary effect of chloride is to abolish the substrate inhibition observed with biliverdin. This effect is mirrored in the NADH kinetics where chloride has little effect on the slope value but increases the apparent turnover number from 1.7 s^{-1} to 5.6 s^{-1}.

Discussion

The initial rate studies indicate that the mechanism obeyed by biliverdin reductase is sequential, as linear intersecting lines were obtained when either substrate was varied at different fixed levels of the other substrate. The mechanism was further investigated by determining the product inhibition patterns [15]. Briefly, since bilirubin is a mixed inhibitor when biliverdin is the variable substrate, Theorell-Chance and rapid-equilibrium random mechanisms are ruled out. A random steady-state mechanism is unlikely as linear product inhibition replots were obtained [15]. These results, taken with our observation that pyridine nucleotides bind to the free enzyme [17], suggest that at pH 9 in the absence of any 'binding protein' the reaction mechanism is ordered. We have been unable to obtain any evidence that biliverdin binds to the free enzyme by analysing difference spectra, by conducting sucrose-density sedimentation experiments in the presence of biliverdin, or by utilising the fact that biliverdin binding to proteins is often accompanied by a distinct spectral change in the presence of a mercaptan [8]. Two minor points concerning the experimental product inhibition patterns and the theoretical patterns for an ordered bi-bi mechanism are worth noting. Firstly, it was not possible to observe the predicted uncompetitive inhibition by bilirubin against NADPH at saturating concentrations of biliverdin as it was not experimentally feasible to saturate with bi-

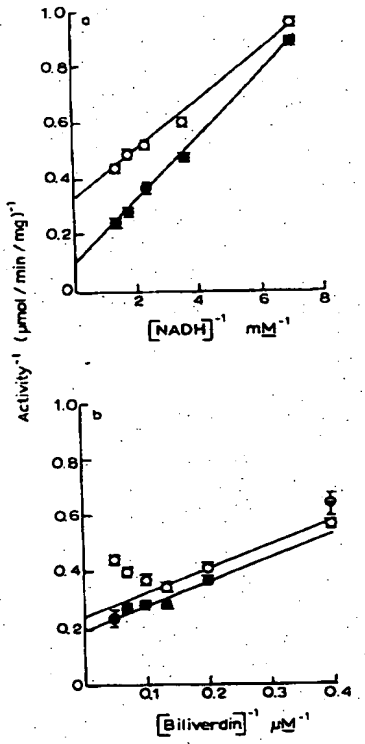

Fig. 6. Effect of chloride on initial rates. Initial rates were measured at pH 7.2 in the absence (○) or presence (●) of 0.5 M KCl. Other conditions are described in the legend to Fig. 5.

liverdin without introducing the complication of substrate inhibition. Secondly, although no inhibition by NADP against biliverdin is predicted at saturating levels of NADPH, significant, albeit reduced, inhibition was observed under these conditions. Cleland [16] has pointed out that in practice one can rarely achieve a high enough concentration of A (NADPH) to negate the effect of Q (NADP) binding. Since NADPH has been shown to bind to biliverdin reductase in the absence of biliverdin [17] it appears that, as with other pyridine-nucleotide linked oxidoreductases, the coenzyme binds before the second substrate [18] in an ordered bi-bi mechanism with bilirubin being the first product to dissociate.

Substrate inhibition studies show that biliverdin inhibited the enzyme uncompetitively at fixed concentrations of NADPH, indicating that biliverdin binds to the enzyme-NADP complex. It should be noted that the substrate inhibition constant increases from approx. 2.5 μM at pH 7.5 to 50 μM at pH 9. It is tempting to ascribe this to deprotonation of a basic residue involved in binding one of the biliverdin propionate side-chains. O'Carra and Colleran [9] have described a reduction in biliverdin reductase activity on esterifying one of the propionate side-chains, although they did not report whether this had an effect on binding. Both results would be compatible with a model where a single salt bridge involving one of the propionate side-chains and a basic residue on the enzyme is less favourable than binding involving two such salt bridges. A similar model will also explain the increase in the apparent K_m for biliverdin as the pH is increased. Dixon plots at high concentrations of biliverdin at pH 9 deviate from linearity to give a limiting reciprocal initial rate (Rigney and Mantle, unpublished data), indicating partial substrate inhibition. It is evident that the enzyme-NADP-biliverdin complex can break down, presumably via an enzyme-biliverdin complex, to regenerate free enzyme. A similar conclusion has been reached at pH 7.2 in the presence of bovine serum albumin [6].

Acknowledgements

This work was supported by the Trinity College Development Fund.

References

1 McDonagh, A.F., Palma, L.A. and Schmid, R. (1981) Biochem. J. 194, 273–282.
2 Stocker, R., Yamamoto, Y., McDonagh, A.F., Glazer, A.N. and Ames, B.N. (1987) Science 235, 1043–1046.
3 Stocker, R., Glazer, A.N. and Ames, B.N. (1987) Proc. Natl. Acad. Sci. USA 84, 5918–5922.
4 Kutty, R.K. and Maines, M.D. (1981) J. Biol. Chem. 256, 3956–3962.
5 Noguchi, M., Yoshida, T. and Kikuchi, G. (1979) J. Biochem. 86, 833–848.
6 Phillips, O. and Mantle, T.J. (1981) Biochem. Soc. Trans. 9, 275–278.
7 Colleran, E. and O'Carra, P. (1977) in Chemistry and Physiology of Bile Pigments (Berk, P.D. and Berlin, N.I., eds.), pp. 69–80, U.S. Department of Health, Education & Welfare, Publication No. 77–1100, Washington, DC.
8 Rigney, E.M. Phillips, O. and Mantle, T.J. (1988) Biochem. J. 255, 431–435.
9 O'Carra, P. and Colleran, E. (1971) Biochem. J. 125, 110P.
10 Phillips, O., Mantle, T.J., Tuffery, A.R., Heyworth, C.M., Wilson, S.R. and Houslay, M.D. (1984) Biochem. Pharm. 33, 1963–1967.
11 Phillips, O. (1981) Ph. D. Thesis, University of Dublin.
12 McDonagh, A.F. (1979) in The Porphyrins (Dolphin, D., ed.), Vol. 6, pp. 453–455, Academic Press, London.
13 Wilkinson, G.N. (1961) Biochem. J. 80, 324–332.
14 Florini, J.R. and Vestling, C.S. (1957) Biochim. Biophys. Acta 25, 575–578.
15 Cleland, W.W. (1963) Biochim. Biophys. Acta 67, 104–137.
16 Cleland, W.W. (1970) in The Enzymes, Vol. 2, (Boyer, P.D., ed.), pp. 1–65.
17 Rigney, E.M. and Mantle, T.J. (1985) Biochem. Soc. Trans. 13, 502.
18 Dalziel, K. (1975) in The Enzymes, Vol. 11 (Boyer, P.D., ed.), pp. 1–61, Academic Press, New York.

Biochem. J. (1989) 259, 709–713 (Printed in Great Britain)

The kinetics of ox kidney biliverdin reductase in the pre-steady state

Evidence that the dissociation of bilirubin is the rate-determining step

Elizabeth RIGNEY,* Timothy J. MANTLE*‡ and F. Mark DICKINSON†

*Department of Biochemistry, Trinity College, Dublin 2, Ireland, and †Department of Biochemistry, University of Hull, Hull, N. Humberside HU6 7RX, U.K.

When the production of bilirubin by biliverdin reductase was monitored at 460 nm by stopped-flow spectrophotometry a 'burst' was observed with a first-order rate constant at pH 8 of 20 s^{-1}. The steady-state rate was established on completion of the 'burst'. When the reaction was monitored at 401 nm there was no observed steady-state rate, but a diminished pre-steady-state 'burst' reaction was still seen with a rate constant of 22 s^{-1}. We argue that the rate-limiting reaction is the dissociation of bilirubin from an enzyme·$NADP^+$·bilirubin complex. With NADPH as the cofactor the hydride-transfer step was shown to exhibit pH-dependence associated with an ionizing group with a pK of 7.2. The kinetics of NADPH binding to the enzyme at pH 7.0 were measured by monitoring the quenching of protein fluorescence on binding the coenzyme.

INTRODUCTION

Biliverdin reductase catalyses the NAD(P)H-dependent reduction of biliverdin to produce bilirubin, which is the major bile pigment in mammalian systems (Colleran & O'Carra, 1977). Bilirubin is recognized as being potentially toxic, so that the conjugation reactions involving glucuronic acid are normally regarded as ensuring the efficient elimination of an undesirable catabolite (Fevery *et al.*, 1972). However, more recent studies have suggested that bilirubin may play an important role as a physiologically important antioxidant (Stocker *et al.*, 1987*a*,*b*; Stocker & Ames, 1987). As biliverdin has been suggested to be the major product in at least one of these model systems (Stocker *et al.*, 1987*b*), it may be that one function of biliverdin reductase is to maintain protective concentrations of a physiologically important antioxidant.

The enzyme exists as a monomer of M_r 34000 in most mammalian species (Noguchi *et al.*, 1979; Kutty & Maines, 1981; Phillips & Mantle, 1981), but has received comparatively little attention. The steady-state kinetics have been studied at pH 9 and shown to follow an ordered mechanism (Rigney & Mantle, 1988). A similar mechanism is probably operative at pH 7.2; however, at this pH the kinetics are not readily amenable to analysis unless a biliverdin-binding protein such as serum albumin is present (see Phillips & Mantle, 1981). The enzyme is subject to potent substrate inhibition as the consequence of the formation of an enzyme·$NADP^+$·biliverdin complex (Rigney & Mantle, 1988). The substrate inhibition is partial both at pH 7.2 and at pH 9, as the enzyme·$NADP^+$·biliverdin complex can break down via an enzyme·biliverdin complex to form the free enzyme (Phillips & Mantle, 1981; Rigney & Mantle, 1988). We now describe some stopped-flow experiments with the enzyme that provide more detailed information about the mechanism of catalysis. In particular, the observation of a 'burst' of bilirubin formation before the establishment of the steady-state rate shows that the rate-limiting step of the reaction occurs after hydride transfer.

MATERIALS AND METHODS

Biliverdin reductase was purified from ox kidney as described previously (Rigney *et al.*, 1988). Biliverdin was synthesized by the method of McDonagh (1979). The conditions for studying the steady-state kinetics have been described in Rigney & Mantle (1988), and for details on the pre-steady-state methods, monitoring changes both in absorbance and fluorescence, see Dickinson & Dickenson (1978). Bilirubin formation was generally monitored spectrophotometrically at 460 nm by using $\Delta\epsilon_{460} = 52\,500\ M^{-1}\cdot cm^{-1}$. For the reverse reaction biliverdin formation was similarly monitored at 660 nm by using $\Delta\epsilon_{660} = 12\,500\ M^{-1}\cdot cm^{-1}$.

RESULTS AND DISCUSSION

Biliverdin–NADPH reactions

When biliverdin reductase was mixed rapidly with NADPH and biliverdin in 10 mM-glycine/HCl buffer, pH 9.0, containing 0.1 M-Na_2HPO_4 at 25 °C a 'burst' at 460 nm was observed before establishment of the steady-state rate (Fig. 1). Similar experiments were performed in 0.1 M-glycine/HCl buffer at pH 9.0 and with NADH replacing NADPH at pH 8.5 and pH 7.0 in 0.1 M-sodium phosphate buffer. A summary of the results of these experiments appears in Table 1. The characteristics shown in Fig. 1 were also seen in all the other experiments, but some points are worthy of note. Changing from 10 mM-glycine buffer, pH 9.0, containing 0.1 M-Na_2HPO_4 with NADPH as coenzyme diminished the 'burst' amplitude and the apparent first-order rate constant for the 'burst' without materially changing the steady-state rate. No further work has been done on this observation and no specific reason for the changes can be offered. The

‡ To whom correspondence should be addressed.

Table 1. Analysis of some stopped-flow experiments with biliverdin reductase at 25 °C

The pre-mixing arrangements were as for Fig. 1. The final concentrations of reactants were 2.7 μM-enzyme, 100 μM-NADPH and 20 μM-biliverdin. The results are expressed as the means and ranges for duplicate experiments.

Buffer	Coenzyme	k_h (s^{-1})	'Burst' amplitude (mol of bilirubin/ mol of enzyme)	Steady-state rate (mol of bilirubin/s per mol of enzyme)
10 mM-Glycine/HCl + 0.1 M-Na_2HPO_4, pH 9.0	NADPH	12.4±0.2	0.6±0.1	0.62±0.02
0.1 M-Glycine/HCl, pH 9.0	NADPH	5.4±0.1	0.2±0.02	0.69±0.08
0.1 M-Sodium phosphate, pH 8.5	NADH	0.09	0.7±0.1	0.02±0.002
0.1 M-Sodium phosphate, pH 7.0	NADH	5.5±1.0	0.3±0.02	0.35±0.07

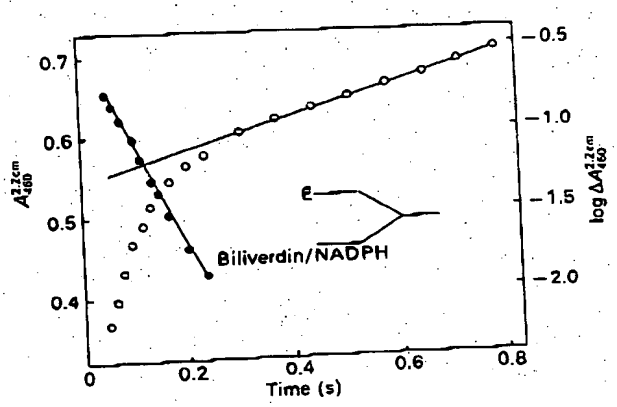

Fig. 1. Pre-steady-state kinetics of biliverdin reductase at pH 9 and 25 °C

Biliverdin reductase was mixed with NADPH and biliverdin to give final concentrations of 3.07 μM, 50 μM and 20 μM respectively, in 0.1 M-Na_2HPO_4/10 mM-glycine/HCl buffer, pH 9. The reaction curve (○, left-hand scale), the analysis of the transient (●, right-hand scale) and the pre-mixing conditions are shown.

steady-state rates ($v/[E]_0$) observed at pH 9.0 with NADPH as coenzyme are in reasonable agreement with the value of 0.46 s^{-1} calculated from eqn. (1):

$$\frac{v}{[E]_0} = \frac{k_{max.}[A][B]}{K_{ia}K_b + K_b[A] + K_a[B] + [A][B]} \quad (1)$$

by using the steady-state parameters determined earlier (Rigney & Mantle, 1988). [In eqn. (1) A and B represent NADPH and biliverdin respectively.] At alkaline pH NADH is clearly a very poor substitute for NADPH with this enzyme. Both the 'burst' rate constant and the steady-state rate are much smaller, although the 'burst' amplitude is similar to that for NADPH. In previous experiments with much smaller concentrations of enzyme we were not able to observe any activity with NADH at pH 8.5 (Rigney & Mantle, 1988). It is clear now that NADH is an effective coenzyme at pH 7.0 and that the broad features of the reaction mechanism are the same as for NADPH.

Stopped-flow experiments with the same pre-mixing arrangements as for Fig. 1 were continued at pH 7.0 in 0.1 M-phosphate buffer. NADPH was the coenzyme. As is shown below, the 'burst' rate constant is much higher than at pH 9.0, although the steady-state rates and 'burst' amplitudes are similar at the two pH values. Variation of the biliverdin concentration (5–80 μM) with 100 μM-NADPH and variation of the NADPH concentration (100–1100 μM) with 5 μM-biliverdin established that the 'burst' rate constant (135±15 s^{-1}), the 'burst' amplitude (0.45±0.5 mol of bilirubin/mol of enzyme) and the specific steady-state rate (1.2±0.15 s^{-1}) remained essentially constant over the concentration ranges tested. Thus the characteristics observed at pH 9.0 (Fig. 1) are also seen at pH 7.0, and it appears that the concentrations used for Fig. 1 and for the experiments described below are saturating.

The effect of pH on the behaviour of the enzyme was examined in a series of experiments with NADPH as coenzyme. The important results appear in Table 2 and Fig. 2. The 'burst' rate constant (k_h) is strongly pH-dependent with an apparent pK_a of 7.2. A finite value of $k_h = 10\ s^{-1}$ seems to be achieved at alkaline pH, suggesting that protonation of this group may not be

Table 2. pH variation of the reaction profiles for biliverdin reductase at 25 °C with NADPH as coenzyme

Experiments were conducted in 0.1 M-sodium phosphate buffers with the pre-mixing arrangement shown in Fig. 1. At pH 9.0 the buffer was 10 mM-glycine/HCl containing 0.1 M-Na_2HPO_4. The final concentrations of reactants were 2.7 μM-enzyme, 100 μM-NADPH and 20 μM-biliverdin. The results are expressed as the means and ranges for duplicate experiments.

pH	k_h (s^{-1})	'Burst' amplitude (mol of bilirubin/ mol of enzyme)	Steady-state rate (mol of bilirubin/s per mol of enzyme)
6.0	162	0.35	1.0
6.5	171±5	0.35±0.02	1.1±0.1
7.0	136±7	0.43±0.02	0.68±0.05
7.25	97	0.44	0.61
7.5	53±5	0.6±0.04	0.72±0.07
8.0	20±1.0	0.63±0.01	0.59±0.1
8.5	13±0.5	0.5±0.01	0.68±0.02
9.0	12±1	0.58±0.05	0.58±0.01

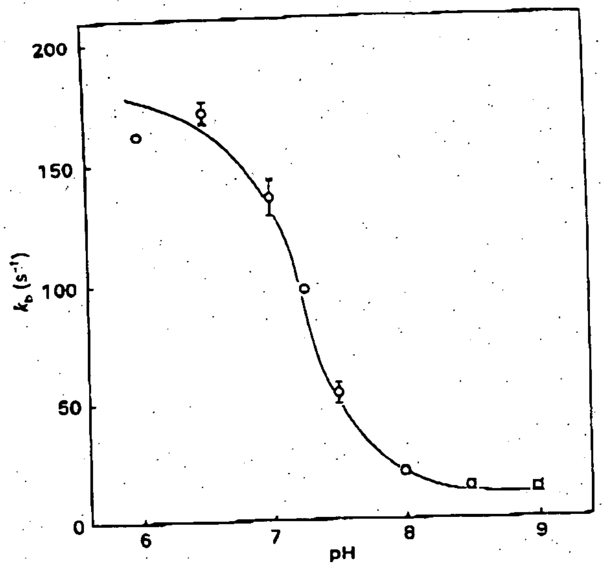

Fig. 2. Effect of pH on the 'burst' rate constant of biliverdin reductase at 25 °C

A solution containing 6.14 μM-biliverdin reductase in 2 mM-sodium phosphate buffer, pH 7.2, was mixed with a solution containing 40 μM-biliverdin and 100 μM-NADPH in the following buffers: 200 mM-sodium phosphate, pH 6–8.5; 200 mM-sodium phosphate/20 mM-glycine, pH 9. The symbols and bars show the means and ranges for duplicate estimates.

absolutely critical for the reaction to proceed with NADPH as coenzyme. The same may not be true for NADH. The limited data of Table 1 show that k_b for NADH changes in the same direction as for NADPH, but much more dramatically between pH 7.0 and pH 8.5. Comparison of the steady-state rates (Tables 1 and 2) with NADPH and NADH also shows a marked difference between the two coenzyme reactions. For NADPH the steady-state rate is rather insensitive to pH, whereas for NADH the rate at pH 7.0 is comparable with that for NADPH but at pH 9.0 is extremely slow. In view of these differences it is interesting that the 'burst' amplitudes for the two coenzymes are quite similar and are relatively pH-independent.

The stopped-flow experiments indicate that the rate-limiting step in biliverdin reduction occurs after hydride transfer and bilirubin formation. A likely mechanism to explain the results is shown in Scheme 1, which describes the events following mixing of enzyme with saturating concentrations of biliverdin and NADPH. In this simple scheme two possible rate-limiting steps occur after hydride transfer, and it is not uncommon to find within the class of NAD(P)-linked dehydrogenases that product coenzyme dissociation is the rate-limiting reaction. In the present case, however, it does not seem that this is so. The 'burst' amplitudes are in all cases significantly less than the 1.0 mol/mol of enzyme expected if $NADP^+$ dissociation is the only rate-limiting step. The low values could be explained if the enzyme preparation was only partially active, but as these preparations were highly active and appear to be homogeneous by various criteria (Rigney & Mantle, 1988) this possibility is for the present discounted. It is also possible that the absorption coefficient of enzyme-bound bilirubin at 460 nm is significantly lowered from that of bilirubin in solution. It seems unlikely on general grounds, however, that the absorption coefficient would be affected by as large a hypochromic shift as would be necessary to be compatible with 'burst' amplitudes of 1.0 mol/mol of enzyme. Certainly the experiments described below at different wavelengths suggest only a limited effect on the absorption spectrum of bound bilirubin.

The data presented can be perhaps best explained by assuming that the rate-limiting step in the reaction is bilirubin dissociation from the product enzyme·$NADP^+$·bilirubin complex. The hydride-transfer step would rapidly equilibrate at a rate determined partly by the state of ionization of the enzyme group having pK_a 7.2, but the equilibrium position of the hydride-transfer step may be roughly in balance. As the bilirubin then dissociates the hydride-transfer step re-equilibrates to maintain the balance and the enzyme·NADPH·biliverdin complex concentration is restored rapidly by combination of substrates with free enzyme liberated by the dissociation of $NADP^+$. With yeast alcohol dehydrogenase, for example, the equilibrium constant for the hydride-transfer step is about 0.1 at pH 7.0 (Dickenson & Dickinson, 1978) whereas the equilibrium constant for the overall reaction is 10^{-4} at this pH (Bäcklin, 1958).

An argument in favour of the above proposal is that in all cases the transient seen in stopped-flow studies is strictly first-order over at least 90% of the reaction course. There is no evidence either in the experiments described above or in those given below that two separate kinetic processes contribute to the appearance of bilirubin in the pre-steady state. If $NADP^+$ dissociation from the terminal enzyme·$NADP^+$ complex is rate-limiting and the hydride-transfer step is rapid and roughly balanced at equilibrium, one would expect to see a biphasic course of bilirubin formation in the pre-steady state whether or not bilirubin and the enzyme·$NADP^+$·bilirubin complex have the same absorption coefficient.

A series of experiments like that described in Fig. 1 were conducted at pH 8.0 with observations being made in the wavelength range 393–413 nm. The results are

$$\text{E·NADPH·biliverdin} \rightleftharpoons \text{E·NADP}^+\text{·bilirubin} \rightarrow \text{E·NADP}^+ \rightarrow \text{E} + \text{NADP}^+$$
$$+ \text{ bilirubin}$$

Scheme 1. Proposed mechanism for biliverdin reductase

The mechanism is a shortened form of a compulsory-order mechanism with coenzyme as the leading substrate. This form of the mechanism is applicable to the stopped-flow experiments described in the text where saturating concentrations of NADPH and biliverdin were used.

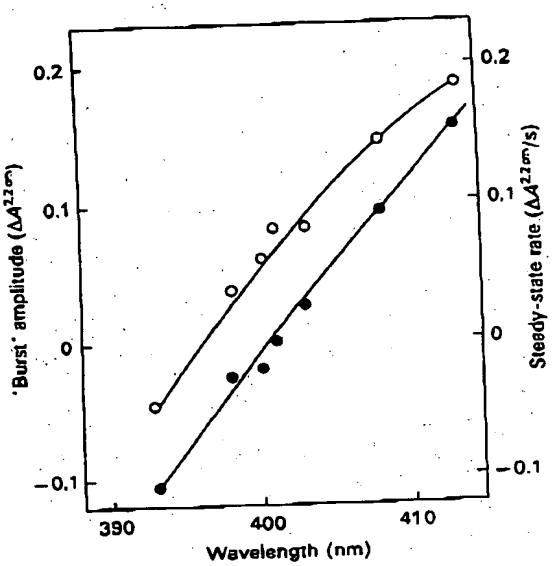

Fig. 3. Wavelength-dependence of 'burst' amplitude and steady-state rate of biliverdin reductase at pH 8.0 and 25 °C

Biliverdin reductase (10.06 μM) was mixed with NADPH (100 μM) and biliverdin (20 μM) in 0.1 mM-sodium phosphate buffer, pH 8.0, in the stopped-flow apparatus. The reactions were monitored at various wavelengths and the 'burst' amplitude (○, left-hand scale) and steady-state rate (●, right-hand scale) were measured.

shown in Fig. 3. It is clear that the 'burst' amplitude decreases as the wavelength decreases. There is an isosbestic point at about 396 nm when no 'burst' is observed, and thereafter the sign of the 'burst' is inverted. The steady-state rate shows the same trend as the 'burst', but the curve is shifted to longer wavelengths and the isosbestic point is at 401 nm. These experiments show that the absorption spectrum of bilirubin in the enzyme·NADPH·bilirubin complex is shifted to shorter wavelengths from that of bilirubin in free solution. The shift is not very great (approx. 4 nm), however, and as the absorption band is rather broad (approx. 90 nm at half maximum) it is unlikely, as stated above, that the absorption coefficient of bound bilirubin at 460 nm is greatly lowered from that of bilirubin in solution.

The transients documented in Fig. 3 are all strictly first-order with experimental error regardless of the sign of the 'burst' and all give values for the 'burst' rate constant in the range of $k_b = 20 \pm 2\ s^{-1}$. Obviously in the region of the isosbestic point the accuracy of the determinations is decreased because of the diminished magnitude of the transient. The fact that the pre-steady-state kinetics of bilirubin formation remain simple across a wide wavelength range supports the view that only one species of enzyme-bound biliurubin is kinetically significant. This encourages belief in the interpretation of the pre-steady-state experiments observed above.

Bilirubin–NADP⁺ reactions

A few stopped-flow experiments were conducted at 25 °C in 0.1 M-sodium phosphate buffer, pH 8.5, in which enzyme was rapidly mixed with a solution of bilirubin and NADP⁺. The final concentrations after mixing were 2.7 μM-enzyme, 80 μM-bilirubin and 1 mM-NADP⁺. The reactions were monitored spectrophotometrically at 660 nm. The reaction profiles were very similar to that of Fig. 1 in that a rapid 'burst' of absorbance was followed by establishment of a slow steady-state rate. In these experiments the 'burst' amplitude was 0.15 ± 0.02 mol of biliverdin/mol of enzyme, the 'burst' rate constant k_b was $5.2 \pm 0.5\ s^{-1}$ and the steady-state rate was 0.02 ± 0.003 mol of biliverdin/s per mol of enzyme. It was not established whether the concentrations of substrates were saturating, but it seems likely that they were.

As for the forward reaction the rate-limiting step in bilirubin oxidation seems to occur after hydride transfer. The hydride-transfer step may equilibrate rapidly, with the equilibrium position being in favour of the enzyme·NADP⁺·bilirubin complex. It is possible that the steady-state rates observed are inhibited rates because of the steady formation of the abortive enzyme·NADP⁺·biliverdin complex (Rigney & Mantle, 1988). Accordingly, no further interpretation of the results seems justified.

Enzyme–NADPH reactions

The binding of NADPH to biliverdin reductase has previously been studied by observing the quenching of protein fluorescence following NADPH binding to the enzyme. At pH 8.5 a value for the dissociation constant of the binary complex of 2.6 μM was obtained (E. M. Rigney & T. J. Mantle, unpublished work). It is not possible to investigate NAD(P)H binding by monitoring nucleotide fluorescence because, unlike most other nicotinamide nucleotide-linked oxidoreductases, no such change was observed on mixing enzyme and either NADPH or NADH. We have now followed the kinetics

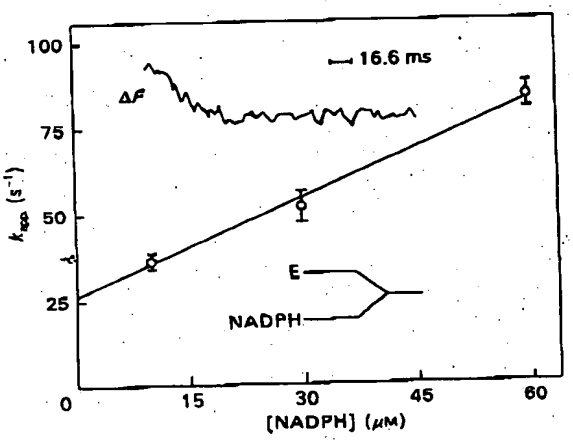

Fig. 4. NADPH binding to biliverdin reductase

The quenching of biliverdin reductase (final concentration 2.57 μM) fluorescence was measured at the concentrations of NADPH indicated by stopped-flow fluorimetry in 50 mM-sodium phosphate buffer, pH 7. The inset shows a trace obtained with 30 μM-NADPH. The symbols and bars show the means and ranges for duplicate experiments. The pre-mixing conditions are indicated.

of NADPH binding to the enzyme by monitoring the quenching of protein fluorescence in a stopped-flow fluorimeter at pH 7.0 and 25 °C.

The results and the conditions of the experiments are shown in Fig. 4. The kinetics show an apparent first-order process, the rate constant of which increases with increasing concentrations of NADPH. The results may be interpreted in terms of the reactions:

$$E + NADPH \underset{k_{-1}}{\overset{k_{+1}}{\rightleftharpoons}} E \cdot NADPH$$

Such a scheme predicts that the slope of Fig. 4 is equal to k_{+1} and the intercept is k_{-1}. Thus $k_{+1} = 0.95 \times 10^6\ M^{-1} \cdot s^{-1}$ and $k_{-1} = 25\ s^{-1}$. The dissociation constant of the complex is calculated to be 26 μM, 10-fold greater than at pH 8.5 (see above), but very similar to the value for the dissociation constant of the enzyme·NADP$^+$ complex of 24 μM at pH 7.0 measured in product-inhibition experiments (Rigney & Mantle, 1988). Commonly nicotinamide nucleotide-linked dehydrogenases bind the reduced form of the coenzyme more tightly than the oxidized form. This does not seem to be true in the present case. The value of $k_{-1} = 25\ s^{-1}$ for NADPH dissociation at pH 7.0 might indicate a similar value for the specific rate of dissociation of the corresponding enzyme·NADP$^+$ complex. If so, it would fit in with our view that bilirubin dissociation from the product ternary complex is the rate-limiting step.

Received 3 October 1988/25 November 1988; accepted 28 November 1988

REFERENCES

Bäcklin, K.-I. (1958) Acta Chem. Scand. **12**, 1279–1285

Colleran, E. & O'Carra, P. (1977) in DHEW Publ. (NIH) U.S. no. 77-1100: Chemistry and Physiology of Bile Pigments (Berk, P. D. & Berlin, N. I., eds.), pp. 69–80, U.S. Department of Health, Education and Welfare, Washington

Dickenson, C. J. & Dickinson, F. M. (1978) Biochem. J. **171**, 613–627

Dickinson, F. M. & Dickenson, C. J. (1978) Biochem. J. **171**, 629–637

Fevery, J. B., Van Damme, R., Michiels, R., DeGroote, J. & Heirwegh, K. P. M. (1972) J. Clin. Invest. **51**, 2482–2492

Kutty, R. K. & Maines, M. D. (1981) J. Biol. Chem. **256**, 3956–3962

McDonagh, A. F. (1979) in The Porphyrins (Dolphin, D., ed.), vol. 6, pp. 453–455, Academic Press, London

Noguchi, M., Yoshida, T. & Kukuchi, G. (1979) J. Biochem. (Tokyo) **86**, 833–848

Phillips, O. & Mantle, T. J. (1981) Biochem. Soc. Trans. **9**, 275–278

Rigney, E. M. & Mantle, T. J. (1988) Biochim. Biophys. Acta **957**, 237–242

Rigney, E. M., Phillips, O. & Mantle, T. J. (1988) Biochem. J. **255**, 431–435

Stocker, R. & Ames, B. N. (1987) Proc. Natl. Acad. Sci. U.S.A. **84**, 8130–8134

Stocker, R., Yamamoto, Y., McDonagh, A. F., Glazer, A. N. & Ames, B. N. (1987*a*) Science **235**, 1043–1046

Stocker, R., Glazer, A. N. & Ames, B. N. (1987*b*) Proc. Natl. Acad. Sci. U.S.A. **84**, 5918–5922

Biochem. J. (1988) 255, 431–435 (Printed in Great Britain)

Some physical and immunological properties of ox kidney biliverdin reductase

Elizabeth M. RIGNEY, Orla PHILLIPS and Timothy J. MANTLE
Department of Biochemistry, Trinity College, Dublin 2, Ireland

The liver, kidney and spleen of the mouse and rat and the kidney and spleen of the ox express a monomeric form of biliverdin reductase (M_r 34000), which in the case of the ox kidney enzyme exists in two forms (pI 5.4 and 5.2) that are probably charge isomers. The livers of the mouse and rat express, in addition, a protein (M_r 46000) that cross-reacts with antibodies raised against the ox kidney enzyme and may be related to form 2 described by Frydman, Tomaro, Awruch & Frydman [(1983) Biochim. Biophys. Acta 759, 257–263]. Higher-M_r forms appear to exist in the guinea pig and hamster. The ox kidney enzyme has three thiol groups, of which two are accessible to 5,5′-dithiobis-(2-nitrobenzoate) in the native enzyme. Immunocytochemical analysis reveals that biliverdin reductase is localized in proximal tubules of the inner cortex of the rat kidney. Biliverdin reductase antiserum also stains proximal tubules in human and ox kidney. The staining of podocytes in glomeruli of ox kidney with antiserum to aldose reductase is particularly prominent. The localization of biliverdin reductase in the inner cortical zone of rat kidney is similar to that described for glutathione *S*-transferase YfYf, and it is suggested that one function of this 'intracellular binding protein' may be to maintain a low free concentration of biliverdin to allow biliverdin reductase to operate efficiently.

INTRODUCTION

Biliverdin reductase catalyses the NAD(P)H-dependent reduction of biliverdin to produce the bile pigment bilirubin. The enzyme has been purified from rat liver, pig spleen and ox kidney (Kutty & Maines, 1981; Noguchi *et al.*, 1979; Phillips & Mantle, 1981) and in each case has been reported to exist as a monomer of M_r 34000-36000. The enzyme has been reported to occur only in mammals (Colleran & O'Carra, 1977), where it is believed to play a role in clearing biliverdin from the foetus (McDonagh *et al.*, 1981). Biliverdin is not known to exhibit any toxicity, and although Okazaki *et al.* (1978) suggested that it might play a role in liver regeneration we have been unable to confirm this suggestion (Phillips *et al.*, 1984). The enzyme is subject to potent substrate inhibition by biliverdin (O'Carra & Colleran, 1971; Phillips & Mantle, 1981), although this effect is probably modulated *in vivo* by intracellular binding proteins (Phillips *et al.*, 1984).

Most studies on the kinetics of this enzyme have included serum albumin in the assay mixture, and as this binds biliverdin it is necessary to apply a correction factor to obtain the free concentration of biliverdin (Phillips & Mantle, 1981). In addition, albumin may have direct effects on the activity of biliverdin reductase (Phillips, 1981; O. Phillips & T. J. Mantle, unpublished work). In order to conduct a detailed kinetic study of this enzyme we have used a slight modification of our original preparation (Phillips & Mantle, 1981) as described elsewhere (Phillips, 1981; Daly & Mantle, 1982) to obtain sufficient quantities of the enzyme. This has allowed us to investigate certain physical and immunological properties of the enzyme, which are described in the present paper.

MATERIALS AND METHODS

Materials

Biliverdin was synthesized by the method of McDonagh (1979). Procion Blue MX-R–Sepharose 4B was prepared as described by Baird *et al.* (1976). NADPH was purchased from Boehringer, and 2′,5′-bisphosphoadenosine–Sepharose and Sephadex G-100 were obtained from Pharmacia.

Purification of biliverdin reductase and aldose reductase

Our current procedure represent minor variations to those described in earlier work (Phillips & Mantle, 1981; Daly & Mantle, 1982). Briefly, ox kidney cytosol is fractionated by $(NH_4)_2SO_4$ fractionation (40–65% saturation), DEAE-cellulose chromatography and chromatography on Procion Blue MX-R–Sepharose. After this step fractions with a specific activity of more than 550 nmol/min per mg were pooled and gel-filtered on Sephadex G-100. After this step the preparation contained two polypeptides of M_r 34000 (biliverdin reductase) and 32000 (aldose reductase). These two proteins were separated on 2′,5′-bisphosphoadenosine–Sepharose as described previously (Phillips, 1981; Daly & Mantle, 1982).

Details of the assay methods for biliverdin reductase and aldose reductase can be found in Phillips *et al.* (1984) and Daly & Mantle (1982).

Electrophoretic methods

SDS/polyacrylamide-gel electrophoresis was carried out according to the method of Laemmli (1970). Isoelectric focusing was performed in flat-bed polyacrylamide gels in an LKB Multiphor apparatus under

native and denaturing (8 M-urea) conditions. Immunoblotting was carried out according to the method of Towbin *et al.* (1979).

Activity stain for biliverdin reductase

After native isoelectric focusing the polyacrylamide gel was overlaid with nitrocellulose paper that had been soaked in 30 μM-biliverdin/100 μM-NADH/50 μM-bovine serum albumin/100 mM-sodium phosphate buffer, pH 7.2, and then blotted dry. Enzyme activity was easily located as yellow bands (bilirubin) against a pale-green background.

Preparation of antisera

Purified preparations of biliverdin reductase and aldose reductase (100 μg of each) were emulsified with Freund's complete adjuvant and injected into multiple sites on the backs of New Zealand White rabbits. Then 2 weeks later the animals were boosted with a further 100 μg of antigen (emulsified with Freund's incomplete adjuvant) by intramuscular injection into the hind leg. After a further 2 weeks the animals were exsanguinated, and the blood was allowed to clot at 4 °C overnight and the serum was stored at −20 °C.

Preparation of cytosols

Animal tissues were obtained from local suppliers with the exception of those from the wallaby, which were kindly supplied by Dr. C. H. Tyndale-Biscoe, C.S.I.R.O., Canberra, A.C.T., Australia. Liver, kidney and spleen from the rat, mouse, hamster, guinea pig, fox and wallaby and human liver were homogenized in 0.25 M-sucrose/10 mM-Tris/HCl/1 mM-EDTA buffer, pH 7.2, in a Polytron homogenizer and centrifuged at 48000 *g* for 20 min. The supernatants were stored at −20 °C at a protein concentration in the range 10–50 mg/ml.

Immunocytochemical analysis

Sections (5 μm) of liver, kidney and spleen from the rat, human and ox that had been fixed in Bouin's fluid were stained by the peroxidase–anti-peroxidase technique of Sternberger *et al.* (1970).

RESULTS AND DISCUSSION

By substituting one Procion dye column instead of two (Phillips & Mantle, 1981) and by including 2',5'-bisphosphoadenosine–Sepharose (Phillips, 1981; Daly & Mantle, 1982) we can now prepare 1–2 mg of electrophoretically homogeneous material in 3 days. The purified enzyme focuses as a single band with a pI of 6.2 under denaturing conditions. However, when the enzyme is focused under native conditions two bands are resolved with isoelectric points of 5.4 and 5.2 (Fig. 1). Both bands are active, as demonstrated by activity staining on nitrocellulose paper (results not shown), demonstrating the existence of two molecular forms of biliverdin reductase, which we term BVR I (pI 5.4) and BVR II (PI 5.2). The separation of two major bands was quite reproducible. However, in some preparations a third band (pI 5.1) was also observed (see, e.g., track 3 in Fig. 1). BVR I and BVR II have identical mobilities on SDS/polyacrylamide-gel electrophoresis, as shown in Fig. 2. The structural relationship between the two forms was examined by peptide mapping with the use of *Staphylococcus aureus* V8 proteinase. No difference between the

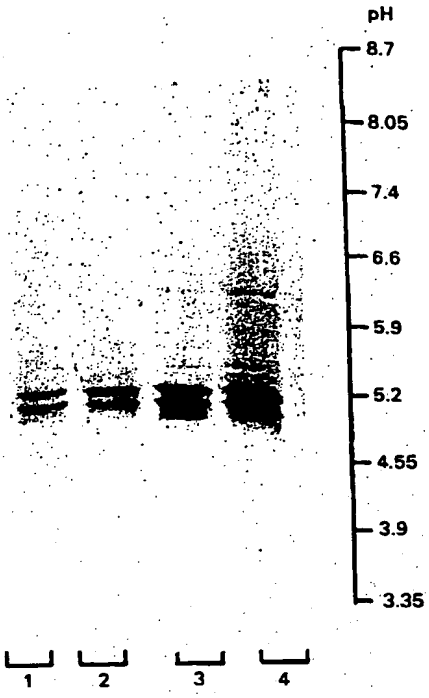

Fig. 1. Isoelectric focusing of ox kidney biliverdin reductase

Tracks 1, 2, 3 and 4 contain 6 μg of ox kidney biliverdin reductase from four preparations.

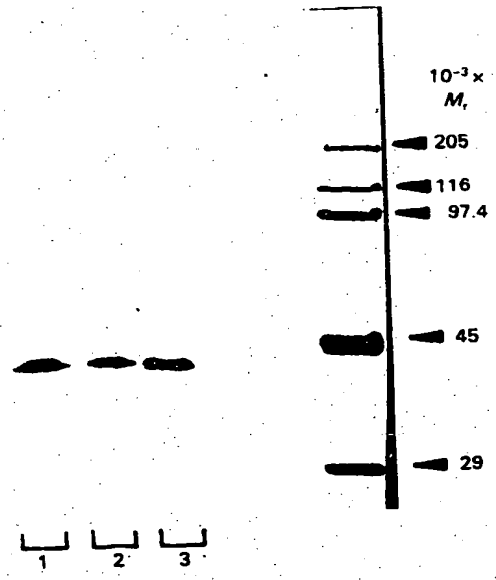

Fig. 2. SDS/polyacrylamide-gel electrophoresis of biliverdin reductase

The two forms of biliverdin reductase (BVR I and BVR II) were excised from the native isoelectric-focusing gel and incubated in 0.125 M-Tris/HCl/1 mM-EDTA/0.1 % SDS for 4 h at 4 °C before SDS/polyacrylamide-gel electrophoresis. Tracks 1, 2 and 3 contain 6 μg of BVR I, BVR II and a mixture of BVR I and BVR II respectively. The mobilities of the M_r markers are indicated. The protein bands were detected by silver staining.

Table 1. Effect of 5,5′-dithiobis-(2-nitrobenzoate) on biliverdin reductase

Reaction of 5,5′-dithiobis-(2-nitrobenzoate) (DTNB) at a final concentration of 25 μM with 2.5 μM enzyme was monitored at 412 nm in 0.1 M-sodium phosphate buffer, pH 8, containing 10 mM-EDTA. Results are shown for a single experiment as a relatively high concentration of enzyme was used. However, the values obtained are in good agreement with results obtained in a separate experiment conducted with 1.47 μM enzyme. The 'protecting' concentrations of substrates were 22 μM and 200 μM for biliverdin and $NADP^+$ respectively.

Substrate present before addition of DTNB	Thiol groups modified (mol/mol of enzyme)		Activity remaining (%)
	No SDS	SDS added	
None	1.66	2.70	0
Biliverdin	0.86	2.82	0
NADP	1.78	3.30	0
Biliverdin plus $NADP^+$	1.10	3.20	30

two forms could be detected by this technique (results not shown). In addition, we have been unable to detect any evidence for kinetic heterogeneity in our steady-state studies (E. M. Rigney & T. J. Mantle, unpublished work). Further attempts to separate BVR I and BVR II by chromatofocusing were not successful; all the activity was eluted in a symmetrical peak at pH 4.6 (results not shown). The two molecular forms of biliverdin reductase are clearly closely related, and we assume that they represent charge isomers. We have not attempted in the present work to define further the relationship between BVR I and BVR II and have conducted the following experiments with preparations containing both forms.

The amino acid composition of biliverdin reductase has been reported previously (Phillips, 1981), but unfortunately no data were presented on the number of thiol groups reactive with 5,5′-dithiobis-(2-nitrobenzoate). Table 1 shows the effect of 5,5′-dithiobis-(2-nitrobenzoate) on biliverdin reductase activity in the presence and in the absence of substrate and also the number of 5,5′-dithiobis-(2-nitrobenzoate) reactive thiol groups per subunit in the absence and in the presence of 1% SDS. It is clear that the polypeptide has three reactive thiol groups of which two are available in the native enzyme. $NADP^+$ did not protect either of the two thiol groups in the native enzyme, whereas biliverdin, either alone or in the presence of $NADP^+$, does appear to protect one of the thiol groups. Neither substrate alone was able to protect enzyme activity. However, 30% activity remained when the enzyme was incubated with 5,5′-dithiobis-(2-nitrobenzoate) in the presence of both substrates. It is unclear why biliverdin, either in the presence or in the absence of $NADP^+$, apparently protects the same thiol group but with different amounts of activity remaining. Ox kidney biliverdin reductase thus resembles the rat liver enzyme, which is also reported to contain three cysteine residues (Kutty & Maines, 1981).

The ability of biliverdin to protect one of the three thiol groups suggests the existence of an enzyme–biliverdin complex. To examine this possibility further we have utilized an earlier observation that when biliverdin is dissolved in a non-aqueous solvent, such as ethyl acetate, in the presence of a thiol a change in colour

Table 2. Species and tissue distribution of biliverdin reductase

Immunoprecipitation was carried out by incubating the respective cytosols with 10 μl of Protein A–Sepharose and 50 μl of antiserum for 6 h at 4 °C and then centrifuging the slurry in a bench centrifuge for 3 min. The supernatants were then assayed for biliverdin reductase activity. Controls in which either the antibody or Protein A–Sepharose had been omitted did not precipitate any biliverdin reductase activity. Abbreviation: N.D., not determined.

Tissue	Specific activity (nmol/min per mg)	Activity remaining after immunoprecipitation (%)
Ox kidney	0.790	0
Ox liver	0.002	0
Pig liver	0.134	0
Guinea-pig liver	0.116	0
Guinea-pig spleen	0.545	0
Guinea-pig kidney	0.401	0
Mouse liver	0.156	0
Mouse spleen	0.585	0
Mouse kidney	0.584	10
Rat liver	0.167	20
Rat spleen	0.436	N.D.
Rat kidney	0.525	19
Hamster liver	0.162	0
Hamster spleen	0.080	0
Hamster kidney	0.060	0
Fox liver	0.144	0
Fox spleen	0.335	0
Fox kidney	0.333	0
Wallaby kidney	0.275	N.D.
Wallaby liver	0.084	N.D.
Wallaby spleen	1.003	N.D.
Human liver	0.053	0

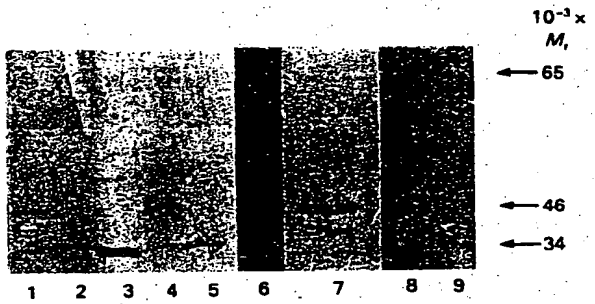

Fig. 3. Immunoblotting cytosols from different species

Cytosols from the different species listed below were immunoblotted with the use of antiserum against the ox kidney enzyme. Tracks 1–9 contained mouse liver (300 μg), mouse spleen (320 μg), mouse kidney (320 μg), rat liver (350 μg), rat spleen (350 μg), rat kidney (350 μg), human liver (350 μg), hamster kidney (160 μg) and fox liver (350 μg) respectively.

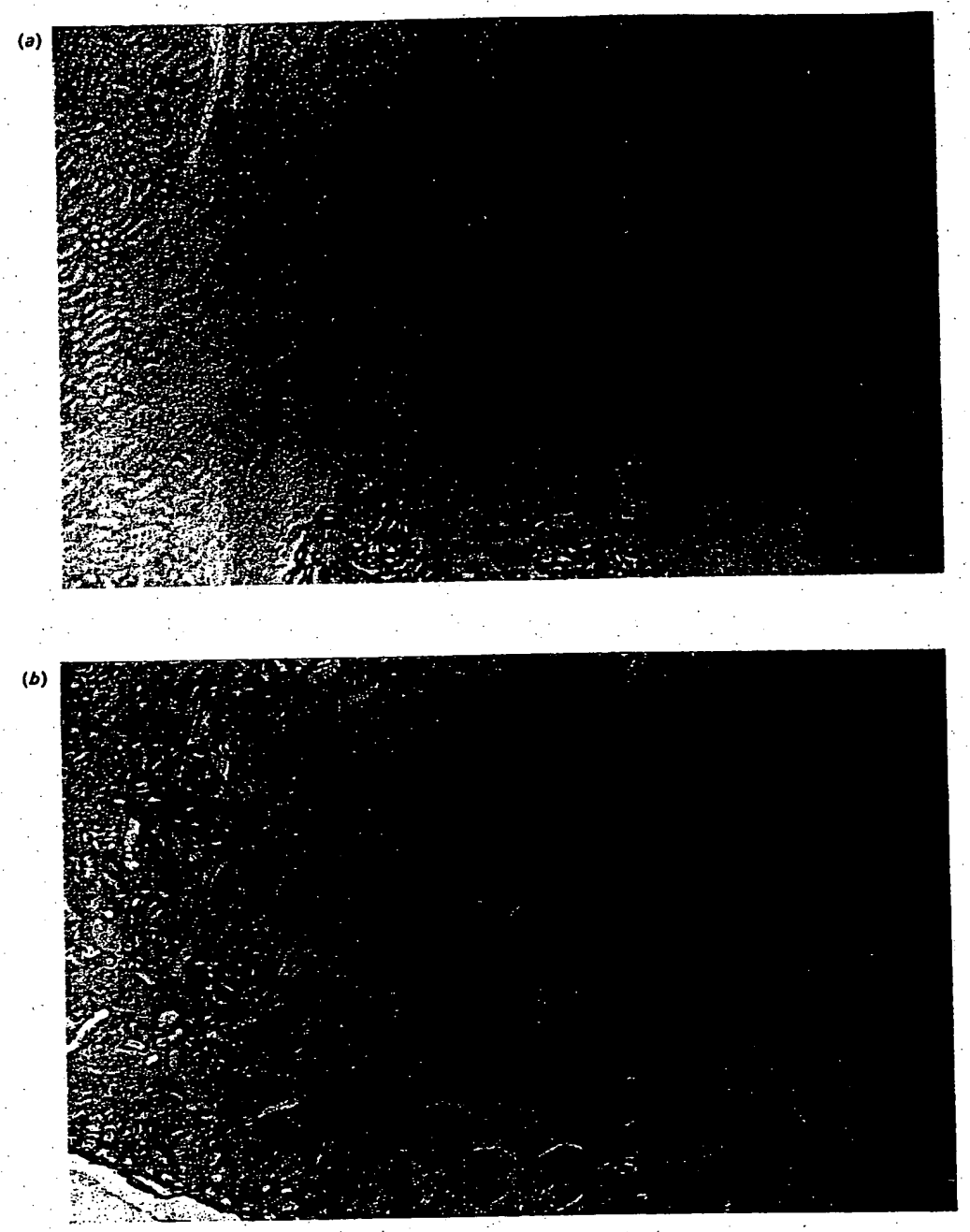

Fig. 4. Immunocytochemical staining of rat kidney and ox kidney

Staining was conducted as described in the text with the use of (*a*) anti-(biliverdin reductase) serum with rat kidney and (*b*) anti-(aldose reductase) serum with ox kidney (*b*).

from green to yellow is observed, which is due to the formation of thioether adduct at the central methylene bridge (Manitto & Monti, 1979). This colour change also occurs when biliverdin is dissoived in aqueous solution in the presence of serum albumin and a mercaptan. We have obtained similar results with dithiothreitol and GSH as mercaptans and with glutathione *S*-transferase YaYc as the biliverdin-binding protein (A. Johns, O. Phillips & T. J. Mantle, unpublished work). We attempted to obtain further evidence for biliverdin binding to the free enzyme by using biliverdin reductase as the 'biliverdin-binding protein' in similar experiments. Unfortunately when biliverdin reductase was used as the 'biliverdin-binding protein' no such effect could be

demonstrated, even in the presence of $NADP^+$. As biliverdin reductase binds biliverdin under these conditions in a ternary enzyme–$NADP^+$–biliverdin complex (Colleran & O'Carra, 1977; Phillips & Mantle, 1981), this suggests that even the smallest mercaptan we used, 2-mercaptoethanol, cannot gain access to the biliverdin-binding site. Clearly no such hindrance exists in the biliverdin-binding proteins such as serum albumin and glutathione *S*-transferase YaYc, which are known to display less selectivity towards hydrophobic ligands and can obviously accommodate the various thioether adducts.

Although biliverdin reductase is believed to be a 'mammalian' enzyme, there have been few surveys to extend the range of species studied. With the availability of antibodies to the ox kidney enzyme we have examined the distribution of this enzyme and the immunological cross-reactivity in several species. Biliverdin reductase activity was present in the kidney, spleen and liver cytosol of all species studied (Table 2), although very low activities were observed in ox liver (see also Colleran & O'Carra, 1977). Biliverdin reductase activity from cytosols of liver, kidney and spleen of the species listed in Table 2 was immunoprecipitated by antibodies to the ox kidney enzyme with the use of Protein A–Sepharose 6B. Under the conditions used 100% immunoprecipitation was achieved in all of the samples with the exception of mouse kidney, rat liver and rat kidney, where 10–20% of the activity remained in the supernatant. Possibly a fraction of biliverdin reductase in mouse kidney, rat liver and rat kidney is immunologically unrelated to the ox kidney enzyme.

Cytosols from the various tissues were also analysed by immunoblotting. From most species cross-reacting material with a subunit M_r of 34000–46000 is clearly seen (Fig. 3). However, hamster kidney (track 7 in Fig. 3) and guinea-pig liver (results not shown) express cross-reacting material with significantly larger M_r values (65000 and 85000 respectively). O'Carra & Colleran (1977) have reported that the guinea-pig enzyme has an M_r of 70000, and the present result is consistent with that observation. Interestingly mouse and rat tissues behaved identically in that liver from both these species contain two cross-reactive proteins with M_r values of 34000 and 46000. Spleen and kidney from both these tissues express only the protein of M_r 34000. It is unclear at the present time whether the proteins of M_r 34000 and 46000 correspond to forms 1 and 2 described by Frydman *et al.* (1983), although in support of this these workers have reported that only their form 1 (M_r 34000) is present in kidney and spleen.

We have studied the localization of biliverdin reductase and aldose reductase in the kidney, liver and spleen of the ox, rat and human. In the rat only the proximal tubules of the inner cortex are stained with anti-(biliverdin reductase) serum (Fig. 4*a*). Interestingly a similar distribution has been noted for glutathione *S*-transferase YfYf and glutathione *S*-transferase YbYb in rat and mouse kidney respectively (Boyce *et al.*, 1987). It is tempting to speculate that these intracellular binding proteins play a functional role with regard to maintaining a low free concentration of biliverdin (Phillips & Mantle, 1981) to allow biliverdin reductase to operate efficiently in these tubules. Biliverdin reductase antiserum also stains proximal tubules in human and ox kidney (results not shown). With antisera to aldose reductase with rat kidney we obtained intense staining of the inner medulla (thin limbs of the loop of Henle and collecting tubules) and weak staining of the inner cortex and glomerular podocytes. A similar finding has been reported by Ludvigson & Sorenson (1980). Similar results were obtained with anti-(aldose reductase) serum staining of human kidney, although there is no precise counterpart of the rat/mouse inner cortical zone in this case. Interestingly the glomerular podocytes of the ox kidney stained very intensely with anti-(aldose reductase) serum (Fig. 4*b*), in contrast with the very weak staining seen with this structure in the rat and human. In the spleen the red pulp but not the splenic nodules stained with biliverdin reductase antiserum (results not shown). This is not surprising as the nodules are not recognized sites of erythrocyte degradation.

This work was supported by the Trinity College Development Fund. We thank S. J. Boyce and S. M. McBennett for performing the immunocytochemical staining and Dr. D. C. Williams for helpful discussions.

REFERENCES

Baird, J. K., Sherwood, R. F., Carr, R. J. C. & Atkinson, A. A. (1976) FEBS Lett. **70**, 61–68
Boyce, S. J., McBennett, S. M., Mantle, T. J. & Hayes, J. D. (1987) in Glutathione *S*-Transferases and Carcinogenesis (Mantle, T. J., Pickett, C. B. & Hayes, J. D., eds.), pp. 69–72, Taylor and Francis, London, New York and Philadelphia
Colleran, E. & O'Carra, P. (1977) in DHEW Publ. (NIH) U.S. no. 77–1100: Chemistry and Physiology of Bile Pigments (Berk, P. D. & Berlin, N. I., eds.), pp. 69–80, U.S. Department of Health, Education and Welfare, Washington
Daly, A. K. & Mantle, T. J. (1982) Biochem. J. **205**, 373–380
Frydman, R. B., Tomaro, M. L., Awruch, J. & Frydman, B. (1983) Biochim. Biophys. Acta **759**, 257–263
Kutty, R. K. & Maines, M. D. (1981) J. Biol. Chem. **256**, 3956–3962
Laemmli, U. K. (1970) Nature (London) **227**, 680–685
Ludvigson, M. A. & Sorenson, R. L. (1980) Diabetes **29**, 450–459
Manitto, P. & Monti, D. (1979) Experientia **35**, 1418–1420
McDonagh, A. F. (1979) in The Porphyrins (Dolphin, D., ed.), vol. 6, pp. 453–455, Academic Press, London
McDonagh, A. F., Palma, L. A. & Schmid, R. (1981) Biochem. J. **194**, 273–282
Noguchi, M., Yoshida, T. & Kikuchi, G. (1979) J. Biochem. (Tokyo) **86**, 833–848
O'Carra, P. & Colleran, E. (1971) Biochem. J. **125**, 110P
Okazaki, K., Nishimura, H., Arizono, H., Nishimura, N. & Suzuki, Y. (1978) Biochem. Biophys. Res. Commun. **81**, 512–520
Phillips, O. (1981) Ph.D. Thesis, University of Dublin
Phillips, O. & Mantle, T. J. (1981) Biochem. Soc. Trans. **9**, 275–278
Phillips, O., Mantle, T. J., Tuffery, A. R., Heyworth, C. M., Wilson, S. R. & Houslay, M. D. (1984) Biochem. Pharmacol. **33**, 1963–1967
Sternberger, L. A., Hardy, P. H., Cuculis, J. J. & Meyer, H. G. (1970) J. Histochem. Cytochem. **18**, 315–333
Towbin, H., Staehelin, T. & Gordon, J. (1979) Proc. Natl. Acad. Sci. U.S.A. **76**, 4350–4354

Received 10 December 1987/14 March 1988; accepted 20 June 1988